University of Puerto Rico, Río Piedras Campus
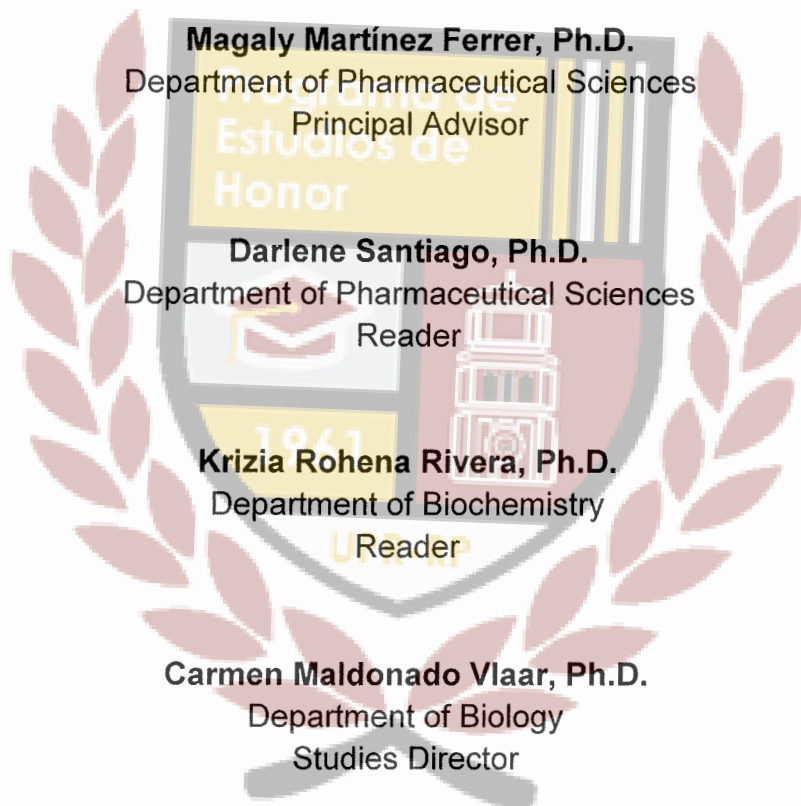**College of Natural Sciences**
Department of Biology

CCL4 and IL-15 Modulate Gene Expression Patterns Associated with the Human PI3-Kinase Signaling Pathway and Cancer Metastasis in Prostate Cancer Tumors

Diana Alexandra Aponte Colón
Honors Program
May 25, 2016

University of Puerto Rico, Río Piedras Campus
College of Natural Sciences
Department of Biology

Thesis Committee:

Magaly Martínez Ferrer, Ph.D.
Department of Pharmaceutical Sciences
Principal Advisor

Darlene Santiago, Ph.D.
Department of Pharmaceutical Sciences
Reader

Krizia Rohena Rivera, Ph.D.
Department of Biochemistry
Reader

Carmen Maldonado Vlaar, Ph.D.
Department of Biology
Studies Director

Marisela Santiago
Department of Accounting
Associate Director, Honors Program

Luis Raul Cámara
Department of Political Sciences
Director, Honors Program

Table of Contents

Abstract

Prostate cancer (PCa) is the second leading cause of cancer-related deaths in the United States and the most frequently diagnosed among men. Inflammation and the Phosphatidylinositol 3-kinase (PI3K) signaling pathway have been linked to PCa development. Macrophage inflammatory protein-1β (CCL4) and Interleukin 15 (IL-15) are inflammatory chemokines that were differentially expressed in patients with PCa recurrence. Given that chemokines are important regulators of inflammation and that the PI3K signaling pathway is considered one of the major drivers of PCa growth, we hypothesized that CCL4 and IL-15 play important roles in the modulation of genes related to prostate cancer progression and metastasis in the PI3K Signaling Pathway. To test our hypothesis, we used an orthotopic xenograft model in which SCID mice were injected with 250,000 22RV1 (androgen-dependent) cells in the anterior prostate lobes. CCL4 or IL-15 were administered bi-weekly, at 0.0013ng/mL or 0.1ng/mL, with intraperitoneal injections during four weeks. Tumor tissue was collected and RNA was extracted. To analyze differentially expressed genes related to cancer metastasis and the human PI3K signaling pathway, we used Qiagen RT^2 Profiler PCR Arrays. Differentially expressed genes were confirmed using Real Time Polymerase Chain Reaction. Our results indicate that BRMS1, CXCR2, ITGA7, FOS, PRKCA, PI3Kα, and AKT1 mRNA expression is differentially expressed ($p<0.05$) in prostate cancer tumors treated with CCL4 when compared to the control. Furthermore, AKT3, CCND1, CD14, FASLG, IGF1, IRS1, MMP2, MMP9, and PTEN mRNA expression is

differentially expressed (p<0.05) in prostate cancer tumors treated with IL-15 when compared to the control. These results support the hypothesis that CCL4 and IL-15 modulate gene expression patterns related to the PI3K signaling pathway in prostate cancer tumors. Furthermore, the determination of these differentially expressed genes can help elucidate the mechanisms underlying prostate cancer progression in tumors treated with CCL4 or IL-15.

Dedication

First and foremost, I would like to dedicate my honors thesis to my grandmother, Antonia Muñiz Miranda. The sacrifices she underwent as a first generation college student inspire me to continue pursuing a higher-education degree. I could not have completed this work without her influence and guidance. I would also like to dedicate this thesis to my father and aunt, Pedro Aponte Muñiz and María de L. Aponte Muñiz, for their unlimited support and to my research and Honors Program mentors. Thank you for providing me the necessary tools to accomplish my goals and for encouraging me to reach my highest potential.
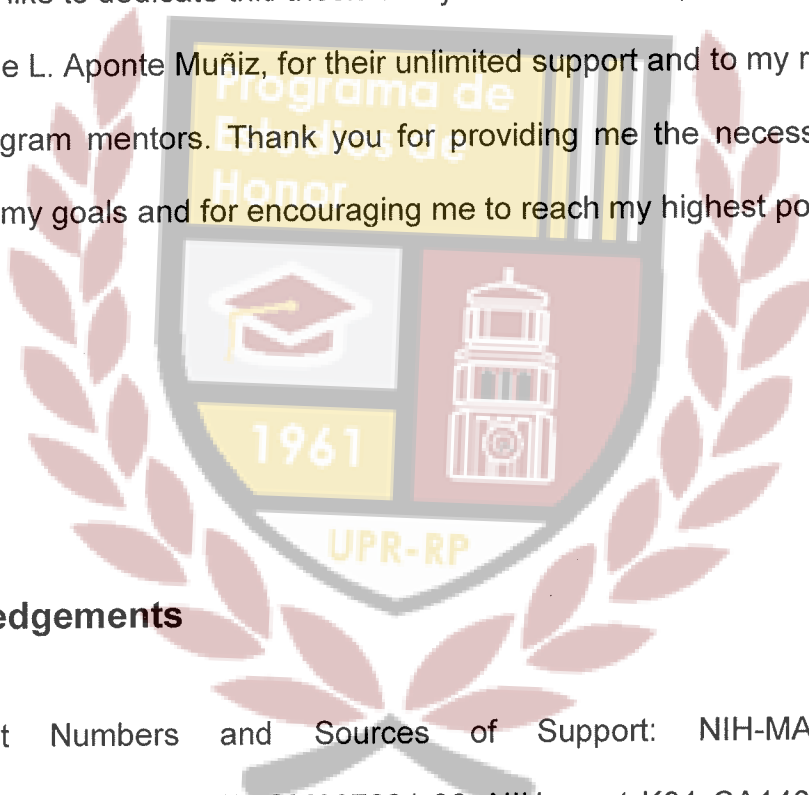
Acknowledgements

List of figures and tables

Figure 1:
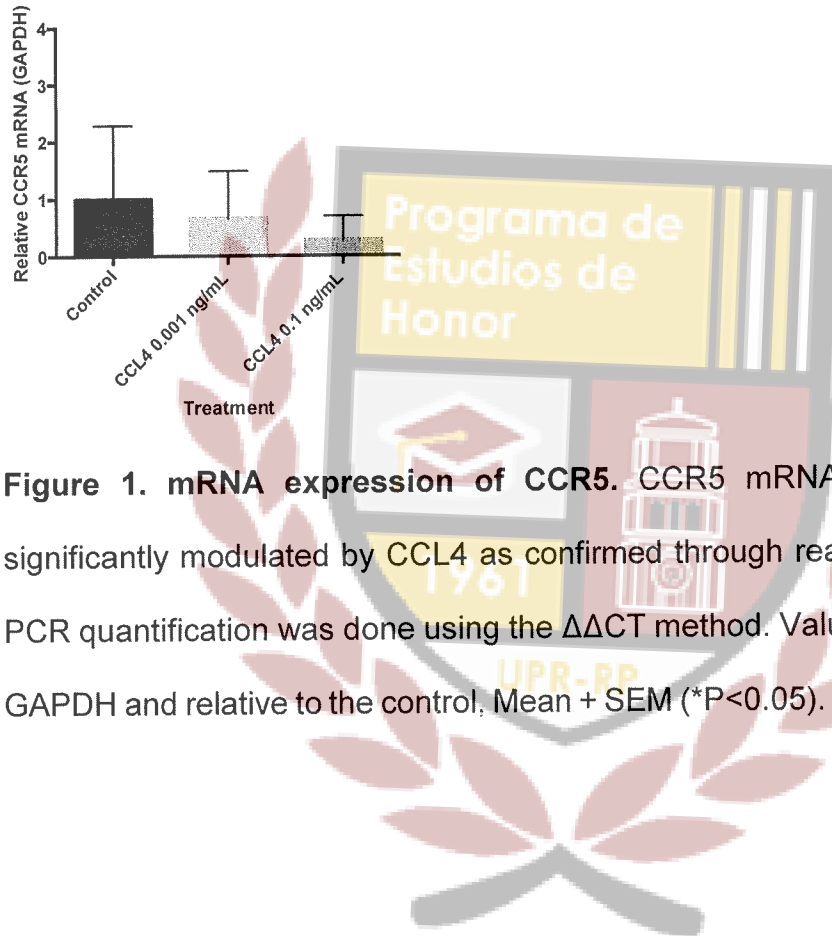
Figure 1. mRNA expression of CCR5. CCR5 mRNA expression was not significantly modulated by CCL4 as confirmed through real time PCR. Real time PCR quantification was done using the $\Delta\Delta CT$ method. Values were normalized to GAPDH and relative to the control. Mean + SEM (*P<0.05). n = 5 tumors per group.

Figure 2:
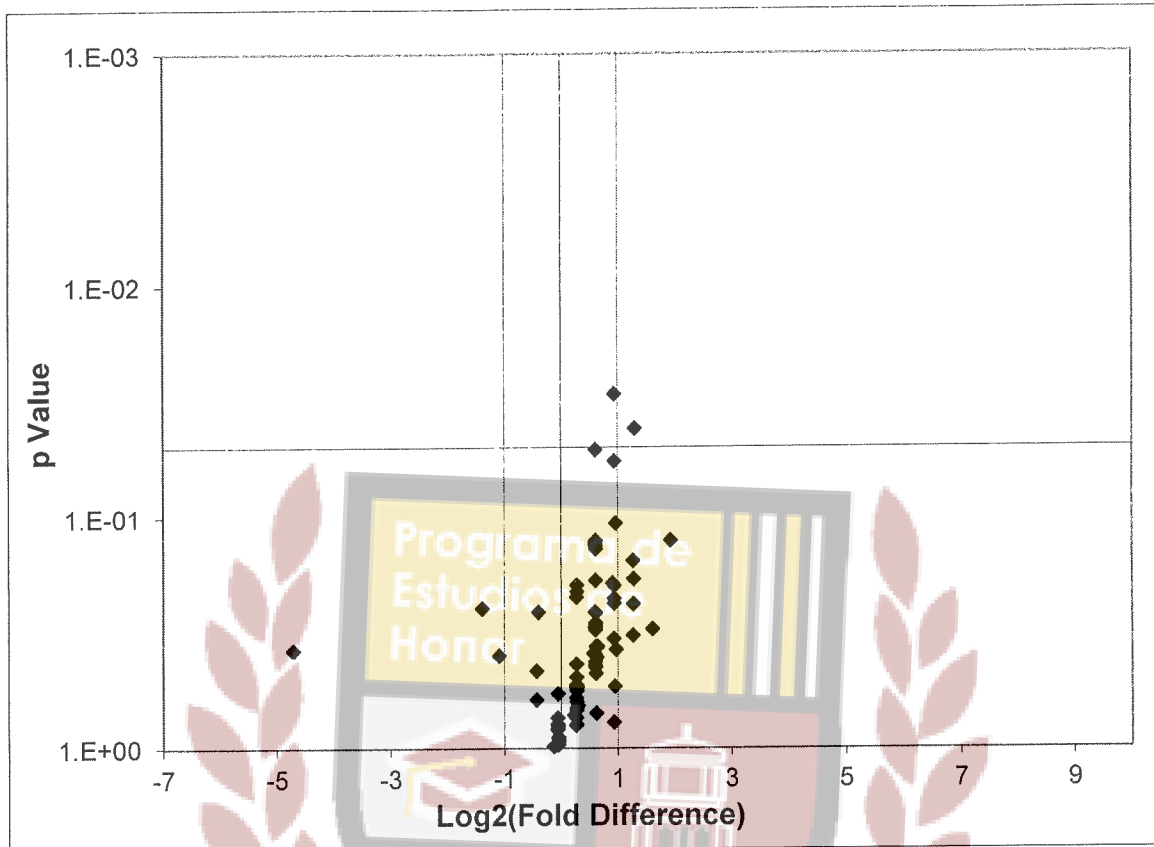
Figure 2. Volcano Plot for CCL4 Tumor Metastasis Array. Volcano plot was obtained from the MS Excel based tool provided by Qiagen (see methods). The black line indicates a fold-change in gene expression of 1. The pink lines indicate the desired fold-change in gene expression threshold, 2. The blue line indicates the desired threshold for the p value of the t-test, 0.05.

Table 1: Results for CCL4 Tumor Metastasis Array.

Symbol	Well	AVG ΔC_t		$2^{-\Delta Ct}$		Fold Change	T-TEST	Fold Up- or Down-Regulation
		Test Sample	Control Sample	Test Sample	Control Sample	Test Sample /Control Sample	p value	Test Sample /Control Sample
APC	A01	8.00	8.59	3.9E-03	2.6E-03	1.51	0.291088	1.51
BRMS1	A02	4.66	5.95	4.0E-02	1.6E-02	2.46	0.041330	2.46
CCL7	A03	12.73	13.64	1.5E-04	7.9E-05	1.87	0.191881	1.87
CD44	A04	5.67	5.93	2.0E-02	1.6E-02	1.20	0.735885	1.20
CD82	A05	9.66	9.60	1.2E-03	1.3E-03	0.96	0.964269	-1.04
CDH1	A06	2.65	2.92	1.6E-01	1.3E-01	1.21	0.549661	1.21
CDH11	A07	13.08	13.70	1.2E-04	7.5E-05	1.54	0.364782	1.54
CDH6	A08	9.66	9.26	1.2E-03	1.6E-03	0.76	0.255332	-1.32
CDKN2A	A09	3.99	4.25	6.3E-02	5.3E-02	1.20	0.681624	1.20
CHD4	A10	3.67	4.27	7.9E-02	5.2E-02	1.51	0.300095	1.51
COL4A2	A11	7.34	8.27	6.2E-03	3.2E-03	1.91	0.234456	1.91
CST7	A12	11.65	12.24	3.1E-04	2.1E-04	1.51	0.297455	1.51
CTBP1	B01	5.00	5.26	3.1E-02	2.6E-02	1.20	0.219439	1.20
CTNNA1	B02	2.34	2.61	2.0E-01	1.6E-01	1.20	0.429419	1.20
CTSK	B03	8.66	9.60	2.5E-03	1.3E-03	1.92	0.057142	1.92
CTSL	B04	3.33	3.92	1.0E-01	6.6E-02	1.51	0.255413	1.51
CXCL12	B05	13.07	13.33	1.2E-04	9.7E-05	1.19	0.534606	1.19
CXCR2	B06	9.66	10.58	1.2E-03	6.5E-04	1.90	0.768629	1.90
CXCR4	B07	9.00	8.93	2.0E-03	2.1E-03	0.95	0.734223	-1.05
DENR	B08	2.33	3.26	2.0E-01	1.0E-01	1.90	0.333436	1.90
EPHB2	B09	13.07	12.93	1.2E-04	1.3E-04	0.91	0.978445	-1.10
ETV4	B10	12.70	13.67	1.5E-04	7.7E-05	1.95	0.371447	1.95
EWSR1	B11	3.34	3.94	9.9E-02	6.5E-02	1.52	0.257883	1.52

FAT1	B12	5.32	5.26	2.5E-02	2.6E-02	0.96	0.823806	-1.05
FGFR4	C01	12.69	12.64	1.5E-04	1.6E-04	0.97	0.932430	-1.03
FLT4	C02	12.36	12.96	1.9E-04	1.3E-04	1.51	0.435172	1.51
FN1	C03	7.99	6.60	3.9E-03	1.0E-02	0.38	0.245304	-2.64
FXYD5	C04	13.10	13.32	1.1E-04	9.7E-05	1.17	0.713593	1.17
GNRH1	C05	6.98	7.92	7.9E-03	4.1E-03	1.91	**0.029332**	1.91
HGF	C06	11.33	11.27	3.9E-04	4.1E-04	0.96	0.576498	-1.04
HPSE	C07	6.98	7.59	7.9E-03	5.2E-03	1.52	0.360548	1.52
HRAS	C08	4.66	4.93	3.9E-02	3.3E-02	1.20	0.552159	1.20
HTATIP2	C09	6.66	6.94	9.9E-03	8.1E-03	1.21	0.537774	1.21
IGF1	C10	9.34	9.27	1.5E-03	1.6E-03	0.95	0.829931	-1.05
IL18	C11	9.98	10.60	9.9E-04	6.5E-04	1.53	0.699941	1.53
IL1B	C12	10.33	11.26	7.8E-04	4.1E-04	1.92	0.537088	1.92
ITGA7	D01	9.67	10.94	1.2E-03	5.1E-04	2.41	0.183606	2.41
ITGB3	D02	11.32	12.25	3.9E-04	2.0E-04	1.91	0.223276	1.91
KISS1	D03	10.67	11.27	6.1E-04	4.0E-04	1.51	0.390471	1.51
KISS1R	D04	8.67	8.61	2.5E-03	2.6E-03	0.96	0.891778	-1.04
KRAS	D05	3.32	3.92	1.0E-01	6.6E-02	1.52	0.186130	1.52
MCAM	D06	8.68	9.94	2.4E-03	1.0E-03	2.40	0.153432	2.40
MDM2	D07	2.66	3.26	1.6E-01	1.0E-01	1.52	0.131791	1.52
MET	D08	8.66	8.92	2.5E-03	2.1E-03	1.20	0.783079	1.20
METAP2	D09	3.00	3.26	1.3E-01	1.0E-01	1.20	0.489057	1.20
MGAT5	D10	5.98	6.91	1.6E-02	8.3E-03	1.91	0.196590	1.91
MMP10	D11	10.32	12.25	7.8E-04	2.1E-04	**3.80**	0.125493	**3.80**
MMP11	D12	9.66	10.26	1.2E-03	8.1E-04	1.52	0.442222	1.52
MMP13	E01	12.36	3.84	1.9E-04	7.0E-02	**0.00**	0.373901	**-366.44**
MMP2	E02	12.01	12.64	2.4E-04	1.6E-04	1.54	0.401589	1.54
MMP3	E03	13.06	13.70	1.2E-04	7.5E-05	1.55	0.359904	1.55

MMP7	E04	13.10	13.66	1.1E-04	7.7E-05	1.48	0.386587	1.48
MMP9	E05	11.00	10.94	4.9E-04	5.1E-04	0.96	0.799793	-1.04
MTA1	E06	3.99	4.27	6.3E-02	5.2E-02	1.21	0.207866	1.21
MTSS1	E07	8.66	8.59	2.5E-03	2.6E-03	0.96	0.783475	-1.05
MYC	E08	2.68	2.94	1.6E-01	1.3E-01	1.20	0.601058	1.20
MYCL	E09	13.04	13.31	1.2E-04	9.9E-05	1.20	0.528614	1.20
NF2	E10	4.67	5.26	3.9E-02	2.6E-02	1.51	0.128163	1.51
NME1	E11	0.99	0.93	5.0E-01	5.3E-01	0.96	0.962765	-1.04
NME4	E12	8.33	8.92	3.1E-03	2.1E-03	1.51	0.420360	1.51
NR4A3	F01	9.33	10.60	1.5E-03	6.4E-04	2.41	0.235802	2.41
PLAUR	F02	8.67	9.27	2.5E-03	1.6E-03	1.51	0.304695	1.51
PNN	F03	3.66	3.93	7.9E-02	6.6E-02	1.21	0.560891	1.21
PTEN	F04	3.98	4.59	6.3E-02	4.2E-02	1.52	0.284579	1.52
RB1	F05	4.67	4.61	3.9E-02	4.1E-02	0.96	0.902003	-1.04
RORB	F06	8.66	9.92	2.5E-03	1.0E-03	2.40	0.322317	2.40
RPSA	F07	-0.34	-0.40	1.3E+00	1.3E+00	0.96	0.906215	-1.04
SERPINE1	F08	7.33	7.94	6.2E-03	4.1E-03	1.53	0.471747	1.53
SET	F09	0.66	1.27	6.3E-01	4.2E-01	1.52	0.125506	1.52
SMAD2	F10	4.66	4.93	3.9E-02	3.3E-02	1.20	0.552142	1.20
SMAD4	F11	4.32	4.59	5.0E-02	4.2E-02	1.20	0.665157	1.20
SRC	F12	7.00	7.25	7.8E-03	6.6E-03	1.19	0.793480	1.19
SSTR2	G01	12.33	12.60	1.9E-04	1.6E-04	1.21	0.624632	1.21
SYK	G02	5.65	6.25	2.0E-02	1.3E-02	1.52	0.136300	1.52
TCF20	G03	5.66	5.93	2.0E-02	1.6E-02	1.21	0.542601	1.21
TGFB1	G04	7.00	7.61	7.8E-03	5.1E-03	1.52	0.050877	1.52
TIMP2	G05	13.00	13.29	1.2E-04	1.0E-04	1.22	0.650276	1.22
TIMP3	G06	12.36	11.93	1.9E-04	2.6E-04	0.74	0.459617	-1.35
TIMP4	G07	12.37	13.33	1.9E-04	9.7E-05	1.95	0.105717	1.95

TNFSF10	G08	13.07	11.97	1.2E-04	2.5E-04	0.47	0.394771	-2.14
TP53	G09	5.99	6.27	1.6E-02	1.3E-02	1.21	0.195546	1.21
TRPM1	G10	13.07	8.35	1.2E-04	3.1E-03	0.04	0.373917	-26.23
TSHR	G11	13.10	12.66	1.1E-04	1.5E-04	0.74	0.613731	-1.35
VEGFA	G12	0.66	2.26	6.3E-01	2.1E-01	3.04	0.302795	3.04
ACTB	H01	-0.68	-0.75	1.6E+00	1.7E+00	0.95	0.936460	-1.05
B2M	H02	1.33	0.94	4.0E-01	5.2E-01	0.76	0.351571	-1.31
GAPDH	H03	-1.32	-1.06	2.5E+00	2.1E+00	1.20	0.576026	1.20
HPRT1	H04	3.67	4.27	7.9E-02	5.2E-02	1.52	0.122269	1.52
RPLP0	H05	-3.00	-3.40	8.0E+00	1.1E+01	0.76	0.609087	-1.32
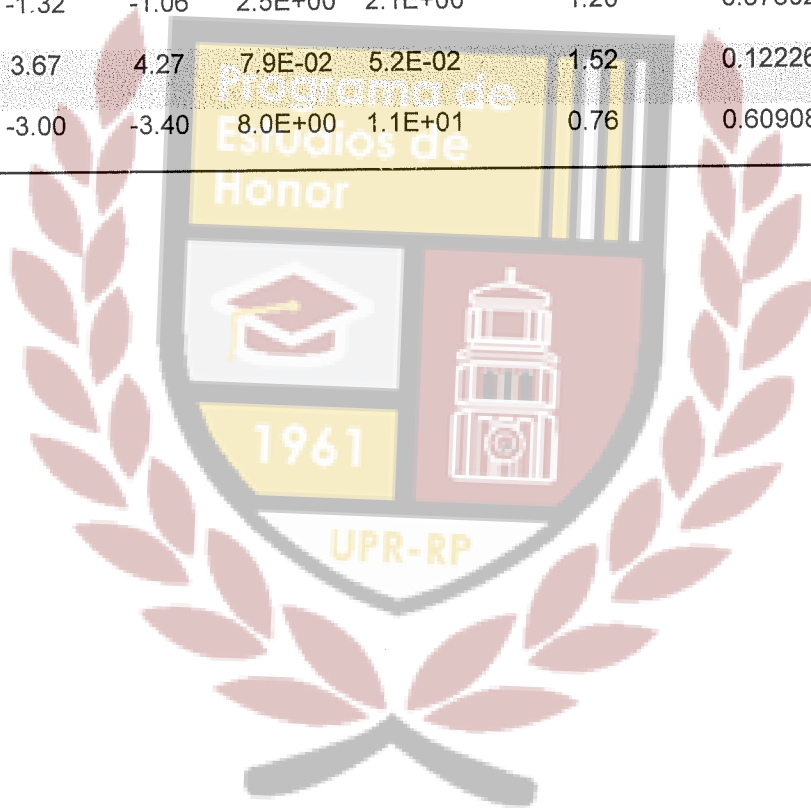
Figure 3:
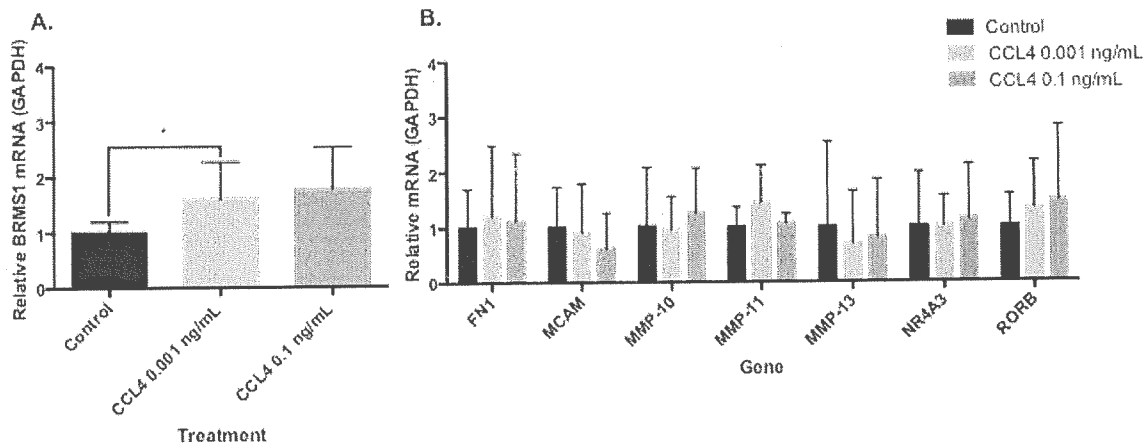
Figure 3. mRNA expression of differentially expressed genes in the Tumor Metastasis Array. A. Quantitative real time PCR revealed BRMS mRNA expression to be induced by CCL4 at a concentration of 0.001 ng/mL. B. mRNA expression of genes that were differentially expressed in the Tumor Metastasis Array but not significantly modulated by CCL4 when confirmed through quantitative real time PCR. Real time PCR quantification was done using the $\Delta\Delta CT$ method. Values were normalized to GAPDH and relative to the control, Mean + SEM (*$P<0.05$). n = 5 tumors per group.

Figure 4:
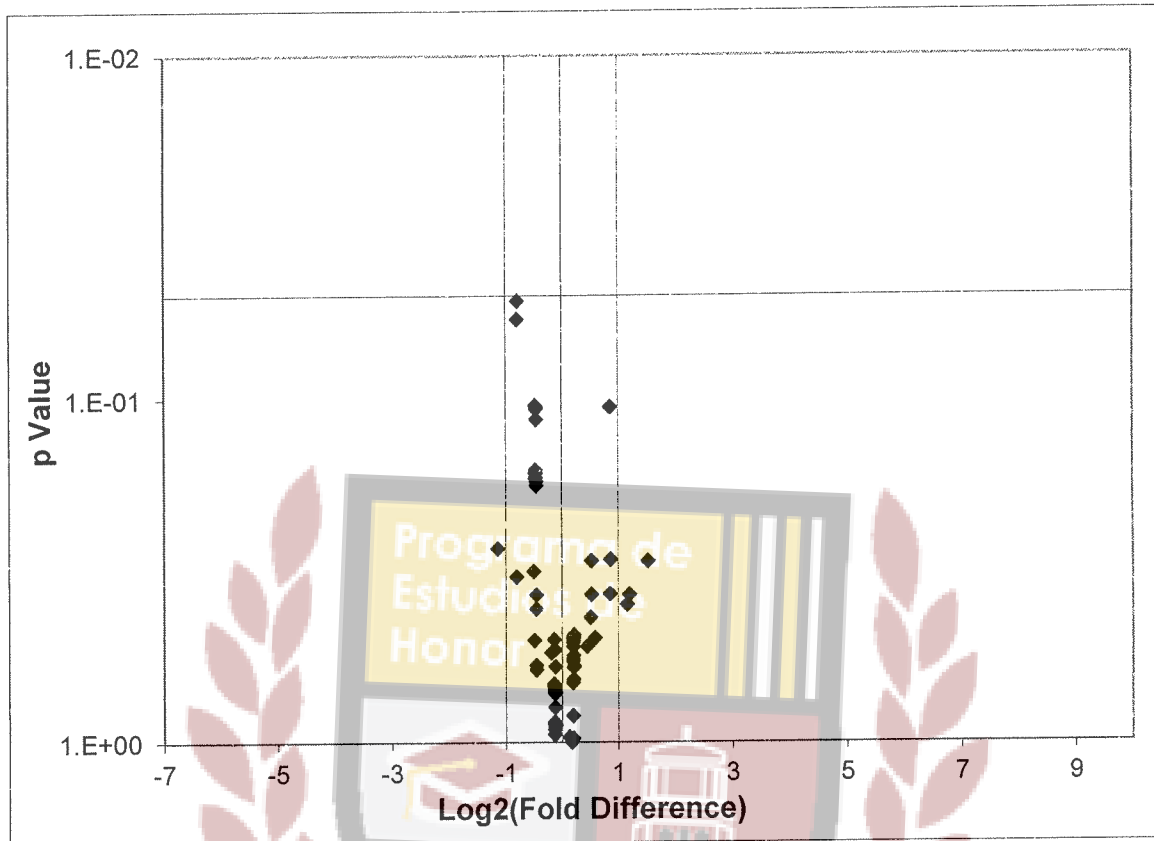
Figure 4. Volcano Plot for the CCL4 PI3-Kinase Array. Volcano plot was obtained from the MS Excel based tool provided by Qiagen (see methods). The black line indicates a fold-change in gene expression of 1. The pink lines indicate the desired fold-change in gene expression threshold, 2. The blue line indicates the desired threshold for the p value of the t-test, 0.05.

Table 2: Results for CCL4 PI3-Kinase Array.

Symbol	Well	AVG ΔC$_t$		2$^{-\Delta Ct}$		Fold Change	T-TEST	Fold Up- or Down-Regulation
		Test Sample	Control Sample	Test Sample	Control Sample	Test Sample /Control Sample	p value	Test Sample /Control Sample
ADAR	A01	4.93	4.45	3.3E-02	4.6E-02	0.72	0.163199	-1.39
AKT1	A02	4.28	4.47	5.1E-02	4.5E-02	1.14	0.579872	1.14
AKT2	A03	4.29	4.16	5.1E-02	5.6E-02	0.91	0.884093	-1.09
AKT3	A04	11.63	11.50	3.2E-04	3.5E-04	0.91	0.917128	-1.10
APC	A05	7.59	7.79	5.2E-03	4.5E-03	1.15	0.656845	1.15
BAD	A06	5.95	5.82	1.6E-02	1.8E-02	0.91	0.689415	-1.10
BTK	A07	12.70	12.87	1.5E-04	1.3E-04	1.12	0.999200	1.12
CASP9	A08	6.27	6.14	1.3E-02	1.4E-02	0.92	0.886866	-1.09
CCND1	A09	-0.10	-0.56	1.1E+00	1.5E+00	0.73	0.177976	-1.37
CD14	A10	12.67	12.47	1.5E-04	1.8E-04	0.87	0.546762	-1.14
CDC42	A11	1.92	2.12	2.6E-01	2.3E-01	1.15	0.486432	1.15
CDKN1B	A12	3.96	4.47	6.4E-02	4.5E-02	1.42	0.431275	1.42
CHUK	B01	5.95	5.81	1.6E-02	1.8E-02	0.91	0.684101	-1.10
CSNK2A1	B02	3.58	3.12	8.4E-02	1.2E-01	0.73	0.614167	-1.38
CTNNB1	B03	3.27	3.48	1.0E-01	9.0E-02	1.15	0.558067	1.15
EIF2AK2	B04	3.92	4.12	6.6E-02	5.7E-02	1.15	0.505462	1.15
EIF4B	B05	2.61	1.81	1.6E-01	2.9E-01	0.57	0.058414	-1.74
EIF4E	B06	5.90	6.11	1.7E-02	1.4E-02	1.16	0.486818	1.16
EIF4EBP1	B07	5.60	5.47	2.1E-02	2.3E-02	0.91	0.536770	-1.09
EIF4G1	B08	4.27	4.47	5.2E-02	4.5E-02	1.15	0.654422	1.15
ELK1	B09	8.93	8.45	2.1E-03	2.9E-03	0.72	0.169619	-1.39
FASLG	B10	12.70	12.90	1.5E-04	1.3E-04	1.15	0.972489	1.15

FKBP1A	B11	4.61	4.14	4.1E-02	5.7E-02	0.72	0.106547	-1.38
FOS	B12	4.96	6.14	3.2E-02	1.4E-02	2.28	0.370037	2.28
FOXO1	C01	8.94	8.47	2.0E-03	2.8E-03	0.72	0.163982	-1.39
FOXO3	C02	6.26	5.45	1.3E-02	2.3E-02	0.57	0.328290	-1.75
GJA1	C03	4.27	4.80	5.2E-02	3.6E-02	1.44	0.294826	1.44
GRB10	C04	8.26	8.46	3.3E-03	2.8E-03	1.15	0.525474	1.15
GRB2	C05	5.61	5.48	2.0E-02	2.2E-02	0.91	0.949602	-1.10
GSK3B	C06	3.92	3.80	6.6E-02	7.2E-02	0.92	0.715321	-1.09
HRAS	C07	4.94	4.80	3.2E-02	3.6E-02	0.90	0.676193	-1.11
HSPB1	C08	3.62	3.82	8.1E-02	7.1E-02	1.15	0.835228	1.15
IGF1	C09	8.94	8.81	2.0E-03	2.2E-03	0.91	0.691166	-1.10
IGF1R	C10	6.61	5.47	1.0E-02	2.3E-02	0.45	0.270977	-2.22
ILK	C11	4.93	4.46	3.3E-02	4.6E-02	0.72	0.168809	-1.39
IRAK1	C12	6.01	6.46	1.6E-02	1.1E-02	1.37	0.523888	1.37
IRS1	D01	8.26	7.80	3.3E-03	4.5E-03	0.73	0.407447	-1.38
ITGB1	D02	2.59	2.78	1.7E-01	1.5E-01	1.14	0.670853	1.14
JUN	D03	6.60	6.80	1.0E-02	9.0E-03	1.15	0.523948	1.15
MAP2K1	D04	4.98	4.47	3.2E-02	4.5E-02	0.71	0.316308	-1.42
MAPK1	D05	3.92	4.13	6.6E-02	5.7E-02	1.15	0.493130	1.15
MAPK14	D06	3.90	4.10	6.7E-02	5.8E-02	1.15	0.500906	1.15
MAPK3	D07	6.62	6.14	1.0E-02	1.4E-02	0.72	0.104011	-1.39
MAPK8	D08	3.92	4.11	6.6E-02	5.8E-02	1.14	0.511212	1.14
MTCP1	D09	9.58	9.12	1.3E-03	1.8E-03	0.73	0.595815	-1.38
MTOR	D10	5.92	5.78	1.7E-02	1.8E-02	0.91	0.689257	-1.10
MYD88	D11	5.26	5.13	2.6E-02	2.9E-02	0.91	0.896552	-1.09
NFKB1	D12	6.29	7.14	1.3E-02	7.1E-03	1.81	0.368330	1.81
NFKBIA	E01	6.60	6.46	1.0E-02	1.1E-02	0.91	0.501503	-1.10
PABPC1	E02	0.93	1.14	5.2E-01	4.5E-01	1.15	0.485146	1.15

PAK1	E03	6.93	6.47	8.2E-03	1.1E-02	0.73	0.172760	-1.38
PDGFRA	E04	12.31	12.90	2.0E-04	1.3E-04	1.50	0.496319	1.50
PDK1	E05	5.59	5.13	2.1E-02	2.9E-02	0.73	0.105758	-1.38
PDK2	E06	8.26	8.13	3.3E-03	3.6E-03	0.91	0.789998	-1.09
PDPK1	E07	5.58	5.79	2.1E-02	1.8E-02	1.16	0.598604	1.16
PIK3CA	E08	4.91	5.12	3.3E-02	2.9E-02	1.15	0.493618	1.15
PIK3CG	E09	12.70	12.90	1.5E-04	1.3E-04	1.15	0.972489	1.15
PIK3R1	E10	5.91	5.79	1.7E-02	1.8E-02	0.92	0.720620	-1.09
PIK3R2	E11	5.94	5.81	1.6E-02	1.8E-02	0.92	0.716140	-1.09
PRKCA	E12	6.33	7.48	1.2E-02	5.6E-03	2.22	0.394765	2.22
PRKCB	F01	10.59	10.46	6.5E-04	7.1E-04	0.92	0.600615	-1.09
PRKCZ	F02	6.96	6.82	8.0E-03	8.8E-03	0.91	0.686057	-1.10
PTEN	F03	3.58	4.44	8.4E-02	4.6E-02	1.81	0.291897	1.81
PTK2	F04	6.27	6.13	1.3E-02	1.4E-02	0.90	0.683190	-1.11
PTPN11	F05	3.94	3.15	6.5E-02	1.1E-01	0.58	0.051586	-1.73
RAC1	F06	1.59	1.46	3.3E-01	3.6E-01	0.91	0.947276	-1.10
RAF1	F07	4.58	4.78	4.2E-02	3.6E-02	1.15	0.604502	1.15
RASA1	F08	4.59	4.46	4.2E-02	4.6E-02	0.91	0.948631	-1.10
RBL2	F09	3.94	4.14	6.5E-02	5.7E-02	1.15	0.497087	1.15
RHEB	F10	5.27	5.15	2.6E-02	2.8E-02	0.92	0.889610	-1.09
RHOA	F11	1.25	1.13	4.2E-01	4.6E-01	0.92	0.890620	-1.09
RPS6KA1	F12	5.31	6.82	2.5E-02	8.9E-03	2.85	0.295200	2.85
RPS6KB1	G01	4.27	4.13	5.2E-02	5.7E-02	0.91	0.873174	-1.10
SHC1	G02	5.93	5.80	1.6E-02	1.8E-02	0.91	0.697522	-1.10
SOS1	G03	4.92	4.45	3.3E-02	4.6E-02	0.72	0.159985	-1.39
SRF	G04	6.62	6.16	1.0E-02	1.4E-02	0.73	0.114167	-1.38
TCL1A	G05	12.29	11.80	2.0E-04	2.8E-04	0.71	0.503505	-1.41
TIRAP	G06	6.94	6.47	8.2E-03	1.1E-02	0.72	0.168110	-1.38

|							
TLR4	G07	12.70	12.83	1.5E-04	1.4E-04	1.09	0.964013	1.09
TOLLIP	G08	7.95	7.82	4.0E-03	4.4E-03	0.91	0.707016	-1.10
TSC1	G09	6.26	5.80	1.3E-02	1.8E-02	0.73	0.370286	-1.37
TSC2	G10	7.28	7.48	6.4E-03	5.6E-03	1.14	0.572205	1.14
WASL	G11	5.95	6.81	1.6E-02	8.9E-03	1.81	0.105258	1.81
YWHAH	G12	2.61	3.14	1.6E-01	1.1E-01	1.44	0.369894	1.44
ACTB	H01	-0.08	-0.55	1.1E+00	1.5E+00	0.72	0.169043	-1.38
B2M	H02	0.93	1.14	5.3E-01	4.6E-01	1.16	0.485448	1.16
GAPDH	H03	-1.05	-1.19	2.1E+00	2.3E+00	0.91	0.823901	-1.10
HPRT1	H04	3.61	4.14	8.2E-02	5.7E-02	1.44	0.059274	1.44
RPLP0	H05	-3.40	-3.54	1.1E+01	1.2E+01	0.91	0.512340	-1.10
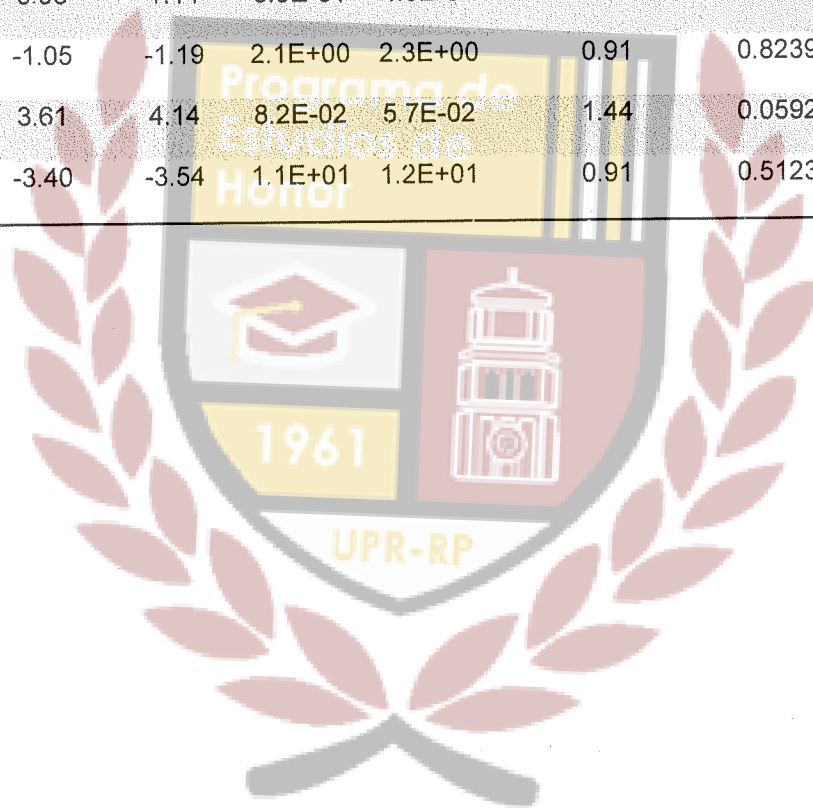
Figure 5:
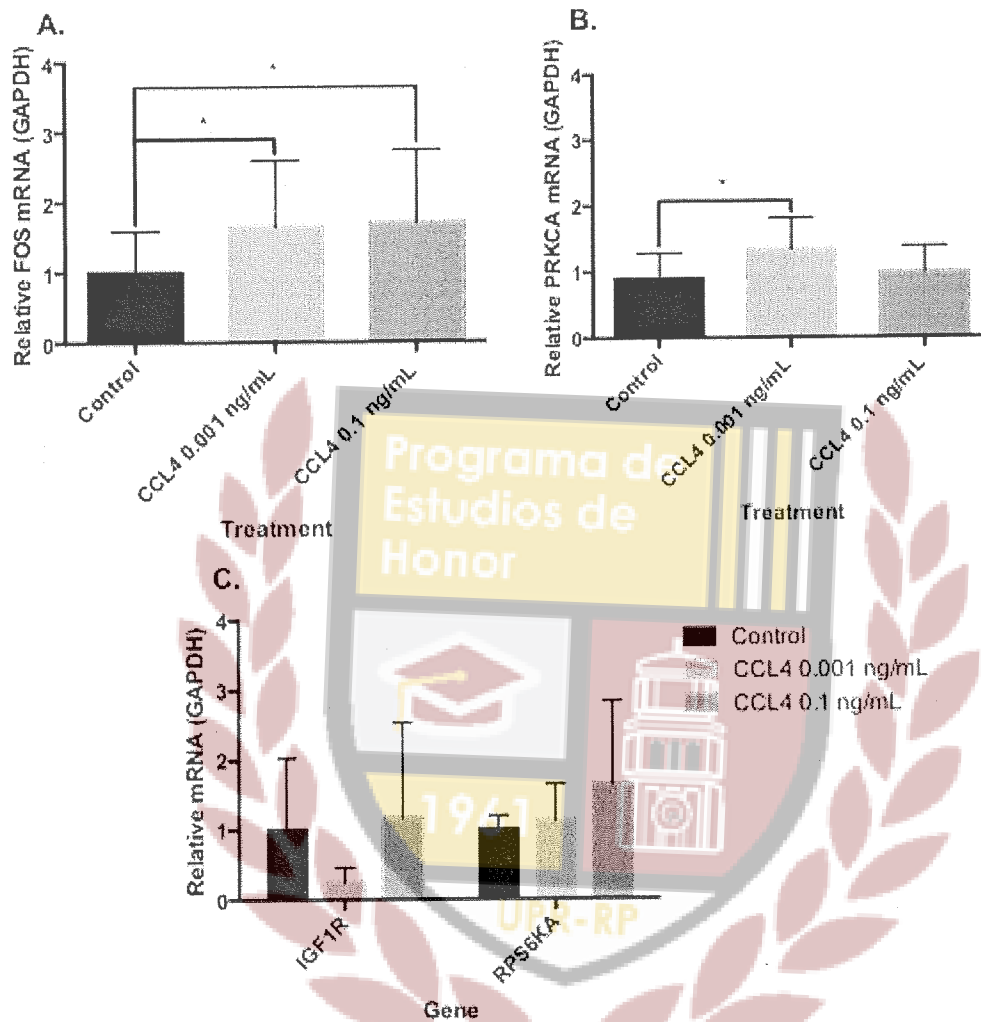
Figure 5. mRNA expression of differentially expressed genes in the PI3-Kinase Array. A. Quantitative real time PCR revealed FOS mRNA expression to be induced by CCL4 at concentrations of 0.001 and 0.1 ng/mL. B. Quantitative real time PCR revealed PRKCA mRNA expression to be induced by CCL4 at a concentration of 0.001 ng/mL. C. mRNA expression of genes that were differentially expressed in the PI3-Kinase Array but not significantly modulated by CCL4 when confirmed through quantitative real time PCR. Real time PCR

quantification was done using the ΔΔCT method. Values were normalized to GAPDH and relative to the control, Mean + SEM (*P<0.05). n = 5 tumors per group.

Figure 6:
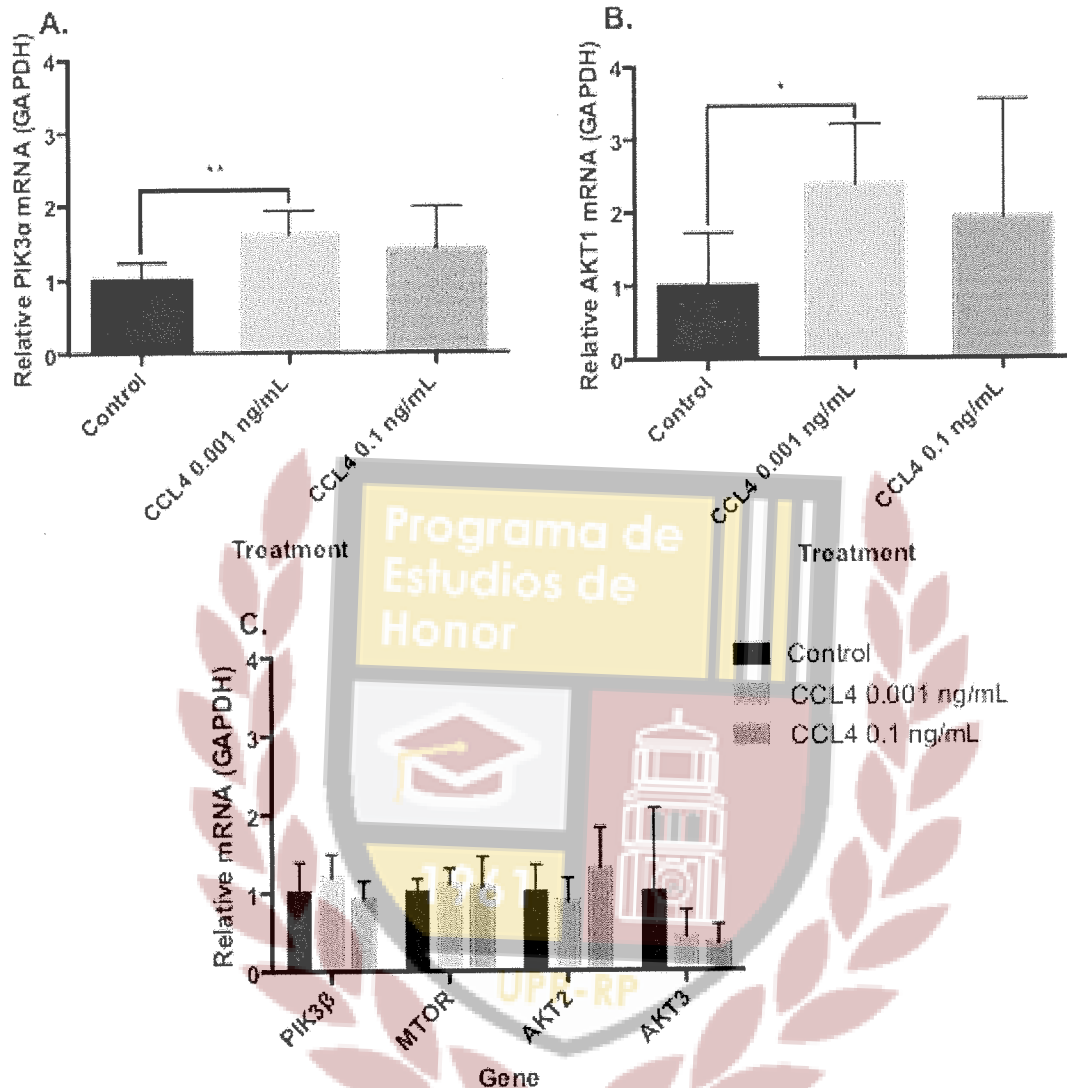
Figure 6. mRNA expression of genes upstream in the PI3-Kinase signaling pathway. A. Quantitative real time PCR revealed PI3K alpha mRNA expression to be induced by CCL4 at a concentration of 0.001 ng/mL. B. Quantitative real time PCR revealed AKT1 mRNA expression to be induced by CCL4 at a concentration of 0.001 ng/mL. C. Several genes upstream in the PI3-Kinase signaling pathway whose mRNA expression was not significantly modulated by CCL4 as confirmed through real time PCR. Real time PCR quantification was done using the $\Delta\Delta CT$

method. Values were normalized to GAPDH and relative to the control, Mean +
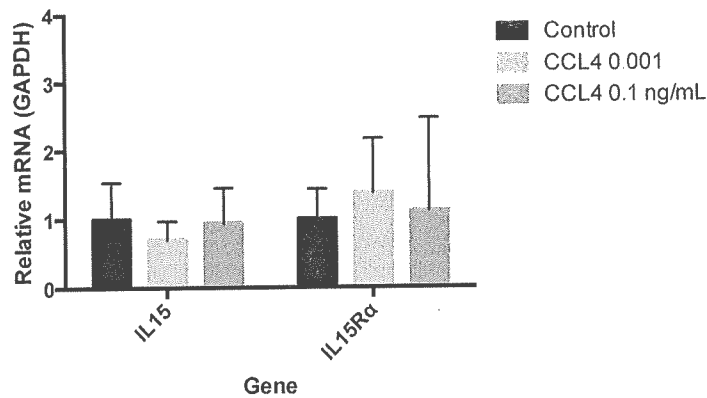
SEM (*P<0.05). n = 5 tumors per group.

Figure 7:

Figure 7. mRNA expression of IL-15 and its receptor, IL-15R alpha. IL-15 nor IL-15R-alpha mRNA expression was significantly modulated by CCL4 as confirmed through real time PCR. Real time PCR quantification was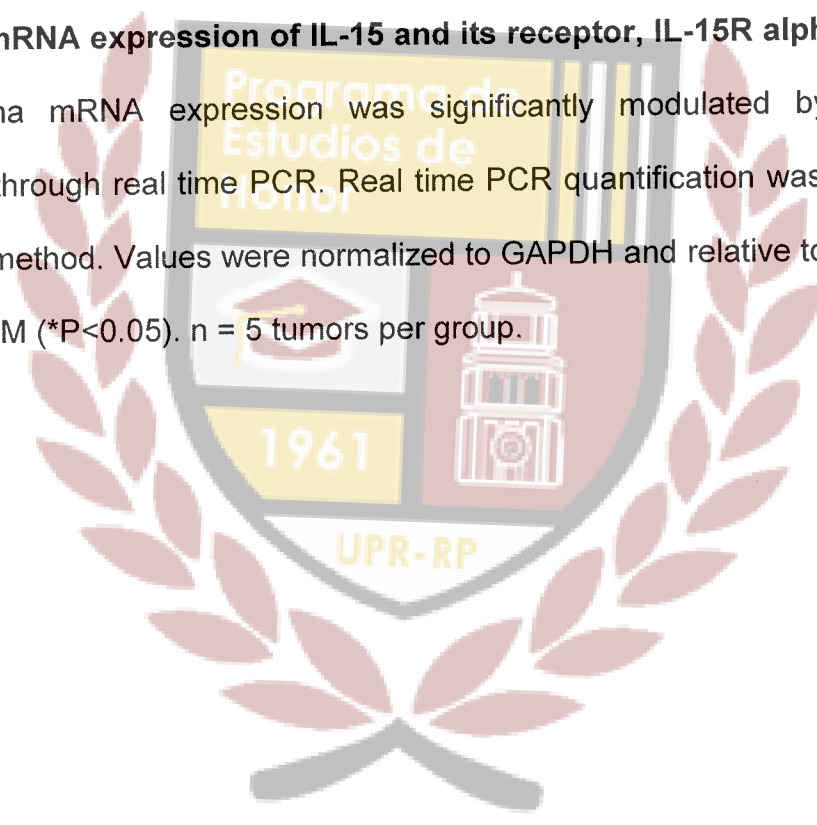 done using the $\Delta\Delta$CT method. Values were normalized to GAPDH and relative to the control, Mean + SEM (*P<0.05). n = 5 tumors per group.

Table 3. Differentially expressed genes in prostate cancer tumors treated with CCL4 0.001 ng/mL

Gene Bank Accession Number	Gene Symbol	Description	Fold Change	P Value
NM_005252	FOS	FBJ murine osteosarcoma viral oncogene homolog.	1.608	0.027
NM_006218	PI3KA	Phosphatidylinositol-4,5-bisphosphate 3-kinase, alpha	1.614	0.009
NM_001014431.1	AKT1	V-akt murine thymoma viral oncogene homolog 1	2.382	0.045
NM_002737	PRKCA	Protein kinase C, alpha	1.342	0.013

Table 4. Differentially expressed genes in prostate cancer tumors treated with CCL4 0.1 ng/mL

Gene Bank Accession Number	Gene Symbol	Description	Fold Change	P Value
NM_015399	BRMS1	Breast cancer metastasis suppressor 1	1.775	0.038
NM_005252	FOS	FBJ murine osteosarcoma viral oncogene homolog.	1.705	0.016

Figure 8:

CCL4 Signaling in Prostate Cancer
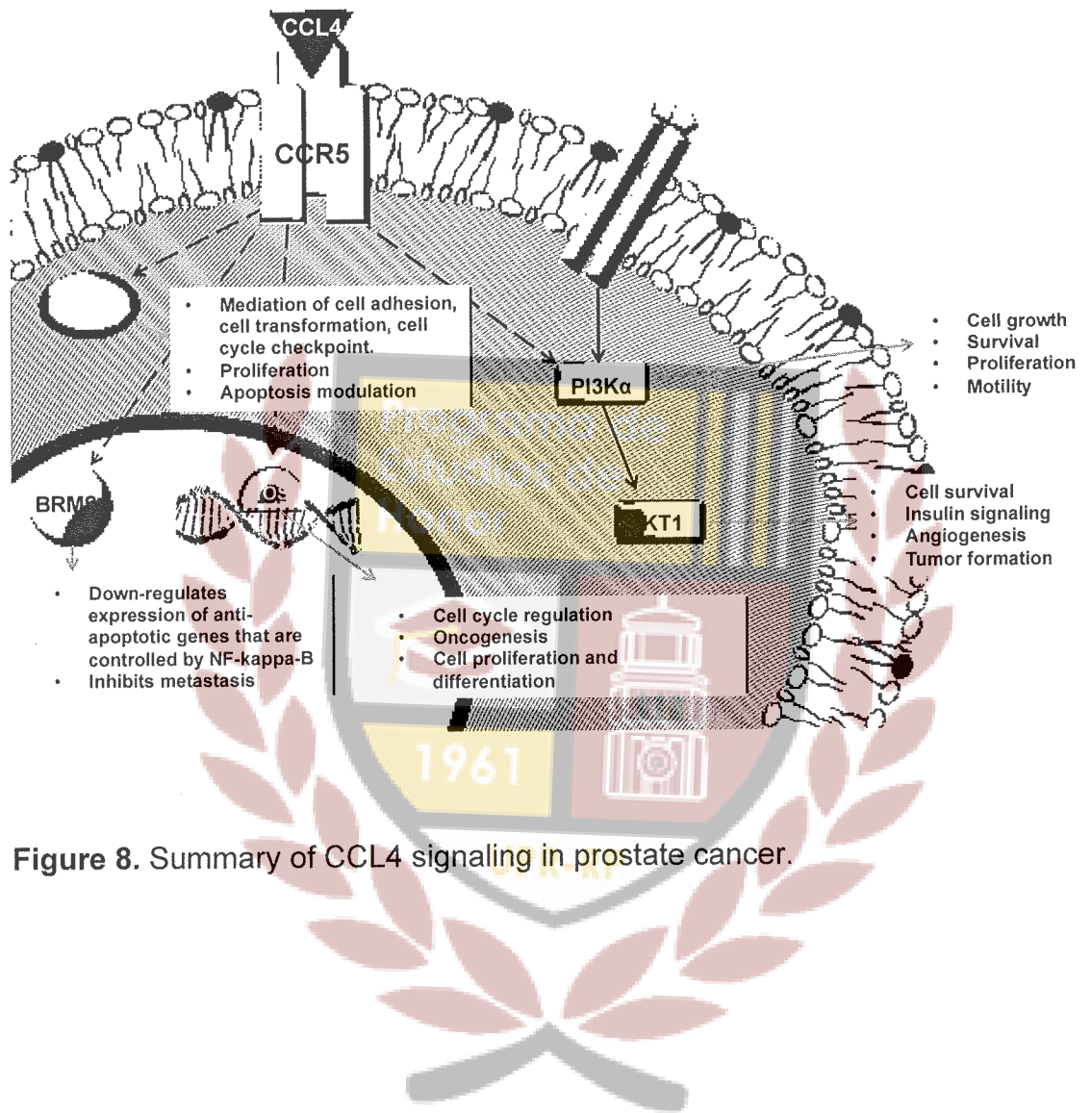
Figure 8. Summary of CCL4 signaling in prostate cancer.

Figure 9:
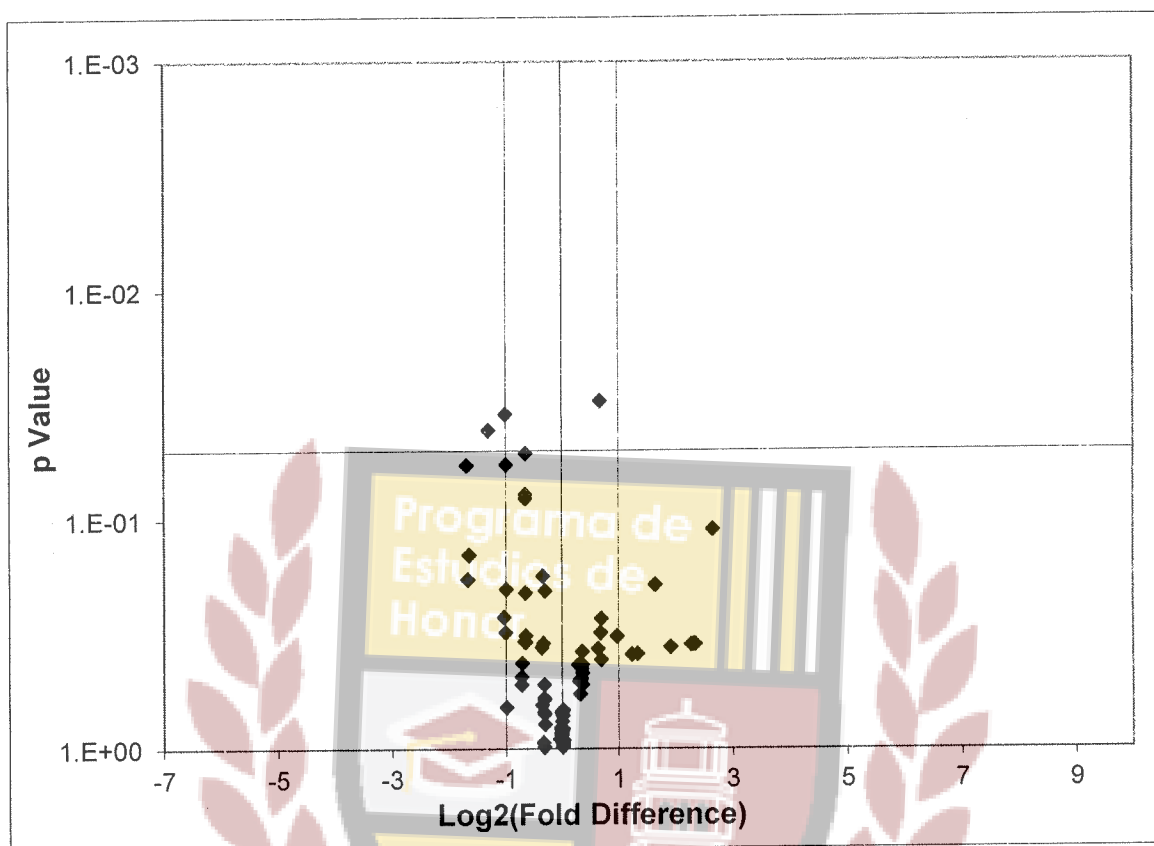
Figure 9. Volcano Plot for the IL-15 PI3-Kinase Array. Volcano plot was obtained from the MS Excel based tool provided by Qiagen (see methods). The black line indicates a fold-change in gene expression of 1. The pink lines indicate the desired fold-change in gene expression threshold, 2. The blue line indicates the desired threshold for the p value of the t-test, 0.05.

Table 5: Results for IL-15 PI3-Kinase Array.

Symbol	Well	AVG ΔC_t		$2^{-\Delta Ct}$		Fold Change	T-TEST	Fold Up- or Down-Regulation
		Test Sample	Control Sample	Test Sample	Control Sample	Test Sample /Control Sample	p value	Test Sample /Control Sample
ADAR	A01	4.80	4.45	3.6E-02	4.6E-02	0.79	0.175860	-1.27
AKT1	A02	4.12	4.47	5.7E-02	4.5E-02	1.28	0.374859	1.28
AKT2	A03	3.80	4.16	7.2E-02	5.6E-02	1.28	0.464112	1.28
AKT3	A04	10.17	11.50	8.7E-04	3.5E-04	2.51	0.383513	2.51
APC	A05	7.47	7.79	5.7E-03	4.5E-03	1.25	0.513373	1.25
BAD	A06	6.13	5.82	1.4E-02	1.8E-02	0.80	0.605734	-1.24
BTK	A07	10.56	12.87	6.6E-04	1.3E-04	4.95	0.348374	4.95
CASP9	A08	5.46	6.14	2.3E-02	1.4E-02	1.61	0.269091	1.61
CCND1	A09	1.13	-0.56	4.6E-01	1.5E+00	0.31	0.057683	-3.23
CD14	A10	10.56	12.47	6.6E-04	1.8E-04	3.75	0.358730	3.75
CDC42	A11	2.13	2.12	2.3E-01	2.3E-01	0.99	0.845658	-1.01
CDKN1B	A12	5.46	4.47	2.3E-02	4.5E-02	0.50	0.657531	-1.99
CHUK	B01	5.80	5.81	1.8E-02	1.8E-02	1.01	0.944513	1.01
CSNK2A1	B02	3.14	3.12	1.1E-01	1.2E-01	0.99	0.859365	-1.01
CTNNB1	B03	4.13	3.48	5.7E-02	9.0E-02	0.63	0.077259	-1.58
EIF2AK2	B04	4.14	4.12	5.7E-02	5.7E-02	0.99	0.691296	-1.01
EIF4B	B05	2.46	1.81	1.8E-01	2.9E-01	0.64	0.340620	-1.57
EIF4E	B06	5.80	6.11	1.8E-02	1.4E-02	1.24	0.498668	1.24
EIF4EBP1	B07	5.12	5.47	2.9E-02	2.3E-02	1.27	0.426465	1.27
EIF4G1	B08	4.47	4.47	4.5E-02	4.5E-02	1.01	0.979196	1.01
ELK1	B09	8.17	8.45	3.5E-03	2.9E-03	1.22	0.426879	1.22
FASLG	B10	10.56	12.90	6.6E-04	1.3E-04	5.06	0.347808	5.06
FKBP1A	B11	4.48	4.14	4.5E-02	5.7E-02	0.79	0.939298	-1.26

FOS	B12	6.80	6.14	9.0E-03	1.4E-02	0.64	0.318995	-1.57
FOXO1	C01	8.51	8.47	2.7E-03	2.8E-03	0.97	0.907634	-1.03
FOXO3	C02	6.46	5.45	1.1E-02	2.3E-02	0.50	0.308926	-2.02
GJA1	C03	4.78	4.80	3.6E-02	3.6E-02	1.01	0.956482	1.01
GRB10	C04	7.79	8.46	4.5E-03	2.8E-03	1.59	0.030207	1.59
GRB2	C05	5.12	5.48	2.9E-02	2.2E-02	1.28	0.524004	1.28
GSK3B	C06	3.79	3.80	7.2E-02	7.2E-02	1.01	0.954317	1.01
HRAS	C07	4.46	4.80	4.5E-02	3.6E-02	1.26	0.490703	1.26
HSPB1	C08	5.47	3.82	2.3E-02	7.1E-02	0.32	0.141700	-3.15
IGF1	C09	6.16	8.81	1.4E-02	2.2E-03	6.26	0.110223	6.26
IGF1R	C10	7.14	5.47	7.1E-03	2.3E-02	0.31	0.181115	-3.19
ILK	C11	5.46	4.46	2.3E-02	4.6E-02	0.50	0.057265	-2.00
IRAK1	C12	5.49	6.46	2.2E-02	1.1E-02	1.96	0.321376	1.96
IRS1	D01	8.84	7.80	2.2E-03	4.5E-03	0.49	0.265059	-2.06
ITGB1	D02	2.80	2.78	1.4E-01	1.5E-01	0.98	0.808430	-1.02
JUN	D03	7.17	6.80	7.0E-03	9.0E-03	0.78	0.359435	-1.29
MAP2K1	D04	5.47	4.47	2.3E-02	4.5E-02	0.50	0.200139	-2.00
MAPK1	D05	4.13	4.13	5.7E-02	5.7E-02	1.00	0.829693	-1.00
MAPK14	D06	4.82	4.10	3.5E-02	5.8E-02	0.61	0.522596	-1.65
MAPK3	D07	6.46	6.14	1.1E-02	1.4E-02	0.80	0.981963	-1.25
MAPK8	D08	4.47	4.11	4.5E-02	5.8E-02	0.78	0.643322	-1.28
MTCP1	D09	8.49	9.12	2.8E-03	1.8E-03	1.55	0.364415	1.55
MTOR	D10	5.47	5.78	2.3E-02	1.8E-02	1.25	0.574701	1.25
MYD88	D11	4.81	5.13	3.6E-02	2.9E-02	1.25	0.496214	1.25
NFKB1	D12	7.80	7.14	4.5E-03	7.1E-03	0.64	0.051143	-1.57
NFKBIA	E01	6.46	6.46	1.1E-02	1.1E-02	1.00	0.755998	-1.00
PABPC1	E02	1.12	1.14	4.6E-01	4.5E-01	1.01	0.914098	1.01
PAK1	E03	6.78	6.47	9.1E-03	1.1E-02	0.81	0.203267	-1.24

PDGFRA	E04	10.56	12.90	6.6E-04	1.3E-04	5.06	0.347808	5.06
PDK1	E05	5.46	5.13	2.3E-02	2.9E-02	0.79	0.344197	-1.26
PDK2	E06	8.85	8.13	2.2E-03	3.6E-03	0.61	0.483721	-1.65
PDPK1	E07	5.81	5.79	1.8E-02	1.8E-02	0.99	0.825770	-1.01
PIK3CA	E08	4.80	5.12	3.6E-02	2.9E-02	1.25	0.503397	1.25
PIK3CG	E09	10.56	12.90	6.6E-04	1.3E-04	5.06	0.347808	5.06
PIK3R1	E10	6.80	5.79	9.0E-03	1.8E-02	0.50	0.034421	-2.01
PIK3R2	E11	7.13	5.81	7.2E-03	1.8E-02	0.40	0.040470	-2.48
PRKCA	E12	6.79	7.48	9.1E-03	5.6E-03	1.61	0.406043	1.61
PRKCB	F01	10.16	10.46	8.7E-04	7.1E-04	1.23	0.505069	1.23
PRKCZ	F02	6.49	6.82	1.1E-02	8.8E-03	1.26	0.443788	1.26
PTEN	F03	2.80	4.44	1.4E-01	4.6E-02	**3.11**	0.191983	**3.11**
PTK2	F04	6.84	6.13	8.7E-03	1.4E-02	0.61	0.420583	-1.64
PTPN11	F05	3.46	3.15	9.1E-02	1.1E-01	0.80	0.702242	-1.24
RAC1	F06	1.45	1.46	3.7E-01	3.6E-01	1.01	0.816233	1.01
RAF1	F07	4.80	4.78	3.6E-02	3.6E-02	0.99	0.871348	-1.01
RASA1	F08	4.46	4.46	4.6E-02	4.6E-02	1.00	0.828189	-1.00
RBL2	F09	4.13	4.14	5.7E-02	5.7E-02	1.00	0.816038	1.00
RHEB	F10	5.14	5.15	2.8E-02	2.8E-02	1.01	0.675214	1.01
RHOA	F11	1.13	1.13	4.6E-01	4.6E-01	1.00	0.936794	1.00
RPS6KA1	F12	7.14	6.82	7.1E-03	8.9E-03	0.80	0.523938	-1.25
RPS6KB1	G01	4.12	4.13	5.7E-02	5.7E-02	1.01	0.681165	1.01
SHC1	G02	5.79	5.80	1.8E-02	1.8E-02	1.01	0.714443	1.01
SOS1	G03	4.47	4.45	4.5E-02	4.6E-02	0.99	0.851921	-1.01
SRF	G04	6.47	6.16	1.1E-02	1.4E-02	0.81	0.778819	-1.24
TCL1A	G05	10.56	11.80	6.6E-04	2.8E-04	2.35	0.386268	2.35
TIRAP	G06	7.13	6.47	7.2E-03	1.1E-02	0.63	0.080492	-1.58
TLR4	G07	10.56	12.83	6.6E-04	1.4E-04	4.81	0.349047	4.81

|							
TOLLIP	G08	8.14	7.82	3.6E-03	4.4E-03	0.80	0.599298	-1.25
TSC1	G09	6.46	5.80	1.1E-02	1.8E-02	0.63	0.207713	-1.58
TSC2	G10	6.80	7.48	9.0E-03	5.6E-03	1.60	0.309604	1.60
WASL	G11	7.48	6.81	5.6E-03	8.9E-03	0.63	0.338009	-1.60
YWHAH	G12	3.46	3.14	9.1E-02	1.1E-01	0.80	0.691006	-1.25
ACTB	H01	0.47	-0.55	7.2E-01	1.5E+00	0.49	0.094359	-2.02
B2M	H02	0.47	1.14	7.2E-01	4.6E-01	1.58	0.281720	1.58
GAPDH	H03	-0.20	-1.19	1.1E+00	2.3E+00	0.50	0.325834	-1.99
HPRT1	H04	3.13	4.14	1.1E-01	5.7E-02	2.02	0.084938	2.02
RPLP0	H05	-3.87	-3.54	1.5E+01	1.2E+01	1.26	0.515265	1.26
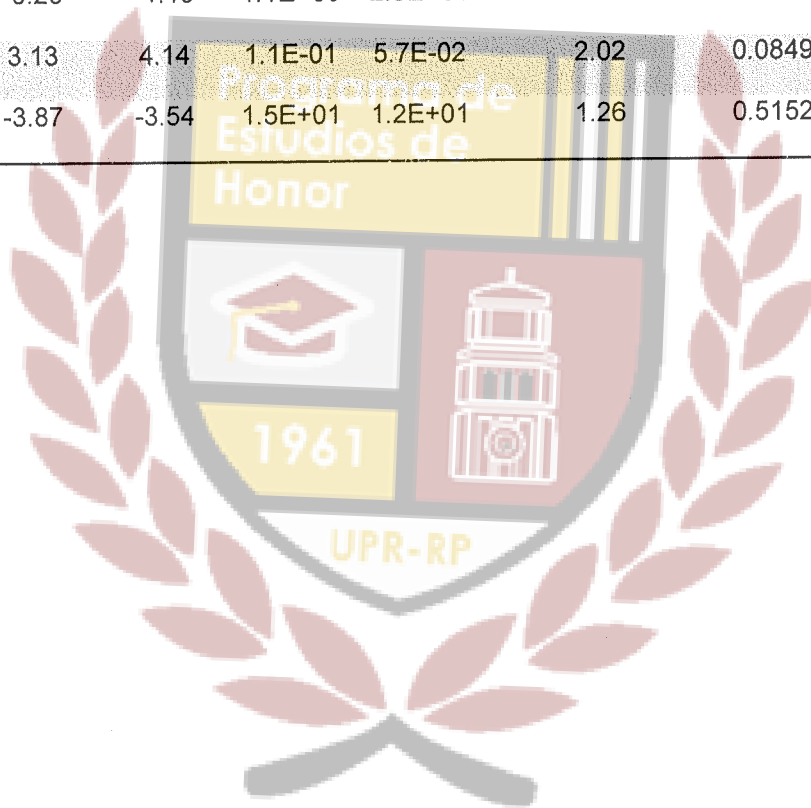
Figure 10:

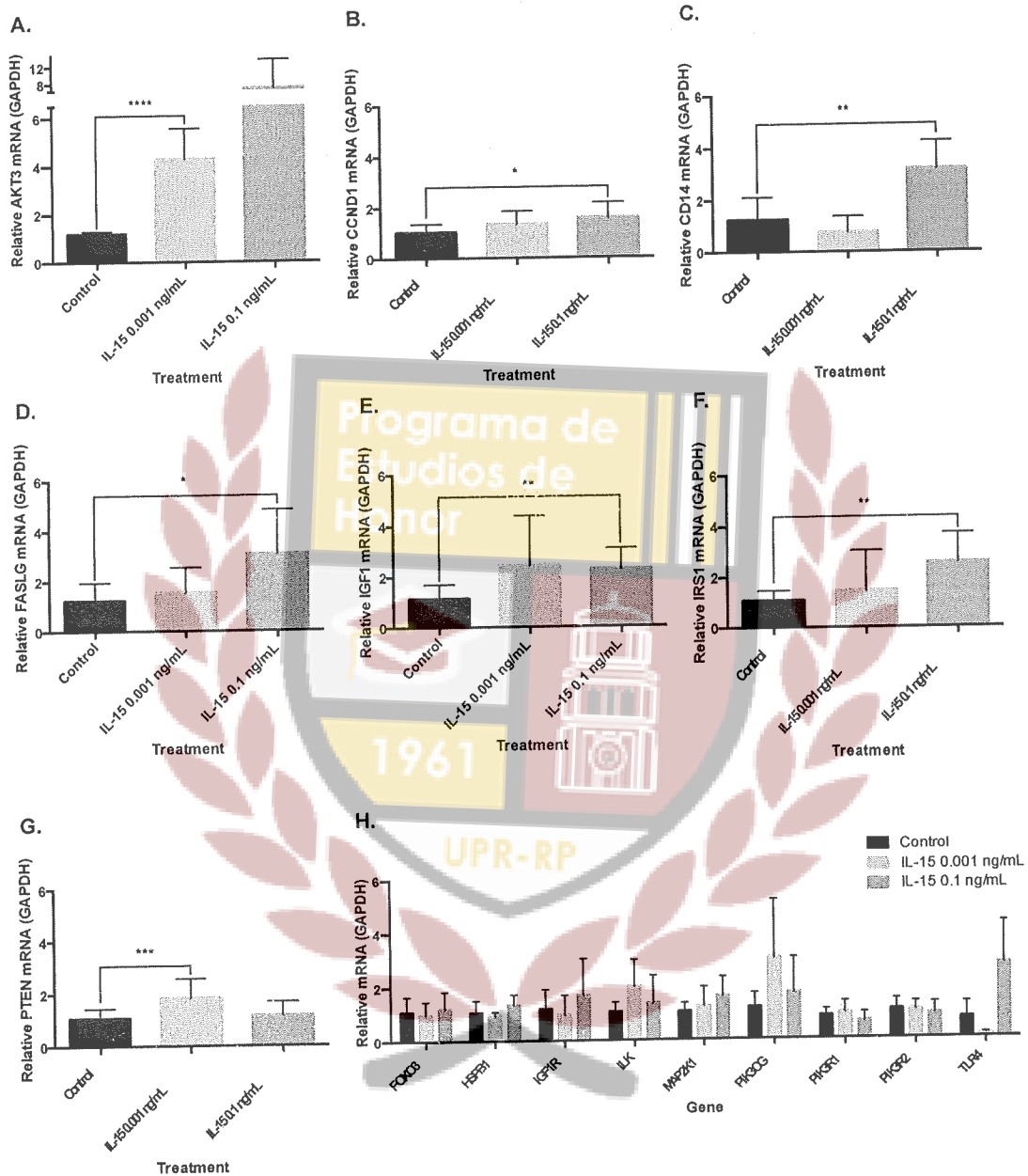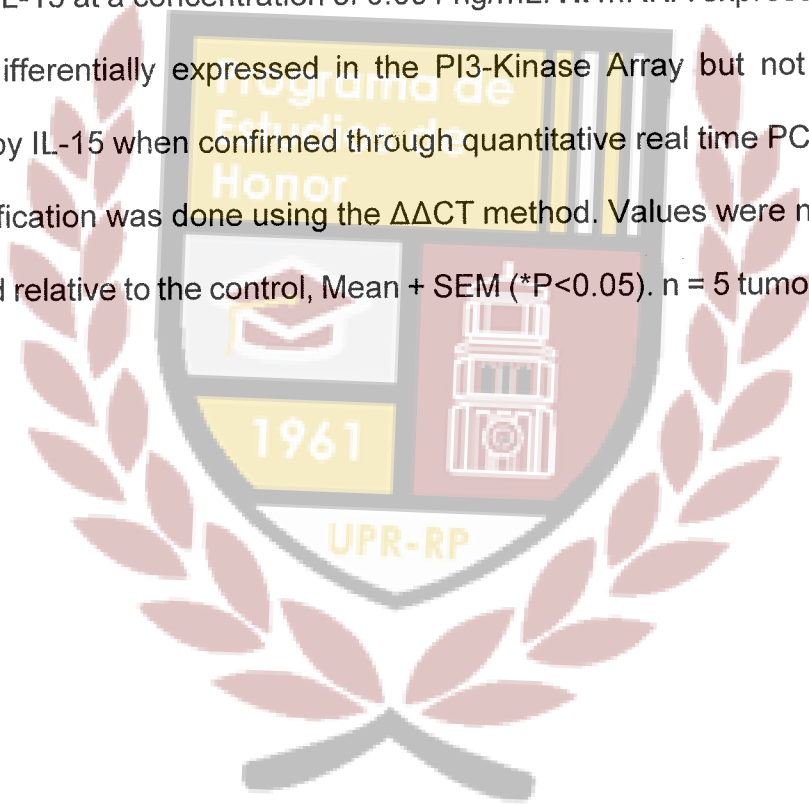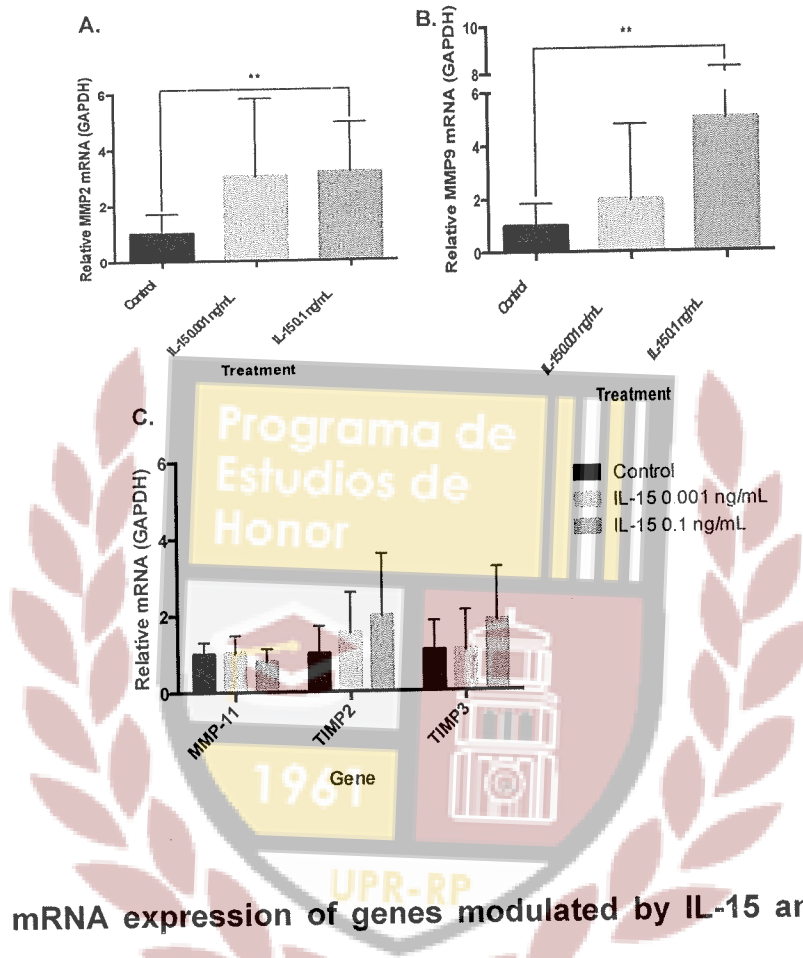**Figure 10. mRNA expression of differentially expressed genes in the PI3-Kinase Array. A.** Quantitative real time PCR revealed AKT3 mRNA expression to be induced by IL-15 at a concentration of 0.001 ng/mL. **B.** Quantitative real time PCR revealed CCND1 mRNA expression to be induced by IL-15 at a concentration of 0.1 ng/mL. **C.** Quantitative real time PCR revealed CD14 mRNA expression to

be induced by IL-15 at a concentration of 0.1 ng/mL. **D.** Quantitative real time PCR revealed FASLG mRNA expression to be induced by IL-15 at a concentration of 0.1 ng/mL. **E.** Quantitative real time PCR revealed IGF1 mRNA expression to be induced by IL-15 at a concentration of 0.1 ng/mL. **F.** Quantitative real time PCR revealed IRS1 mRNA expression to be induced by IL-15 at a concentration of 0.1 ng/mL. **G.** Quantitative real time PCR revealed PTEN mRNA expression to be induced by IL-15 at a concentration of 0.001 ng/mL. **H.** mRNA expression of genes that were differentially expressed in the PI3-Kinase Array but not significantly modulated by IL-15 when confirmed through quantitative real time PCR. Real time PCR quantification was done using the $\Delta\Delta CT$ method. Values were normalized to GAPDH and relative to the control, Mean + SEM (*P<0.05). n = 5 tumors per group.

Figure 11:

Figure 11. mRNA expression of genes modulated by IL-15 and related to cancer metastasis. **A.** Quantitative real time PCR revealed MMP2 mRNA expression to be induced by IL-15 at a concentration of 0.1 ng/mL. **B.** Quantitative real time PCR revealed MMP9 mRNA expression to be induced by IL-15 at a concentration of 0.1 ng/mL. **C.** mRNA expression of genes that were not significantly modulated by IL-15 when confirmed through quantitative real time PCR. Real time PCR quantification was done using the $\Delta\Delta$CT method. Values were normalized to GAPDH and relative to the control, Mean + SEM (*$P<0.05$). n = 5 tumors per group.

Table 6. Differentially expressed genes in prostate cancer tumors treated with IL-15 0.001 ng/mL

Gene Bank Accession Number	Gene Symbol	Description	Fold Change	P Value
NM_001206729.1	AKT3	V-akt murine thymoma viral oncogene homolog 3	3.717	< 0.0001
NM_000314.6	PTEN	Phosphatase and tensin homolog	1.845	0.0002
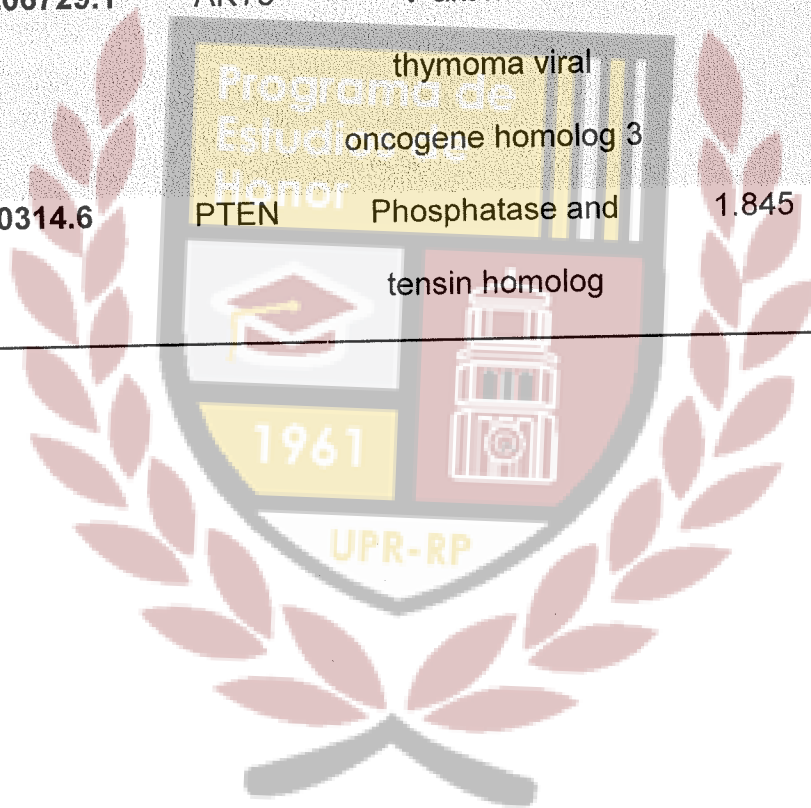
Table 7. Differentially expressed genes in prostate cancer tumors treated with IL-15 0.1 ng/mL

Gene Bank Accession Number	Gene Symbol	Description	Fold Change	P Value
NM_053056.2	CCND1	Cyclin D1	1.5832	0.0222
NM_000591.3	CD14	CD14 molecule	3.1926	0.0027
NM_000639.2	FASLG	Fas ligand	3.104	0.0176
NM_000618.4	IGF1	Insulin like growth factor 1	2.2837	0.0049
NM_005544.2	IRS1	Insulin receptor substrate 1	2.5636	0.0035
NM_001127891.2	MMP2	Matrix metallopeptidase 2	3.1793	0.0053
NM_004994.2	MMP9	Matrix metallopeptidase 9	5.0202	0.0043

Figure 12:

IL-15 Signaling in Prostate Cancer

- Degradation of basement membrane
- Breakdown of extracellular matrix

- Cellular proliferation
- Apoptosis inhibition
- Angiogenesis
- Metastasis
- Important for Prostate Cancer initiation
- May serve protective role in advanced metastasis (?)

- Mediates recognition and phagocytosis of apoptotic cells
- Associated with low metastasis risk

- Tumor growth
- Tumor proliferation
- LNCaP cells- may help protect against metastasis (?)

- Cell cycle progression
- Overexpression contributes to tumorigenesis

- Tumor suppressor
- Modulates cell cycle progression and cell survival

- Cell survival
- Insulin signaling
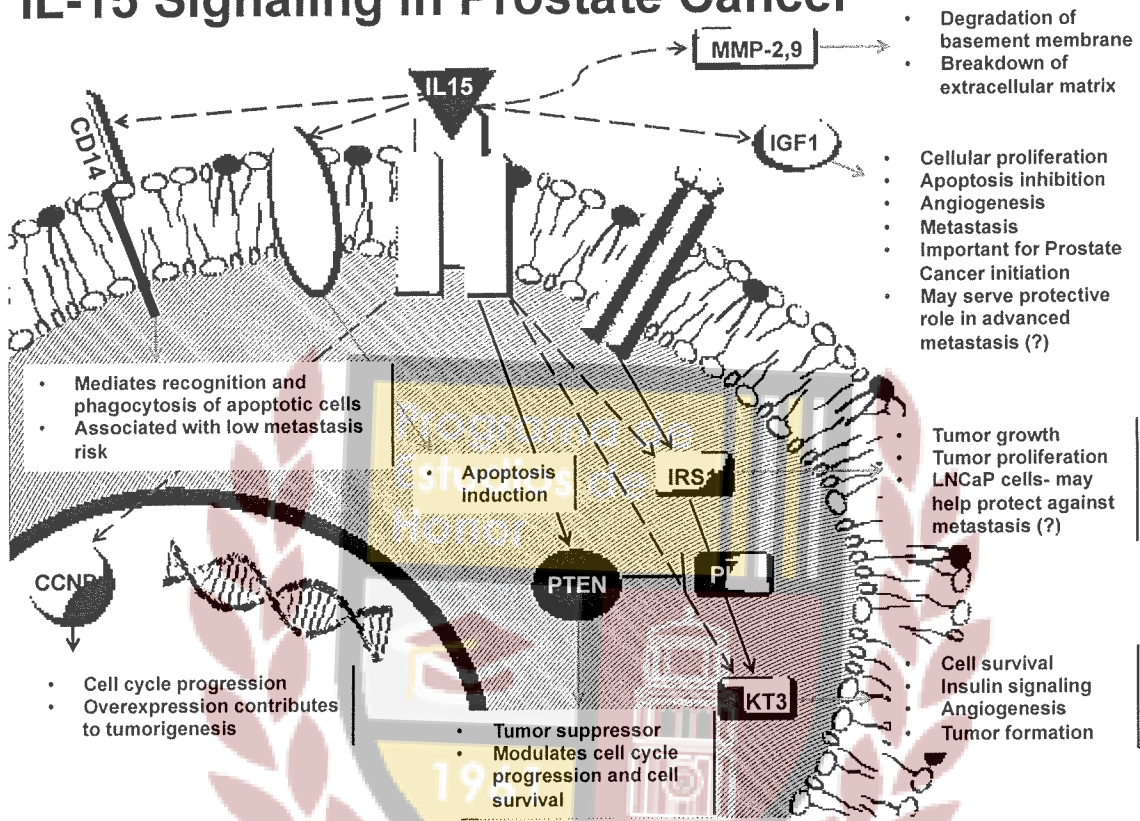- Angiogenesis
- Tumor formation

Figure 12. Summary of IL-15 signaling in prostate cancer.

List of abbreviations:

ACSL3- Acyl-CoA synthetase long-chain family member 3

ADAR- Adenosine deaminase, RNA-specific

AKT1- V-akt murine thymoma viral oncogene homolog 1

AKT2- V-akt murine thymoma viral oncogene homolog 2

AKT3- V-akt murine thymoma viral oncogene homolog 3

APC- Adenomatosis polyposis coli

BAD- BCL2 associated agonist of cell death

BRMS1- Breast cancer metastasis suppressor 1

BTK- Bruton agammaglobulinemia tyrosine kinase

CASP9- Caspase 9

CCL- CC-chemokine ligand

CCL3- Macrophage inflammatory protein-1α, *also known as* C-C motif chemokine ligand 3 (*See MIPα*)

CCL4- Macrophage inflammatory protein-1β, *also known as* C-C motif chemokine ligand 4 (*See MIPβ*)

CCL7- C-C motif chemokine ligand 7

CCND1- Cyclin D1

CCR5- CC-chemokine receptor 5

CD14- CD14 molecule

CD44- CD44 molecule

CD82- CD82 molecule

CDC42- Cell division cycle 42

CDH1- Cadherin 1

CDH6- Cadherin 6

CDH11- Cadherin 11

CDKN1B- Cyclin-dependent kinase inhibitor 1B

CDKN2A- cyclin-dependent kinase inhibitor 2A

cDNA- Complementary DNA (*see DNA*)

CHD4- Chromodomain helicase DNA binding protein 4

CHUK- Conserved helix-loop-helix ubiquitous kinase

COL4A2- Collagen, type IV, alpha 2

CPT2- Carnitine palmitoyltransferase 2

CSNK2A1- Casein kinase 2 alpha 1

CST7- Cystatin F

CTBP1- C-terminal binding protein 1

CTNNA1- Catenin alpha 1

CTNNB1- Catenin beta 1

CTR9- CTR9 homolog, Paf1/RNA polymerase II complex component

CTSK- Cathepsin K

CTSL- Cathepsin L

CXCL12- C-X-C motif chemokine ligand 12

CXCR2- C-X-C motif chemokine receptor 2

CXCR4- C-X-C motif chemokine receptor 4

DENR- Density-regulated protein

DNA- Deoxyribonucleic acid

DTX1- Deltex 1

EIF2AK2- Eukaryotic translation initiation factor 2 alpha kinase 2

EIF4B- Eukaryotic translation initiation factor 4B

EIF4E- Eukaryotic translation initiation factor 4E

EIF4EBP1- Eukaryotic translation initiation factor 4E binding protein 1

EIF4G1- Eukaryotic translation initiation factor 4 gamma 1

ELK1- ELK1, ETS transcription factor

EPHB2- Eph receptor B2

ETV4- Ets variant 4

EWSR1- EWS RNA binding protein 1

FABP4- Fatty acid binding protein 4

FASLG- Fas ligand

FAT1- FAT atypical cadherin 1

FGFR4- Fibroblast growth factor receptor 4

FKBP1A- FK506 binding protein 1A

FLT4- Fms related tyrosine kinase 4

FN1- Fibronectin 1

FOS- FBJ osteosarcoma oncogene

FOXO1- Forkhead box O1

FOXO3- Forkhead box O3

FXYD5- FXYD domain containing ion transport regulator 5

GATA3- GATA binding protein 3

GJA1- Gap junction protein, alpha 1

GNRH1- Gonadotropin releasing hormone 1

GOT2- Glutamic-oxaloacetic transaminase 2

GRB2- Growth factor receptor bound protein 2

GRB10- Growth factor receptor bound protein 10

GSK3B- Glycogen synthase kinase 3 beta

HGF- Hepatocyte growth factor

HPSE- Heparanase

HRAS- Harvey rat sarcoma viral oncogene homolog

HSPB1- Heat shock protein family B (small) member 1

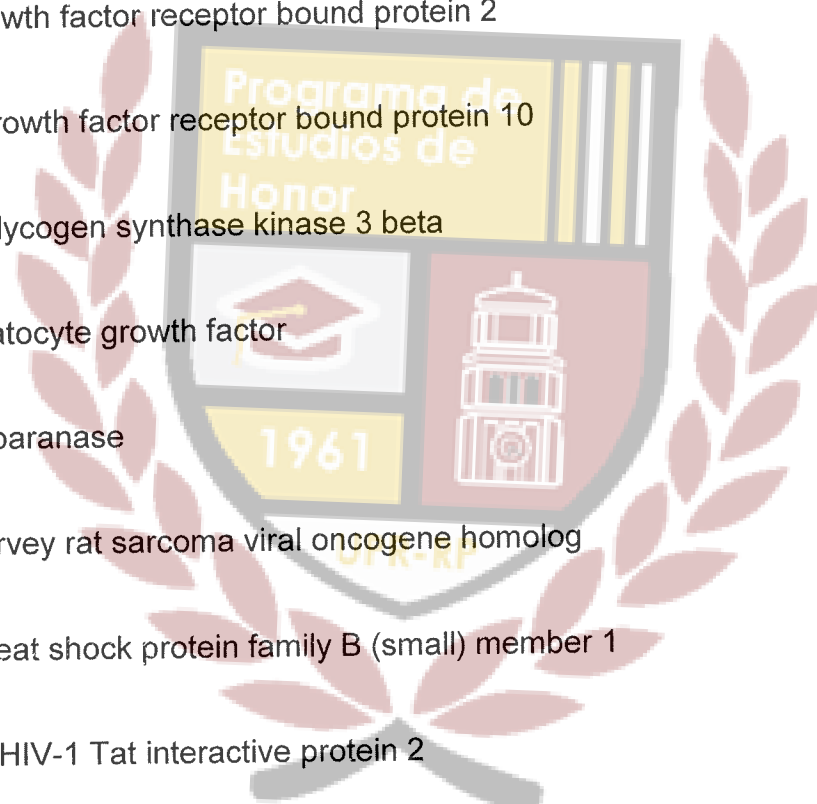**HTATIP2**- HIV-1 Tat interactive protein 2

IGF1- Insulin like growth factor 1

IGF1R- Insulin like growth factor 1 receptor

IL-15- Interleukin 15

IL18- Interleukin 18

IL1B- Interleukin 1 beta

ILK- Integrin linked kinase

IRAK1- Interleukin 1 receptor associated kinase 1

IRS1- Insulin receptor substrate 1

ITGA7- Integrin alpha 7

ITGB1- Integrin subunit beta 1

ITGB3- Integrin subunit beta 3

JUN- Jun proto-oncogene

KISS1- KiSS-1 metastasis-suppressor

KISS1R- KISS1 receptor (*see KISS1*)

KRAS- Kirsten rat sarcoma viral oncogene homolog

MAP2K1- Mitogen-activated protein kinase kinase 1

MAPK1- Mitogen-activated protein kinase 1

MAPK3- Mitogen-activated protein kinase 3

MAPK8- Mitogen-activated protein kinase 8

MAPK14- Mitogen-activated protein kinase 14

MCAM- Melanoma cell adhesion molecule

MDM2- MDM2 proto-oncogene

MET- MET proto-oncogene, receptor tyrosine kinase

METAP2- Methionyl aminopeptidase 2

MGAT5- Mannosyl (alpha-1,6-)-glycoprotein beta-1,6-N-acetyl-glucosaminyltransferase

MIP1- Macrophage inflammatory protein 1

MIP1α- Macrophage inflammatory protein 1α (*see CCL3 and MIP1*)

MIP1β- Macrophage inflammatory protein 1β (*see CCL4 and MIP1*)

MMP2- Matrix metallopeptidase 2

MMP3- Matrix metallopeptidase 3

MMP7- Matrix metallopeptidase 7

MMP9- Matrix metallopeptidase 9
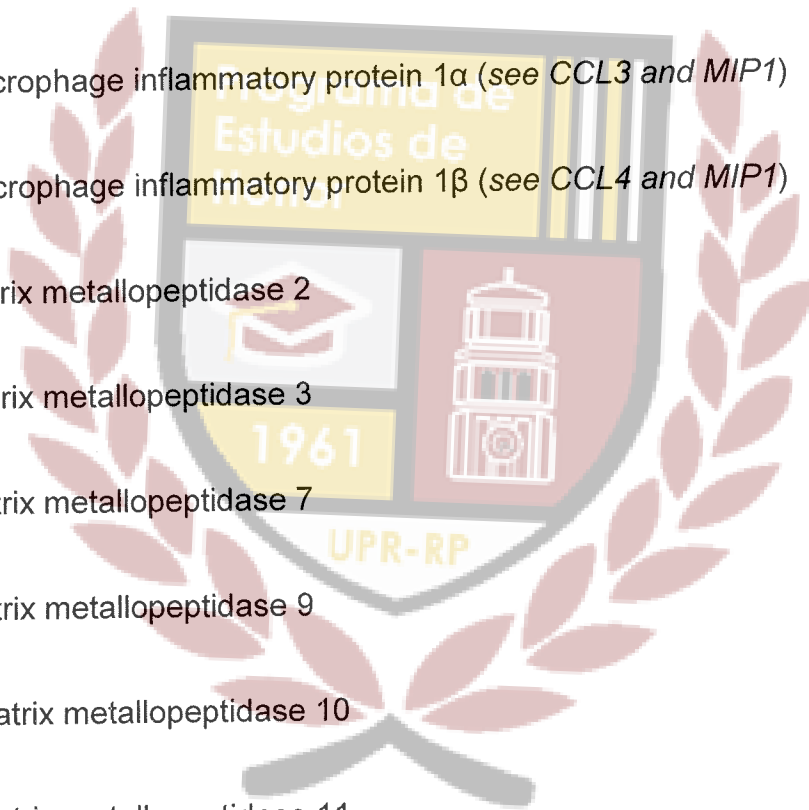
MMP10- Matrix metallopeptidase 10

MMP11- Matrix metallopeptidase 11

MMP13- Matrix metallopeptidase 13

MSR1- Macrophage scavenger receptor 1

MTA1- Metastasis associated 1

MTCP1- Mature T-cell proliferation 1

mTOR- Mechanistic Target Of Rapamycin

MTSS1- Metastasis suppressor 1

MYC- V-myc avian myelocytomatosis viral oncogene homolog

MYCL- V-myc avian myelocytomatosis viral oncogene lung carcinoma derived homolog

MYD88- Myeloid differentiation primary response gene 88

NF2- Neurofibromin 2 (merlin)

NFKB- Nuclear factor kappa B

NFKB1- Nuclear factor of kappa light polypeptide gene enhancer in B-cells 1 (*see NFKB*)

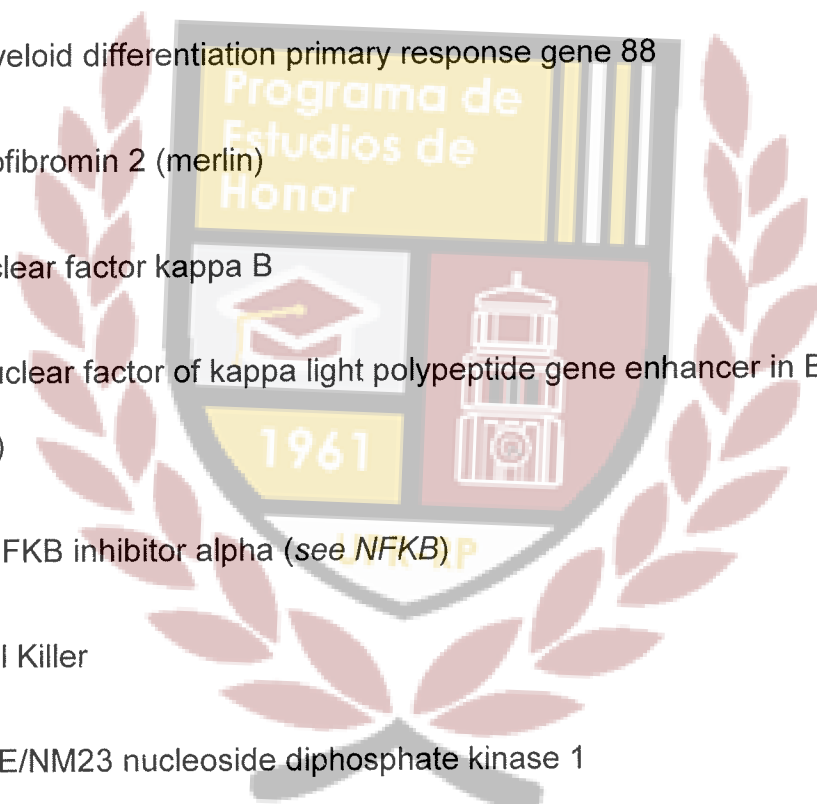**NFKBIA**- NFKB inhibitor alpha (*see NFKB*)

NK- Natural Killer

NME1- NME/NM23 nucleoside diphosphate kinase 1

NME4- NME/NM23 nucleoside diphosphate kinase 4

NR4A3- Nuclear receptor subfamily 4 group A member 3

PABPC1- Poly(A) binding protein cytoplasmic 1

PAK1- p21 protein (Cdc42/Rac)-activated kinase 1

PCR- Polymerase Chain Reaction

PDGFRA- Platelet derived growth factor receptor alpha

PDK1- Pyruvate dehydrogenase kinase 1

PDK2- Pyruvate dehydrogenase kinase 2

PDPK1- 3-phosphoinositide dependent protein kinase 1

PH- Pleckstrin homology

PI3K- Phosphatidylinositol 3-kinase (*also known as PIK3*)

PIK3CA- Phosphatidylinositol-4,5-bisphosphate 3-kinase catalytic subunit alpha (*see PI3K*)

PIK3CG- Phosphatidylinositol-4,5-bisphosphate 3-kinase catalytic subunit gamma (*see PI3K*)

PIK3R1- Phosphoinositide-3-kinase regulatory subunit 1

PIK3R2- Phosphoinositide-3-kinase regulatory subunit 2

PIP$_2$- Phosphatidylinositol 4,5-bisphosphate

PIP$_3$- phosphatidylinositol (3,4,5)-triphosphate

PKB- Protein Kinase B

PLAUR- Plasminogen activator, urokinase receptor

PLCG2- Phospholipase C gamma 2

PLIN2- Perilipin 2

PNN- Pinin, desmosome associated protein

PRKCA- Protein kinase C alpha

PRKCB- Protein kinase C beta

PRKCZ- Protein kinase C zeta

PTEN- Phosphatase and tensin homolog

PTK2- Protein tyrosine kinase 2

PTPN11- Protein tyrosine phosphatase, non-receptor type 11

qRT-PCR- Quantitative Real Time Polymerase Chain Reaction

RAC1- Ras-related C3 botulinum toxin substrate 1 (rho family, small GTP binding

protein Rac1)

RAF1- Raf-1 proto-oncogene, serine/threonine kinase

RASA1- RAS p21 protein activator 1

RB1- Retinoblastoma 1

RBL2- Retinoblastoma-like 2

RHEB- Ras homolog enriched in brain

RHOA- Ras homolog family member A

RNA- Ribonucleic acid

RORB- RAR-related orphan receptor beta

RPS6KA1- Ribosomal protein S6 kinase A1

RPS6KB1- Ribosomal protein S6 kinase B1

RPSA- Ribosomal protein SA

SCID- Severe combined immunodeficiency

SERPINE1- Serpin family E member 1

SET- SET nuclear proto-oncogene

SHC1- SHC (Src homology 2 domain containing) transforming protein 1

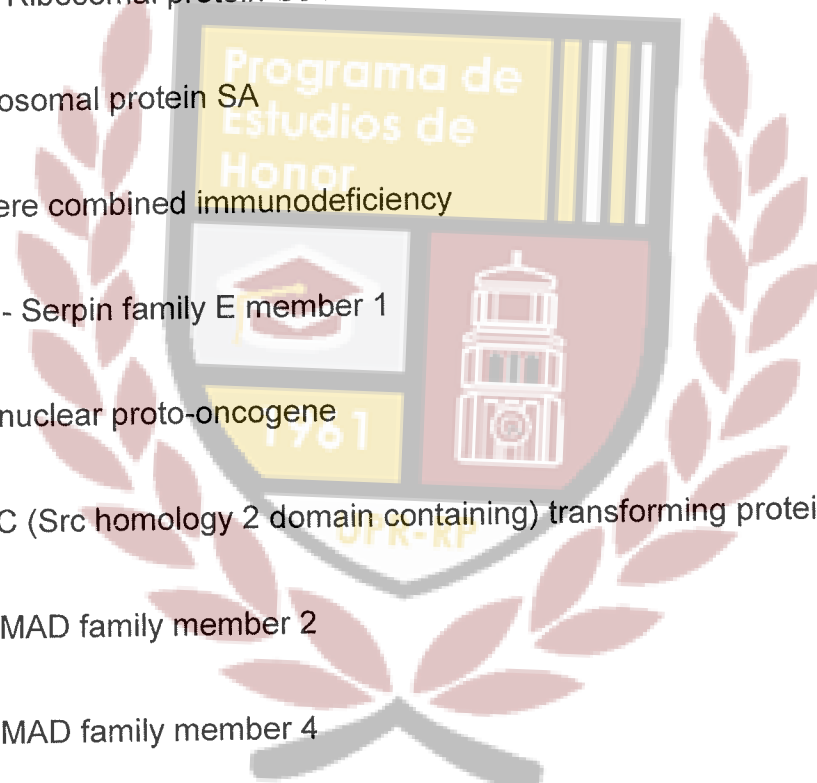**SMAD2**- SMAD family member 2

SMAD4- SMAD family member 4

SOS1- SOS Ras/Rac guanine nucleotide exchange factor 1

SRF- Serum response factor

STAT3- Signal transducer and activator of transcription 3

SRC- SRC proto-oncogene, non-receptor tyrosine kinase

SSTR2- Somatostatin receptor 2

SYC- Cysteinyl-tRNA synthetase

TAPBP- TAP binding protein (tapasin)

TCF4- Transcription factor 4

TCF20- Transcription factor 20 (AR1)

TCL1A- T-cell leukemia/lymphoma 1A

TGFB1- Transforming growth factor beta 1

TIMP- Tissue inhibitor of metalloproteases

TIMP2- TIMP metallopeptidase inhibitor 2 (*see TIMP*)

TIMP3- TIMP metallopeptidase inhibitor 3 (*see TIMP*)

TIMP4- TIMP metallopeptidase inhibitor 4 (*see TIMP*)

TIRAP- Toll-interleukin 1 receptor (TIR) domain containing adaptor protein
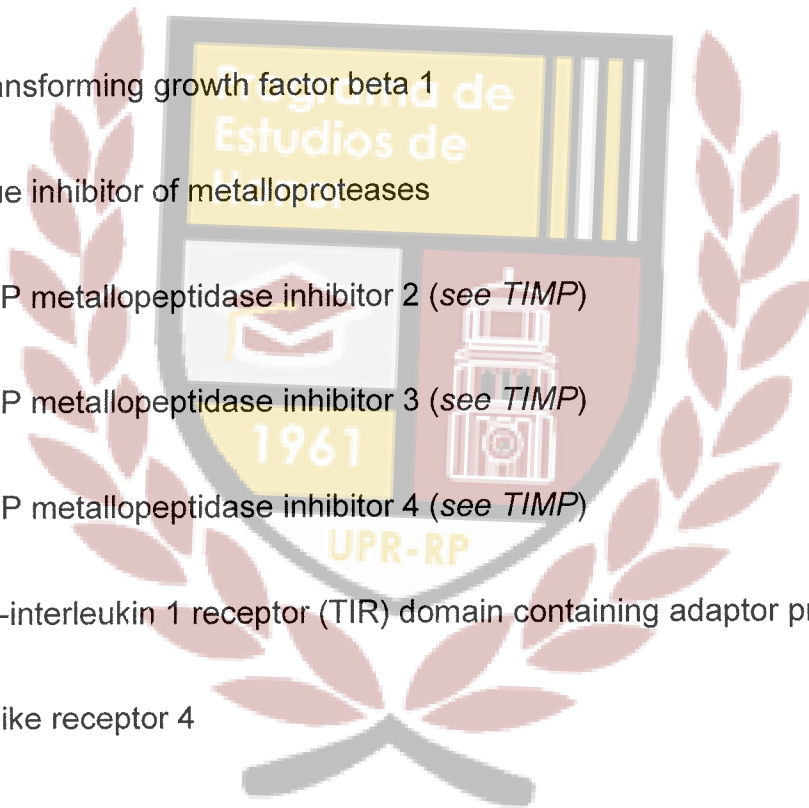
TLR4- Toll-like receptor 4

TNFα- Tumor necrosis factor alpha

TNFSF10- Tumor necrosis factor superfamily member 10

TOLLIP- Toll interacting protein

TP53- Tumor protein p53

TRPM1- Transient receptor potential cation channel subfamily M member 1

TSC1- Tuberous sclerosis 1

TSC2- Tuberous sclerosis 2

TSHR- Thyroid stimulating hormone receptor

VEGFA- Vascular endothelial growth factor A

WASL- Wiskott-Aldrich syndrome like

YWHAH- Tyrosine 3-monooxygenase/tryptophan 5-monooxygenase activation protein eta

Introduction

Chapter 1: Cancer, an Enduring Problem Worldwide

Cancer, a disease characterized by uncontrolled cell growth and abnormal spread of cells, is an ongoing problem that currently affects millions of people on a global scale. According to the American Cancer Society (2015), around 14.1 million new cancer cases occurred in 2012 worldwide. That same year, approximately 8.2 million people in the world died of cancer. Also, In the United States alone, 1,665,540 new cancer cases were diagnosed in 2012. The cancer deaths in the United States that year were 585,720. The American Cancer Society estimates that approximately 1,658,370 new cancer cases will be diagnosed in the United States in 2015. Also, around 589,430 Americans are expected to die of cancer in 2015; that number equals the death of 1,620 individuals per day. Accounting for approximately 1 of every 4 deaths in the United States and representing the second leading cause of death in the same nation, cancer is an unremitting nuisance. Now, more than ever, cancer research is an imperative endeavor that must be conducted to better understand the molecular biology behind the disease. A better understanding of the mechanisms behind cancer can later on be translated to new treatments that will be aimed at improving the quality of life of the millions of patients that suffer from the disease.

According to the National Cancer Institute (2015), the most frequently diagnosed cancers in the United States include: bladder cancer, breast cancer,

colon and rectal cancer, endometrial cancer, kidney cancer, leukemia, lung cancer, melanoma, non-Hodgkin lymphoma, pancreatic cancer, prostate cancer, and thyroid cancer. This list excludes non-melanoma skin cancers. The National Cancer Institute (2015) also sates that the most common type of cancer in the United States is breast cancer, followed by prostate or lung cancer.

Chapter 2: Biology and Hallmarks of Cancer

Most cancers start with a single cell that undergoes a series of mutations. Alberts (2015) reports that as the cell divides, additional hereditable changes accumulate, eventually leading to the development of a primary tumor that emerges in a particular organ. Since most cancers have features that mirror their origins, cancers derived from different cell types are considered distinctive diseases. As a result, Alberts (2015) states that cancers are classified based on the tissue and cell type from which they develop. He explains that a tumor is considered benign if its cells are not invasive, but once tumor cells invade neighboring tissue, a tumor will be considered malignant and a true cancer. The more a tumor undergoes metastasis and spreads to other parts of the body, the harder it is to eliminate the cancer and the greater the risk of death for the patient.

Unlike normal cells, cancer cells are immortal: they can be defined by their enhanced ability to reproduce without limits (Hanahan and Weinberg, 2000; Hayflick, 1997; Wright et al., 1989). As cancer cells reproduce, they avoid cellular

2

signals that control cell growth and replication, migrate to, and occupy areas that are normally inhabited by other cells (Alberts, 2015). Hanahan and Weinberg (2011) comment on six common hallmarks that facilitate the growth and metastatic progression of tumors: the ability of cancer cells to maintain proliferative signaling, to avoid growth suppressors, to resist cell death, to replicate perpetually, to induce the formation of new blood vessels, and to activate invasion and metastasis. Inflammation promotes the hallmark functions described above and genome instability creates genetic multiplicity in cancer, they say. These features provide solid groundwork for the study and comprehension of cancer biology.

Chapter 3: Possible Causes Underlie Cancer Development

Cancers are complex and variable: they do not have a single, attributable cause. Instead, the American Cancer Society (2015) states that internal factors, such as inherited genetic mutations, hormones, and immune conditions, and external factors, such as unhealthy diets, infectious organisms, and tobacco, may act in parallel or in sequence to cause cancer. De Marzo et al. (2007) say that chronic inflammation has also been related to the development of different human cancers; many of them associated with environmental contact and/or infective agents. Additionally, both the innate and adaptive immune systems are involved in the pathogenesis of cancers associated with inflammation. The connection between inflammation and a favorable immune response is important to understand its role in treating prostate cancer, the focus of this study.

Chapter 4: Inflammatory Responses Mediated by the Immune System have a Key Role in Cancer Development

An introduction to immunology and the immune cells is vital to have a clear understanding of the role of the immune system in cancer development. In this chapter, I will first give an introduction to immunology as previously reviewed by Silverthorn, Murphy, and Kennedy (Silverthorn et al., 2013; Murphy et al., 2012; Kennedy, 2010) in order to subsequently explain the role of inflammation in cancer development.

Part A: Introduction to Immunology

Immunology is the study of the immune system, our biological machinery for identifying and eliminating pathogens. Anatomically, the immune system has two main constituents: the lymphoid tissues and immune cells. The lymphoid tissues can be further subdivided into primary or secondary tissues; the former includes the thymus and bone marrow where immune cells form and mature, and the latter includes the lymph nodes and spleen, among other components, where mature naïve immune cells are kept and adaptive immune responses commenced. The innate immune response is the first line of defense against a broad range of

pathogens, while the adaptive immune response mediates specific immune responses.

Leukocytes, or white blood cells, are immune cells that are derived from the bone marrow and mediate both innate and adaptive immune responses. The hematopoietic stem cells in the bone marrow give rise to the lymphoid and myeloid cell lineages, among other components of blood. The myeloid lineage gives rise to the majority of the cells if the innate immune response: dendritic cells, granulocytes, mast cells, neutrophils, eosinophils, basophils, and macrophages. The lymphoid lineage, on the other hand, gives rise to the natural killer (NK) cells of the innate response and the white blood cells of the adaptive response, B cells and T cells.

As previously mentioned, the innate immunity is composed of a group of cells with diverse functions. Both basophils and mast cells contribute to inflammation by releasing chemicals that mediate allergic and inflammatory responses. Neutrophils, the most abundant white blood cells, are phagocytic cells that ingest and destroy pathogens. They also secrete cytokines and chemicals that mediate inflammatory responses. Eosinophils are immune cells whose primary function is to destroy invaders, predominantly parasites that have been coated by antibodies. They can also participate in allergic reactions by discharging toxic enzymes and other substances. Monocytes, on the other hand, are the precursors of macrophages, scavenger phagocytic cells that can ingest and destroy pathogens. Because of their role as antigen-presenting cells, macrophages are also important in the development of an acquired immunity. Dendritic cells are

immune cells whose primary function is to identify pathogens and activate other immune cells by presenting antigens. They act as a link between innate and adaptive responses, as antigen binding contributes to the activation of lymphocytes. Finally, NK cells are components of the adaptive response because they lack antigen-specific receptors, even though they are derived from the lymphoid lineage. These cells are cytotoxic, as they release lytic granules that can kill virus-infested cells. NK cells also have important roles defending cells against intracellular pathogens by killing infected or cancerous cells and secreting cytokines such as interferons and tumor necrosis factor alpha (TNFα).

Lymphocytes are key components of the adaptive immune response due to the fact that they are the only immune cells that have specificity and create immunological memory (Kennedy, 2010). B and T cells generate a wide variety of receptors with different specificities by several molecular processes. One of those processes, called gene rearrangement, occurs in antigen receptors during lymphocyte development.

Lymphocytes can be further subdivided into B cells and T cells according to their functions and surface markers. B lymphocytes develop and mature in the bone marrow. After encountering antigens, they can differentiate into plasma cells, whose effector functions include secreting antibodies, and memory cells, that are long-lived cells that create immunological memory. B cells can also act as antigen-presenting cells for T cells. T cells, on the other hand, develop in the thymus. They can only identify antigens when bound to self-MHC molecules and can be mainly subdivided into CD4$^+$ T$_H$ and CD8$^+$ T$_C$ cells. CD4$^+$ T$_H$ cells express CD4 in their

membrane and are also known as helper T cells because they mediate specific responses through the excretion of cytokines, immunological messengers, and the expression of molecules in their surfaces. $CD4^+$ T_H cells can activate infected macrophages and T cells. Another subset of T cells, the $CD8^+$ T_C cells, are also known as cytotoxic T cells because they induce apoptosis in infected cells. Finally, γδ T cells only comprise 1-5% of T cells and have CD3 expressed in their membrane, instead of CD4 or CD8. They have regulatory and cytotoxic functions and are involved in the primary immune response because they can recognize antigens without the need of MHC molecules. γδ T cells can recognize antigens that are not proteins and secrete cytokines that promote inflammation (Wu et al., 2014).

Part B: Inflammation

As alluded in the previous part of this chapter, cytokines are cell-signaling proteins that facilitate cellular communication during immune responses by disturbing the behavior of other cells that have the appropriate receptors (Mandal, 2013; Murphy et al., 2012). According to Wong and Fish (2003), inflammatory chemokines are a small family of structurally related cytokines that act primarily as chemotactic and immunoregulatory molecules. Additionally, they can recruit and activate lymphocytes into inflamed tissue (Karp, 2013). Both cytokines and chemokines are critical in immune responses, as they initiate the process of inflammation after being secreted by activated macrophages. Inflammation can be
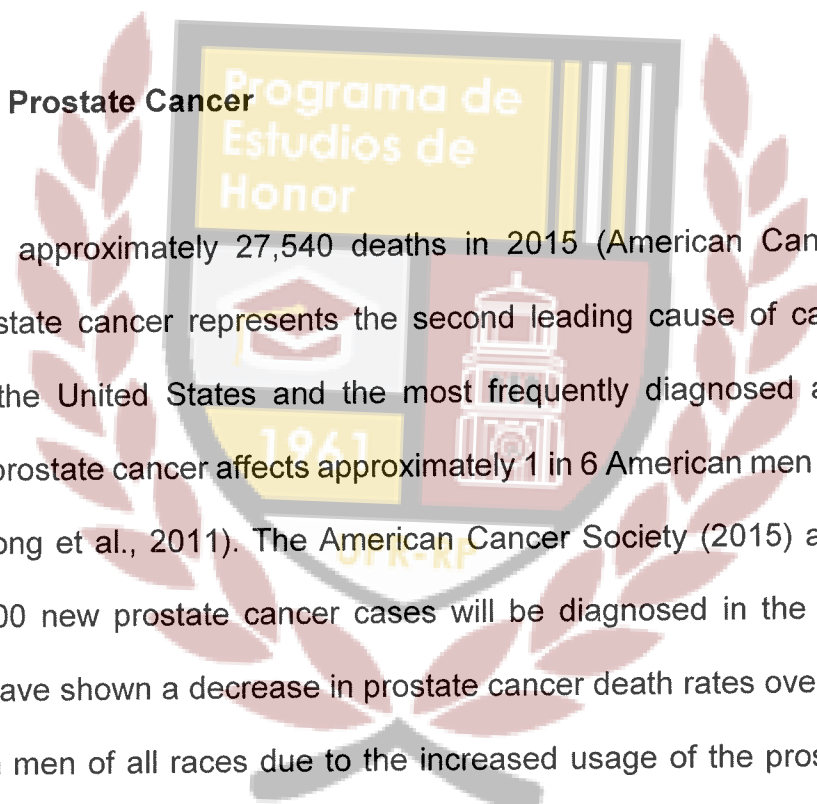
beneficial to the organism, as it helps recruit proteins and cells into the target tissue to combat pathogens. Furthermore, inflammation facilitates the activation of lymphocytes that can initiate adaptive responses. Following tissue damage or infection and the release of cytokines and chemokines, vasoactive and chemotactic factors are released (Kennedy, 2010). This leads to increased vascular permeability and vasodilation, which causes the characteristic redness, swelling, and heat of inflammation. Furthermore, inflammatory cells are able to migrate into the tissue, where they release inflammatory mediators that cause pain (Murphy et al., 2012).

Part C: Inflammation in Cancer Development

Inflammation has been linked to prostate cancer development. As part of the inflammatory process, activated phagocytic cells of the innate immune system release extremely reactive chemical compounds. As a result, DNA in epithelial cells can be damaged and reactive chemical compounds can initiate a free-radical chain response by reacting with other components of the cell (De Marzo et al., 2007). Inácio Pinto et al. (2015) also mention other bioactive molecules that are part of the pro-inflammatory environment and increase the risk of cancer: cytokines, growth factors, and chemokines. They state that, in conjunction, these bioactive molecules maintain cancer cell proliferation rate, inhibit apoptosis, stimulate angiogenesis, and stimulate the production of enzymes that modify the extracellular matrix; ultimately promoting epithelial-mesenchymal transition. De

Marzo et al. (2007) state that a disturbance in the regulation of cytokine production can cause augmented inflammation and cancer. Furthermore, McCarron et al. (2002) have found that single nucleotide polymorphisms that are associated with increased cytokine production are also associated with the development of cancer through the regulation of the tumor angiogenesis pathway.

Chapter 5: Prostate Cancer

With approximately 27,540 deaths in 2015 (American Cancer Society, 2015), prostate cancer represents the second leading cause of cancer-related deaths in the United States and the most frequently diagnosed among men. Currently, prostate cancer affects approximately 1 in 6 American men in the United States (Jeong et al., 2011). The American Cancer Society (2015) approximates that 220,800 new prostate cancer cases will be diagnosed in the US in 2015. Statistics have shown a decrease in prostate cancer death rates over the last two decades in men of all races due to the increased usage of the prostate-specific antigen (PSA) blood test for screening (American Cancer Society, 2015). Nevertheless, the incidence of prostate cancer is estimated to increase as a result of the ageing baby boomer population (Sfanos and De Marzo, 2012).

On a molecular level, prostate cancer advances through the collection of both somatic and epigenetic changes in the cells' genomes. These changes lead to the inactivation of tumor-suppressor genes and activation of oncogenes (De

Marzo et al., 2007), which ultimately result in aberrant cell division, progression of tumors, and cancer metastasis. In its early stages, prostate cancer usually shows no symptoms. The American Cancer Society (2015) affirms that advancement of the disease brings problems such as: disturbed urine flow, incapacity or difficulties urinating and stopping urine flow, urge to urinate recurrently, pain while urinating, and blood in the urine. It also states that prostate cancer undergoes metastasis and spreads to the bones in its advanced stages.

Established prostate cancer risk factors include: diets high in processed meats, dairy foods, obesity, smoking, and toxic combustion products. Additionally, several factors have been attributed to the development of prostate cancer, including: chronic prostatic inflammation, increasing age, genetics, and environmental exposures (Sfanos and De Marzo, 2012; Sfanos et al., 2013; De Marzo et al., 2007). The cause of prostate cancer development has also been associated with infections, dietary habits, urine reflux, corpora amylacea (Jeong et al., 2011), and hormonal changes (Sfanos and De Marzo, 2012).

Chapter 6: The Tumor Microenvironment, Inflammation, and Prostate Cancer

The tumor microenvironment - which is composed of immune cells, fibroblasts, blood vessels, mesenchymal stem cells, fat cells, and other factors such as cytokines, chemokines, and extracellular matrices (Shiao et al., 2016) - undergoes complex changes as tumors progress. In the past years, several

studies and reviews have stressed the importance of the tumor microenvironment in prostate cancer pathogenesis and advancement (De Marzo et al., 2007; Taverna et al., 2015; Shiao et al., 2016). In prostate cancer development, alterations in the epithelium cause transformations in the cell types present in the stroma, a supportive network that is mainly comprised of connective tissue (Hägglöf and Bergh, 2012). In fact, the stroma has been considered a vital regulator of prostate malignancy, as changes in it also lead to accretion and alteration of tissue extracellular matrices, which results in the secretion of inflammatory cytokines and chemokines in response to the injured tissue (Shiao et al., 2016). Although in normal conditions an inflammatory response helps regenerate the damaged tissue, in cancer, the interaction between the microenvironment, tumor cells, and stroma generates an inflammatory response that has adverse effects. Epidemiological, histopathological, and molecular pathological studies serve as emerging evidence of the essential role of inflammation in the development and progression of prostate cancer (Blum et al., 2008). Shiao et al. (2016) state that both inflammation and stromal activation are cancer-promoting processes that co-exist and regulate each other in tumor development through the continuous assembly of growth factors and chemokines that attract other inflammatory cells and promote cell growth.

De Marzo et al. (2007) state that, even though the exact cause of inflammation in prostate cancer is still unknown, the initiation of the inflammatory process has been attributed to direct infections, reflux of urine, dietary patterns, and estrogens. On a molecular level, as prostate cancer progresses to a higher

grade, the cells accumulate more mutations, that lead to their recognition by the immune system (Schumacher and Schreiber, 2015). Cells from both the innate and adaptive immune responses are important players in the prostate cancer microenvironment.

As reviewed by Shiao et al. (2016), macrophages, NK cells, dendritic cells, and mast cells – which are part of the innate response – have been associated with cancer patient outcomes. NK cells have been associated with anti-cancerous effects (Frankel et al., 2010), as they can have direct cytotoxicity against cancerous cells and can release cytokines and chemokines that regulate and recruit other immune cells. On the other hand, neutrophils (Okada et al., 2000), macrophages (Fang et al., 2013), and mast cells (Pittoni and Colombo, 2012) are mostly associated with pro-cancerous effects. Neutrophils are associated with prostate cancer progression through the recruitment of immunosuppressive immune cells, but can also have anti-tumorous effects through the direction of cancer cell lysis. Macrophages can aid in the development and progression of prostate cancers through the promotion of angiogenesis, invasiveness, tumor proliferation, metastasis, and chemotaxis. They also modulate prostate cancer tumorigenesis by mediating CCL4-STAT signaling though the androgen receptor (Fang et al., 2013). On the other hand, macrophages may mediate anti-tumorigenic outcomes by releasing cytotoxic cytokines and presenting antigens to T cells. Mast cells have been associated with both anti and pro-tumorigenic effects, the former through the release of inflammatory cytokines, and the latter through the suppression of T cell functions and promotion of tumor progression.

B and T lymphocytes - which are part of the adaptive and anti-tumorigenic immune responses (Hanahan and Coussens, 2012) – have been associated with cancer development and advancement. Increased numbers of T cells, specifically CD4+, CD8+, or regulatory T cells, are associated with worse prostate cancer survival and invasion (McArdle et al., 2004; Ness et al., 2014; Liu et al., 2013; Davidsson et al., 2013). Although T cells are associated with pro-cancerous effects through the release of cytokines that promote tumor formation, they can also mediate anti-cancerous effects by directly lysing cancer cells (Tc CD8$^+$) or releasing cytotoxic cytokines (Shiao et al., 2016). Furthermore, as stated by Shiao et al. (2016), although regulatory T cells are associated with pro-tumorous effects through the stimulation of production of inflammatory cytokines and suppression of anti-cancerous immunological responses, they can also be related to anti-cancer outcomes by helping restore homeostasis to decrease inflammation. Finally, increased levels of infiltrating B cells are correlated with higher prostate cancer grades and increased risk of biochemical recurrence (Woo et al., 2014). They are also known to modulate macrophages, that can induce pro-cancerous effects (Affara et al., 2014) as previously stated. In short, although the role of the adaptive immune response in prostate cancer complex and not entirely understood, increased numbers of T and B cell infiltrates are associated with bad prognoses. Further studies are needed to have a better understanding of both the adaptive and immune responses in prostate cancer.

Chapter 7: Current alternatives for Prostate Cancer Treatment

The recommendation of whether or not men should undergo regular prostate cancer screening depends on their risk of acquiring prostate cancer. According to the American Cancer Society (2015), regular prostate cancer screening is not endorsed for men at average prostate cancer risk because of the serious concerns about cancer over-diagnosis in slow-growing tumors that are not detrimental and because of the unfavorable side effects associated with the treatments. Also, two large clinical trials devised to determine the efficiency of Prostate Specific Antigen testing for the decrease of prostate cancer deaths yielded inconsistent results. The American Cancer Society (2015) does consider black men or men that have close relatives diagnosed with prostate cancer prior to the age of 65 to be at high risk for prostate cancer development. These men should incur in regular prostate cancer screening from the age of 45. Finally, the American Cancer Society (2015) considers men with numerous close relatives diagnosed with prostate cancer at a young age to be at higher risk of acquiring prostate cancer. Therefore, they should have regular prostate cancer screening from the age of 40.

When it comes to treating prostate cancer, treatments differ according to the aggressiveness and advancement of the cancer and age of the patient. The Gleason score, or the tumor's appointed grade, is an indicator of the cancer's aggressiveness (National Cancer Institute). According to the American Cancer Society, a cancer with a score of 6 is considered low grade and less aggressive

while a cancer with a score of 10 is considered high grade and very aggressive. Therefore, the American Cancer Society explains that older men, or those with tumors that are less aggressive and/or at an early stage, should undergo a process of active surveillance where the patient is carefully observed.

Surgery comprises one of the treatment options for prostate cancer; it can be conducted in several ways: open, laparoscopic, or robotic-assisted. Other treatment options include radioactive seed implants or external beam radiation. In more advanced cases, cancer can be treated with chemotherapy, radiation therapy, or hormonal therapy. Although hormone therapy can help limit the growth of the cancerous tumor (thereby helping control advanced prostate cancer for prolonged periods) some men develop resistance to hormone therapy. Current data obtained by the American Cancer Society (2015) does not support any of the treatments mentioned above as the best one to treat prostate cancer. To improve treatment, researchers are exploring new biomarkers that can help differentiate between low grade and more aggressive cancers; this would minimize unnecessary treatment and associated side effects that ultimately have a negative impact on quality of life.

Chapter 8: Macrophage Inflammatory Protein 1β (CCL4) and Interleukin 15 (IL-15) as Novel Biomarkers for Assessing Prostate Cancer Recurrence

In a previous study, researchers have identified inflammatory chemokines

that act as biomarkers for distinguishing patients with high risk of developing biochemical prostate cancer recurrence. To test their hypothesis, Blum et al. (2008) conducted a study that included 82 subjects with biochemical recurrence within 5 years of prostatectomy. Furthermore, the control group was composed of 98 subjects that did not develop prostate cancer recurrence after a prostatectomy. Researchers used Multiplex Elisa to analyze and distinguish the expression of chemokines between these two populations (control and experimental subjects). Blum et al. (2008) found that the inflammatory cytokines Macrophage inflammatory protein-1β (CCL4) and Interleukin-15 (IL-15) were differentially expressed among patients that had prostate cancer recurrence. Specifically, CCL4 was found to be upregulated in patients that developed biochemical recurrence within five years of a prostatectomy and IL-15 was found to be downregulated in such patients. Even though these different findings suggest that these chemokines may be considered independent predictors of prostate cancer recurrence, the combination of chemokines with other clinicopathologic variables (such as prostate-specific antigen, Gleason score, surgical margin, and seminal vesicle status) was able to better distinguish patients at risk for prostate cancer recurrence. To bring these biomarkers into the clinic and potentially aid in the better detection of prostate cancer recurrence, further research is needed to elucidate the role of CCL4 and IL-15 in prostate cancer. This study looks at how CCL4 and IL-15 modulate gene expression patterns in prostate cancer tumors.

Chapter 9: Macrophage Inflammatory Protein 1β (CCL4)

The chemokine CCL4, also known as Macrophage Inflammatory Protein 1β, is a member of the largest family of chemokines: CC-chemokine ligand (CCL). It is located on chromosome 17 and closely related to the other CC-chemokine ligand protein Macrophage Inflammatory Protein 1α (also known as CCL3). Both CCL4 and CCL3, known as Macrophage Inflammatory Protein1 (MIP1), were discovered as a protein doublet in 1988 by the Cerami laboratory and named due to its inflammatory properties (Wolpe et al., 1988). Further characterization resulted in two distinct proteins that have deviating signal capabilities despite their 68% similarity in primary protein structure. Mature human CCL4 is composed of 69 residues with a molecular weight of 7.8 kD. It is manufactured and secreted by activated macrophages, B cells, and T cells and function to attract inflammatory cells, including macrophages, to the location of inflammation (Krzysiek et al., 1999). NK cells, mast cells, neutrophils, dendritic cells, and B and T lymphocytes can also produce large amounts of MIP1 proteins (Oliva et al., 1998; Lapinet et al., 2000; Sallusto et al., 1999). As indicated by Maurer and von Stebut (2004), other cells can also produce smaller amounts of MIP1 proteins. They also state that the production and excretion of MIP1 proteins usually requires cell activation, which can be mediated by the pro-inflammatory proteins TNFα, IFNγ, and IL-1α and β.

CCL4 is well known for mediating chemotactic and pro-inflammatory responses, but it has also been implicated in homeostasis (Maurer and von Stebut, 2004). It mediates its effects by binding to its receptor, CC-chemokine receptor 5

(CCR5), with high affinity (Saika et al., 2012). CCR5 has been found to be highly expressed on memory T cells, NK cells, and dendritic cells (Lee et al., 1999). Additionally, CCR5 has been found to be expressed in monocytes and macrophages, CD3+ lymphocytes, CD4+ lymphocytes, CD8+ lymphocytes, T helper 1 lymphocytes, and CD34+ bone marrow cells (Menten et al., 2002). Binding to CCR5, a cell surface CC chemokine receptor and G-protein coupled receptor, leads to signal transduction events that can ultimately lead to the activation of the PI3K signaling pathway as well as the MAP kinases and JAK/STAT signaling cascades. The downstream events modulated by CCL4 have not been well characterized.

CCL4 has been shown to be a potent lymphocyte chemoattractant (Menten et al., 2002) that is up-regulated under inflammatory conditions. It can orchestrate inflammatory reactions by principally recruiting other inflammatory cells, including (but not limited to) monocytes, NK cells, and dendritic cells. CCL4 can also mediated inflammatory responses through its role in the differentiation of T helper cells. According to Maurer and von Stebut (2004), CCR5 activation by CCL4 can also lead to an increased expression of inflammatory markers and pro-inflammatory mediators.

CCL4 has been found to be highly expressed in some cancers, including gastric cancer (Saito et al., 2003). As previously mentioned, CCL4 was found to be upregulated in patients with prostate cancer recurrence. Recent data from our group show that CCL4 increases PC3 cell migration and 22RV1 cell invasion. Additionally, CCL4 increases tumor volume in an *in vivo* prostate cancer xenograft

model with 22RV1 (androgen-dependent) cells. Its effects appear to be mediated through the androgen receptor, since tumors with PC3 cells that were posteriorly treated with CCL4 were not significantly larger compared to the control group. Other researchers have found that the androgen receptor-CCL4-STAT3 signaling axis is a key regulator of prostate tumor origination (Fang et al., 2013). Additionally, Prostate cancer tumors with the 22RV1 cell line show increased angiogenesis and express higher levels of phospho-histone 3 and desmin. In order have a better understanding of the role of CCL4 in prostate cancer, we must explore the transcriptional changes that are being mediated at a molecular level. Thus, this project aims to elucidate the target genes related to metastasis or a specific pathway whose activation is directly modulated by CCL4 in prostate cancer.

Chapter 10: Interleukin 15 (IL-15)

The chemokine Interleukin 15, also known as IL-15, is a member of the four α-helix bundle cytokine family and was concurrently co-discovered by the Waldmann and Giri laboratories in 1994 (Burton et al., 1994; Grabstein et al., 1994). Originally, it was described as a novel T cell growth factor and lymphokine that shared components of the IL-2 receptor. We now know that IL-15 is a 14-15 kDa glycoprotein that encoded on chromosome 4q31. Furthermore, we also know that there are two IL-15 mRNA isoforms that produce the same mature protein, but differ in the lengths of their signal peptides (Steel et al., 2012). The isoform with the long signal peptide is targeted to the secretory pathway, whereas the mRNA

isoform with the short signal peptide is not secreted. Instead, it remains in the cytoplasm or nucleus, where it can modulate transcription (Tagaya et al., 1997). Although the production of IL-15 can be regulated through transcription, evidence points out that the majority of the regulation occurs post-transcriptionally (Burton et al., 1994). IL-15 translation must be tightly regulated in order to avoid autoimmunity, since IL-15 has the capability to induce potent cytokines, such as tumor necrosis factor alpha and interferon-γ (Steel et al., 2012; Waldmann, 2004).

IL-15 signals through a heterotrimeric receptor, IL-15R, which is comprised of α, β, and γc chains. The IL-15Rβ chain (CD122) shared with the Interleukin-2 receptor, while the common gamma chain (CD132) is shared with the Interleukin-2, 4, 7, 9, and 21 receptors. Thus, the alpha chain bestows IL-15 its receptor specificity (Giri et al., 1995). Instead of directly interacting with IL-15R in the cellular membrane, the bioactivity of IL-15 is conferred through a trans-presentation mechanism where a complex of IL-15 and the alpha subunit of the receptor is presented to NK, NKT, or T cells (Wu, 2013). IL-15 alpha expression is independent of IL-15R beta or common gamma chain. Pilipow et al. states that although the IL-15Rβγ complex is found in target cells, IL-15Rα can be found on the surface of distinct types of cells, including endothelial cells, activated monocytes, and dendritic cells. Activation of the IL-15 receptor has been linked to the activation of multiple signaling pathways such as: JAK/STAT, Ras/MAPK, and PI3K pathway (Menten et al., 2002; Huntington et al., 2007; Miyazaki et al., 1994; Miyazaki et al., 1995; Adunyah et al., 1997; Saika et al., 2012; Johnston et al., 1995; Pilipow et al., 2015). In lymphocytes, exposition of membrane-bound IL-15

to IL-15Rβ-γc can result in the expression of *bcl-2*, *c-myc*, *c-fos/jun* and activation of NF-κB.

IL-15 plays an important role in immunobiology due to its involvement in the development and proliferation of several innate and adaptive immune cells, as reviewd by Steel et al. IL-15 can stimulate the propagation of activated CD4-CD8-, CD4+CD8+, CD4+, and CD8+ T cells. Furthermore, IL-15 has been known to promote durability of antigen-specific CD8+ T cells, preservation of CD8+CD44hi memory T cells, activation of γδ T cells, and act as an anti-apoptotic factor for T cells (Marks-Konczalik et al., 2000; Oh et al., 2008; Kanegane and Tosato, 1996; Ribot et al., 2014). IL-15 also modulates NK-cell proliferation and subsequent activation (Waldmann and Tagaya, 1999), aside from providing vital positive homeostatic roles, whose importance can be noted in knockout mice models that lack IL-15 or IL-15R alpha (Lodolce et al., 1998; Kennedy et al., 2000). Effects on other components of the immune system include: protecting neutrophils and mast cells from apoptosis, acting as a growth factor for mast cells, inducing B lymphocyte propagation and differentiation, increasing antibody secretion, and permitting partially CD4-independent induction of immunoglobulin responses (Tagaya et al., 1996; Armitage et al., 1995).

Due to its effects as a powerful immunostimulatory chemokine, IL-15 may have an important role in immunosurveillance in cancer. Although IL-15 is not associated with positive outcomes in hematological malignancies (Steel et al., 2012), administration of IL-15 has shown anti-tumor effects in mice tumor models

(Munger et al., 1995; Oh et al., 2003; Zhang et al., 2009; Yu et al., 2010). IL-15 has been called the "cancer cure cytokine" (Wu, 2013), and clinical trials have begun to use IL-15 as a treatment against cancer, including metastatic melanoma and renal cell carcinoma. Patients have shown an improvement in the responsiveness of host CD8+ T cells, NK cells, and production of memory T cells with high avidity and long half-life (Pilipow et al., 2015).

Studying the role of IL-15 in prostate cancer is important, since increased levels of circulating IL-15 have been found in patients with early stage prostate cancer as compared with patients with benign prostatic hyperplasia (Mengus et al., 2011) and since IL-15 has been implicated as a biomarker that may help predict prostate cancer recurrence (Blum et al., 2008). Nevertheless, few studies have explored the role of IL-15 in prostate cancer. These have shown that IL-15 augments anti-tumor action through NK and CD8+ cells propagation and activation in prostate cancer cell lines (Wu and Xu, 2010; Wu et al., 2004; Suzuki et al., 2001) and that IL-15 reverses Wilms' tumor antigen-specific CTL's unresponsiveness in prostate cancer patients (King et al., 2009). Additionally, IL-15 can increase dendritic cell survival in the tumor microenvironment, which has been demonstrated to be almost lacking of dendritic cells, through an augmented expression of Bcl-x(L), an anti-apoptotic protein, and an enlarged resistance of dendritic cells to prostate cancer-induced cell death (Pirtskhalaishvili et al., 2000). Data from our group indicate that IL-15 decreases cell motility. In tumors, Immunohistochemical analysis revealed that IL-15 decreases phospho histone 3 expression and increases neutrophil infiltration, adiponectin expression, desmin,

and alpha smooth muscle actin. This data hints that IL-15 possibly decreases prostate cancer metastasis. Although previous research projects have focused on studying the effects that are indirectly mediated by IL-15 though immune cells, this project aims to elucidate the transcriptional changes mediated by IL-15 independently of the adaptive immune response in prostate cancer.

Chapter 11: The PI3-Kinase Signaling Pathway is linked to Prostate Cancer Development

The phosphatidylinositol 3-kinase (PI3K) pathway is frequently mutated in cancer. The PI3K pathway, which is evolutionarily conserved from yeast to mammals, regulates diverse cellular processes in higher eukaryotes including: metabolism, survival, proliferation, apoptosis, growth, and cell division Chalhoub and Baker, 2009). The pathway is also critical for cell growth control, one of the necessary signals for cancer cells to grow and divide along with a loss of restraints on cell-cycle progression. Although the PI3K Signaling pathway is activated by various extracellular signal proteins (such as insulin and insulin-like growth factors) in non-cancerous cells, the pathway is normally activated by a mutation in cancer cells. This mutation permits cell growth even in the absence of extracellular signal proteins (Alberts, 2015). Aside from a mutation, the pathway can be activated by high levels of insulin in the bloodstream, abnormal activation of a growth factor receptor, and/or a loss of the Phosphatase and tensin homolog (PTEN) phosphatase tumor-suppressor gene (Alberts, 2015). The PTEN phosphatase

gene codes for an enzyme that inhibits the PI3K signaling pathway by dephosphorylating the phosphatidylinositol (3,4,5)-triphosphate (PIP$_3$) molecules that the PI3KF forms (Alberts, 2015). As a result of the activation of the PI3K Signaling pathway, the protein kinases Protein Kinase B (PKB) and Mechanistic Target Of Rapamycin (mTOR) are also activated. Their activation stimulates protein synthesis, increases glucose uptake by the cell, and increases production of the acetyl CoA in the cytosol, which is necessary for cell lipid synthesis (Alberts, 2015).

In response to extracellular signaling cues, class I PI3Ks catalytic subunits are recruited to activated membrane receptors. The activated PI3Ks then catalyze the formation of the second messenger PIP$_3$ from the membrane-bound phospholipid Phosphatidylinositol 4,5-bisphosphate (PIP$_2$). PIP$_3$ subsequently binds to the pleckstrin homology (PH) domains of proteins; activating signals and recruiting the proteins to the membrane (Engelman et al., 2006; Chalhoub and Baker, 2009). PKB also interacts at the plasma membrane with PIP$_3$ by means of a PH domain. PKB undergoes a change in conformation after interacting with PIP$_3$. This change in conformation makes PKB a substrate for another PIP$_3$-bound kinase (PDK1) that phosphorylates PKB. PKB is also phosphorylated by a second kinase, most likely mTOR. After being phosphorylated twice, PKB is activated and subsequently dissociated from the plasma membrane; it can move to the cytosol and nucleus and interact in diverse signaling pathways (Karp, 2013). These pathways can ultimately result in the arrangement of the cytoskeleton, cell growth,

translation, apoptosis, cell-cycle arrest, DNA repair, and changes in glucose metabolism (Chalhoub and Baker, 2009).

A wide range of human cancers are associated with the PI3K signaling pathway, including: prostate, breast, endometrium, colon, urinary tract, upper aerodigestive track, ovary, stomach, liver, esophagus, pancreas, central nervous system, hematopoietic and lymphoid tissue, lung, skin, and thyroid (Table 1 – Appendix). The biggest percentage of tumors with PI3K mutations, however, can be seen in prostate cancer. About 40% of primary and 70% of metastatic prostate cancers have genomic alterations in the PI3K signaling pathway. This pathway is therefore considered one of the major drivers of prostate cancer growth (Marques et al., 2015).

The activation of PKB in prostate cancer is frequently linked to the loss of tumor suppressor Phosphatase and tesin homologue delete in chromosome *ten* (PTEN) (Axanova et al., 2010; Li et al., 2005; Rubin et al., 2000). About 20% of primary prostate cancer tumors have a loss of PTEN protein; this statistic also correlates with a 50% of metastatic tumors experiencing a loss of PTEN protein (Engelman et al., 2006; Sansal and Sellers, 2004). Progression of prostate cancer may be associated with PTEN loss or accumulation of mutations in the PTEN gene (Engelman et al., 2006); this results in increased activity of the PI3K signaling pathway (Chalhoub and Baker, 2009).

Chapter 12: Using a xenograft model with the 22RV1 human prostate cancer cell line in SCID mice to study the transcriptional patterns modulated by CCL4 and IL-15 in prostate cancer

As stated above, the PI3K signaling pathway can be clearly linked to prostate cancer. Inflammation has also been linked to the etiology and progression of prostate cancer; in part because of the presence of chemokines, such as CCL4 and IL-15, which are differentially expressed in patients with prostate cancer recurrence. However, in the presence of CCL4 or IL-15, the PI3K signaling pathway has not been linked to prostate cancer and inflammation. This project studies the gene expression patterns associated with the PI3K pathway and cancer metastasis in tumors treated with CCL4 or IL-15.

Part A: Hypothesis

We expect to detect an upregulation of the oncogenes and the genes associated with apoptosis inhibition and cell survival in the PI3K signaling pathway in tumors treated with CCL4. We also expect to detect an upregulation in the genes associated with cell proliferation and cancer metastasis in tumors treated with CCL4. On the other hand, we expect IL-15 to adversely effect the genes related to the PI3K signaling pathway; causing the downregulation of oncogenes and genes associated with apoptosis inhibition, cell survival, cell proliferation, and cancer

metastasis. By helping to elucidate the mechanisms of action of CCL4 and IL-15 in prostate cancer, this project will contribute to the field of prostate cancer research and will eventually have important implications for future therapeutics.

Part B: Xenograft model with the 22RV1 cell line in SCID mice

In order to test our hypothesis, we used an orthotopic xenograft model with the 22RV1 human prostate cancer cell line in SCID mice. SCID mice fail to develop B and T lymphocytes due to a flaw in gene rearrangement (*see Chapter 4, Part B*). For such reason, these mice are immunocompromised and cannot deliver a proper adaptive immune response. They have been used to create models of human tumor cell metastasis (Yano et al., 1996), including human prostate cancer cells (Klein et al., 1997; Sato et al., 1997). Although these mice do not have functional B or T lymphocytes, they do contain the other immune cells associated with a primary immune response, including macrophages, neutrophils, and NK cells. This controlled model allows us to study the biological effects of CCL4 or IL-15 independently of the adaptive immune response. Aside from the mouse model, the 22RV1 human prostate carcinoma cell line, which is derived from the human prostatic carcinoma xenograft CWR22R (Sramkoski et al., 1999), was chosen for the orthotopic xenograft model due to the known importance of androgen and its receptor in prostate cancer progression.

Methods and Materials

Orthotopic Mouse Model

Male ICR-SCID mice (7-8 weeks old) were housed and maintained in a pathogen-free environment at The University of Puerto Rico Medical Sciences Campus animal facility, under the Institutional Animal Care and Use Committee regulations. Animals received food and water ad libitum with a 12-hour light cycle. An orthotopic xenograft model in which 22RV1 (250,000 cells) were injected in the anterior prostate lobes of ICR-SCID mice (IcrTac:IcrCrl-SCID) (Taconic,

Germantown, NY, USA) was used to develop 2 prostate tumors per mice. Cell suspensions in PBS were placed in 30 µL of collagen I (Becton Dickinson, Franklin Lakes, NJ, USA) and allowed to partially solidify to hold cells in place and reduce leakage in the peritoneal cavity during surgery. Mice were intraperitoneally injected bi-weekly with CCL4 (0.001 or 0.1 ng/mL), IL-15 (0.001 or 0.1 ng/mL), or vehicle (Saline). At 4 weeks of treatment, tumors were collected. Tumor volume was determined using caliper measurements. Results were analyzed using the student's t-test at a 95 % confidence interval. $n_{control}$=26 tumors, n_{CCL4}=21 tumors, n_{IL-15}=20 tumors .

Tissue Collection and Processing

Tumor samples ($n_{control}$=26 tumors, n_{CCL4}=21 tumors, n_{IL-15}= 20 tumors) were collected and divided in two sections. The frozen tissue section was used to isolate RNA for gene expression assays.

RNA Isolation

RNA was extracted and purified from frozen mice tumors using the RNeasy Mini Kit (Qiagen Inc., Valencia; CA, USA). The resultant RNA was

spectrophotometrically quantified and qualified at 260 and 280 nm on a Nanodrop spectrophotometer. Gel analysis was performed as well. All of the collected RNA was stored at -80°C after quantitation.

Gene Expression Analysis and Confirmation

A. Arrays

To evaluate changes in gene expression at the RNA level, the Qiagen RT^2 PCR arrays (human tumor metastasis and PI3K pathway) were used (Qiagen Inc., Valencia; CA, USA). RNA (2 μg per array) was copied to cDNA using the RT^2 First Strand Kit including DNA elimination procedure (Qiagen Inc., Valencia; CA, USA). Results were analyzed using the MS Excel based tool provided by Qiagen (PCR Array Analysis V4, available for download at https://www.qiagen.com/us/resources/resourcedetail?id= d8d1813e-e5ba-4d29-8fdf-07a3f4227e0a&lang=en).

B. Confirmation

Complementary DNA (cDNA) was synthesized from previously extracted RNA using the iScript cDNA Synthesis Kit (Bio-Rad, Hercules, CA, USA). To validate results, quantitative Real time PCR (qRT-PCR) was performed under standard conditions using the Step One Plus Real-time PCR System (Applied Biosystems, Carlsbad; CA, USA). Real-time PCR was performed using SYBR super mix (Bio-Rad, Hercules, CA, USA) in a total volume of 10 μL. Depending on

the gene of interest the cycle was, at 95 °C for 15 seconds and 62 °C for 1 minute or 95 °C for 15 seconds and 56 °C for 1 minute. PCR efficiency was examined using serial dilutions of the template cDNA and the melting curve data was collected for PCR specificity. GAPDH was used as housekeeping gene. Results were quantified using the $\Delta\Delta C_t$ method. No PCR product was detected in control samples in which the template was omitted. Primer sequences are available upon request. PCR arrays: n = 3 tumors per group, randomly chosen. Real-time PCR confirmation: n = 5 representative tumors per group.

Statistical Analysis

All data are presented as means ± standard deviations. Unpaired student t-tests were employed in the statistical analysis of gene transcript expression. Outliers were identified and eliminated using the ROUT method, Q = 1%.
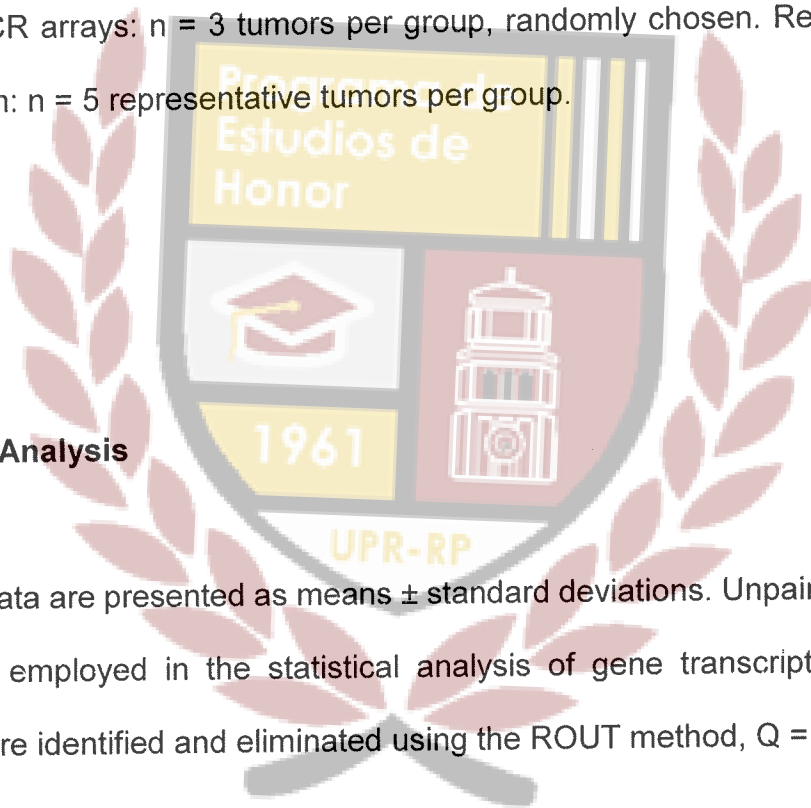
Results:

An orthotopic xenograft model in which SCID mice were injected with 250,000 22RV1 (androgen-dependent) cells in the anterior prostate lobes was performed. CCL4 or IL-15 were administered bi-weekly at 0.001 ng/mL or 0.1 ng/mL with intraperitoneal injections during four weeks. Tumor tissue was collected; a total of two prostatic tumors were obtained per mouse. One of the tumors was used for RNA analysis; the other one was embedded with paraffin and sectioned for future immunohistochemical analysis experiments. RNA was extracted from one of the tumors (from each mice) and its concentration was quantified.

Part A: CCL4 modulates genes related to cancer metastasis and the PI3K signaling pathway

Before studying the gene expression patterns related to the PI3K signaling pathway and cancer metastasis that are modulated by CCL4, we decided to study the mRNA expression of CCR5, CCL4's receptor. As seen in Figure 1, CCR5 mRNA expression was not significantly modulated by CCL4 as confirmed by real time PCR.

We then proceeded to performing the Tumor Metastasis PCR Array. The Volcano Plot provided by the MS Excel based tool for the Tumor Metastasis PCR Array can be seen in Figure 2, where the black line indicates a fold change in gene expression of one, the pink lines indicate a fold change of two, and the blue lines indicate a p value of the t-test of 0.05. The numerical results of the array can be seen in Table 1. Because only one gene surpassed the desired fold change and p value (2 and 0.05, respectively), we decided to exclusively use the fold change values to elect which genes were going to be confirmed through real time PCR. Out of all the genes in Table 1, we decided to confirm the following genes in the Tumor Metastasis Array: BRMS1, FN1, MCAM, MMP10, MMP11, MMP13, NR4A3, and RORB. ITGA7 and CXCR2, although part of the array, had been previously confirmed by the lab and found to be upregulated in prostate cancer tumors treated with CCL4 0.001 ng/mL (*data not shown*; Rohena-Rivera et al. (2016)). After confirming the list of genes through real time PCR, we were able to corroborate that BRMS1 mRNA expression is upregulated by CCL4 0.001 ng/mL

in prostate cancer tumors (Figure 3A). FN1, MCAM, MMP10, MMP11, MMP13, NR4A3, and RORB mRNA expression is not differentially expressed in prostate cancer tumors treated with CCL4 (Figure 3B).

After studying the mRNA expression of genes in the Tumor Metastasis Array, we proceeded to performing the PI3K PCR Array with RNA from the prostate cancer tumors treated with CCL4 0.001 ng/mL and 0.1 ng/mL. The Volcano Plot provided by the MS Excel based tool for the PI3K PCR Array can be seen in Figure 4, where the black line indicates a fold change in gene expression of one, the pink lines indicate a fold change of two, and the blue lines indicate a p value of the t-test of 0.05. The numerical data for the array can be seen in Table 2. Once again, we decided to use the fold change values to choose the genes that would be confirmed through real time PCR. From the list of genes in Table 2, we decided to confirm the following genes in the PI3K Array through real time PCR: FOS, IGF1R, PRKCA, and RPS6KA1. As seen in Figure 5, FOS mRNA was found to be induced by CCL4 at concentrations of 0.001 and 0.1 ng/mL (p value= 0.027 and 0.016, respectively). PRKCA mRNA was also upregulated by CCL4, but only at a concentration of 0.001 ng/mL (p value=0.013). IGF1R and RPS6KA mRNA expression was not differentially expressed in prostate cancer tumors treated with CCL4.

We proceeded to asking ourselves whether the effects of CCL4 on the PI3K signaling pathway were mainly in genes found downstream, or whether CCL4 also induced the pathway upstream. For such reason, we decided to evaluate the mRNA expression of the following genes: AKT1, AKT2, AKT3, MTOR, PI3Kα, and

34

PI3Kβ. After performing real time PCR experiments, our data indicated that CCL4 induces PI3Kα and AKT1 mRNA expression at a concentration of 0.001 ng/mL (Figure 6; p value= 0.009 and 0.045, respectively). PI3Kβ, MTOR, AKT2, and AKT3 mRNA expression was not differentially expressed in prostate cancer tumors treated with CCL4.

Finally, knowing that CCL4 and IL-15 were both differentially expressed in patients with biochemical prostate cancer recurrence (CCL4 was upregulated and IL-15 was downregulated), we decided to study whether CCL4 decreased IL-15 or IL-15Rα mRNA expression. Our results, seen in Figure 7, indicate that CCL4 does not significantly modulate IL-15 or IL-15Rα mRNA expression, as confirmed by real time PCR. The summaries for fold change and p values of genes that are modulated by CCL4 at concentrations of 0.001 and 0.1 ng/mL can be seen in Tables 3 and 4, respectively. A visual summary of the genes that are differentially expressed in prostate cancer tumors treated with CCL4 can be appreciated in Figure 8.

Part B: IL-15 modulates genes related to the PI3K signaling pathway and cancer metastasis

We performed the PI3K signaling pathway Array with RNA extracted from prostate cancer tumors treated with IL-15 at concentrations of 0.001 or 0.1 ng/mL. The Volcano Plot provided by the MS Excel based tool for the PI3K Array can be

appreciated in Figure 9, where the black line indicates a fold change in gene expression of one, the pink lines indicate a fold change of two, and the blue lines indicate a p value of the t-test of 0.05. The numerical data from the array can be seen in Table 5. We decided to confirm the following genes through real time PCR based on the fold change values in Table 5: AKT3, BTK, CCND1, CD14, FASLG, FOXO3, HSPB1, IGF1, IGF1R, ILK, IRS1, MAP2K1, PDGFRA, PIK3CG, PIK3R1, PIK3R2, PTEN, and TLR4. As can be seen in Figures 10A and 10G, IL-15 0.001 ng/mL induces the mRNA expression of AKT1 and PTEN (p values= <0.0001 and 0.0002, respectively). IL-15 0.1 ng/mL, on the other hand, induces the expression of the following genes: CCND1, CD14, FASLG, IGF1, and IRS1 (Figure 10, p values= 0.0222, 0.0027, 0.0176, 0.0049, and 0.0035; respectively. FOXO3, HSPB1, IGF1R, ILK, MAP2K1, PIK3CG, PIK3R1, PIK3R2, and TLR4 mRNA expression is not significantly modulated by IL-15 (Figure 10H).

We proceeded to studying genes related to the degradation of the extracellular matrix due to the importance of this process in cancer metastasis. Both MMP2 and MMP9 mRNA expression was found to be upregulated in prostate cancer tumors treated with IL-15 as compared to the control (Figure 11A and B, P-values= 0.0053 and 0.0043, respectively). On the other hand, our real time PCR experiments showed that MMP11, TIMP2, and TIMP3 mRNA expression is not significantly modulated by IL-15 (Figure 11C). The summaries for fold change and p values of genes that are modulated by IL-15 at concentrations of 0.001 and 0.1 ng/mL can be seen in Tables 6 and 7, respectively. A visual summary of the genes

that are differentially expressed in prostate cancer tumors treated with IL-15 can be appreciated in Figure 12.

Discussion:

This study aimed to characterize the transcriptional patterns related to the PI3K signaling pathway or cancer metastasis and regulated by CCL4 or IL-15 in prostate cancer. Because CCL4 was over-expressed in patients with prostate cancer recurrence (Blum et al., 2008), we hypothesized it was associated with prostate cancer malignancy and would therefore upregulate oncogenes or genes associated with apoptosis inhibition, cell survival, cell proliferation, and cancer metastasis. On the other side, since IL-15 was downregulated in such patients (Blum et al., 2008), we expected it to be associated with better prostate cancer

37

prognosis. We also hypothesized that IL-15 would cause the downregulation of oncogenes and genes associated with apoptosis inhibition, cell survival, cell proliferation, and cancer metastasis.

As shown by PCR array analysis and real time PCR confirmation, CCL4 altered the expression of genes related to the PI3K signaling pathway and cancer metastasis. It is important to acknowledge that the effects of CCL4 in prostate cancer are concentration dependent – both concentrations used (0.001 ng/mL and 0.1 ng/mL) yielded different gene expression patterns. One of the genes that was activated at both concentration, FOS, has previously been linked with cancer progression. As reviewed by Mahner et al. (2008), members of the FOS family dimerize with Jun to form Activating Protein 1 (AP-1), a transcription factor. Furthermore, they explain that FOS has been linked to cell differentiation and proliferation through signal transduction. Other studies have found that FOS promotes tumorigenesis by decreasing the expression of tumor-suppressor genes and inducing cancer invasion and cell growth (Bakin and Curran, 1999; Hu et al., 1994). In androgen-independent prostate cancer, elevated levels of c-FOS have been found (Edwards et al., 2004). These, in turn, correlate with augmented proliferation and invasiveness of prostate cancer cells. The results of our study suggest that CCL4 may promote prostate cancer invasiveness through its effects on the activation of FOS. Another gene that has been associated with prostate cancer and is was over-expressed at low CCL4 concentration is PRKCA. PRKCA has been linked to apoptosis modulation and cell proliferation in prostate cancer (Lahn et al., 2004). The effects of PRKCA on apoptosis, nonetheless, have been

shown to depend on hormone responsiveness, since the LNCaP (hormone-responsive) prostate cell line induces apoptosis while the hormone-insensitive PC3 cell line is associated with apoptosis inhibition. Further studies are needed to characterize the effects of PRKCA in apoptosis and proliferation in the cell line used for our xenograft model, 22RV1. BRMS1, upregulated in tumors treated with CCL4 0.1 ng/mL, is a tumor suppressor gene that suppresses cancer metastasis without constraining its tumorigenicity (Meehan et al., 2004). Although these results do not directly support our hypothesis, they can be expected since CCL4 can potentially activate a wide range of genes that can also be involved in signal transduction. Finally, other two genes that are upregulated at low CCL4 concentrations are PI3KA and AKT1. As mentioned in the introduction, one of the pathways that are prominently activated in early stages of prostate cancer is the PI3K-AKT signaling pathway, which is associated with cell growth and survival. The over-expression of these genes in tumors treated by CCL4 supports our hypothesis and the current literature that links this pathway with prostate cancer progression. Together, these results suggest that CCL4 controls transcriptional patterns that promote negative events in prostate cancer.

Also shown by PCR array analysis and confirmed through real time PCR, IL-15 altered the expression of genes related to the PI3K signaling pathway and cancer metastasis. Even though we expected to se a downregulation of genes associated with the PI3K signaling pathway, we saw an upregulation of AKT3 mRNA. AKT3 is a serine/threonine protein kinase that modulates diverse cell responses. Levels of phosphorylated AKT have previously been correlated with

increased Gleason score (Hammarsten et al., 2012). A recent study suggests that AKT3 promotes the growth proliferation of cancer cells independent of AKT1 or AKT2 (Lin et al., 2015). In line with those results, tumors treated with IL-15 also had increased levels of CCND1 mRNA. The CCND1 encodes the protein Cyclin-D1, which is necessary for the cell cycle to progress across G1 phase (Baldin et al., 1993). Upregulation of ATK3 has previously been linked to an increase in Cyclin D1 (Lin et al., 2015). This suggests that IL-15 may mediate progression of the cell cycle though its effect in AKT3 and CCND1 mRNA. IL-15 also upregulates the mRNA expression of MMP2 and MMP9, two metalloproteinases that are involved in the degradation of extracellular matrix proteins. MMP2 has been established as a predictor of decreased prostate cancer-free survival (Trudel et al., 2003) and its expression has been associated with prostate cancer malignancy grade (Xie et al., 2015). Moreover, the upregulation of MMP9 has been linked to invasiveness in the LNCaP prostate cancer cell line (Aalinkeel et al., 2011). Thus, it appears that IL-15 can mediate negative outcomes in prostate cancer.

As hypothesized, IL-15 also modulates genes that may be associated to a better prostate cancer prognosis. Our results show that IL-15 induces IGF1 mRNA expression in prostate cancer tumors. IGF1 is necessary for prostate growth and development in rats and mice. It also has an important role in stimulating the proliferation of epithelial cells extracted from human prostates (Roberts, 2004). Although increased levels of IGF1 have been suggested as predictors for prostate cancer risk (Wolk et al., 1998), and even though IGF1 is important for prostate cancer initiation, diminished IGF expression and downregulation of the IGF1

receptor has been associated with advanced cancer metastasis (Roberts, 2004). Since we are using a mouse model that already has prostate cancer and since we are aiming to study prostate cancer recurrence, the increased expression of IGF1 in prostate cancer tumors treated with IL-15 may serve a protective function against advanced cancer metastasis. As with IGF1, IL-15 also induces the expression of IRS1, a gene associated with PI3K activation, cytoskeleton organization, and prostate cancer risk and etiology (Neuhausen et al., 2005). In LNCaP cells, the expression of IRS1 augments cell adhesion and diminishes cell motility independent of IGF1 and dependent of PI3K (Reiss et al., 2001). Reiss et al. (2000) interprets a loss of LNCaP IRS1 expression as a mechanism used to increase metastasis. The results from our experiments suggest that IRS1 upregulation may help protect against metastasis, but future experiments are needed to confirm this. Usually, aside from having decreased levels of IGF1 and IRS1, prostate cancer cells have mutations in the PTEN, a gene that encodes a protein whose role is the inhibition of the PI3K pathway. Our results show that IL-15 induces PTEN mRNA expression, thus contributing to the downregulation of such pathway that is normally very active in cancer. Aside from the genes that were previously mentioned, IL-15 also induces the expression of FASLG, a gene involved in Fas-mediated apoptosis, which has been explored as a strategy against prostate cancer (Nakanishi et al., 2003; Hedlund et al., 1999; Rubinchik et al., 2001; Schimmer et al., 2006; Hyer et al., 2003; Hsieh, 2009; Hedlund et al., 1998). Thus, this gene may be involved in the promotion of prostate cancer apoptosis in tumors treated with IL-15. Furthermore, tumors treated with IL-15 also

had increased levels of CD14 mRNA. CD14 is a monocyte marker that has been associated with low metastasis risk (Brandt et al., 1997). In prostate cancer patients, high percentages of myeloid-derived immunosuppressive CD14(+)HLA-DR(low/-) have been found (Vuk-Pavlović et al., 2010; Brusa et al., 2013). Further studies are needed to characterize the effects of CD14 upregulation in prostate cancer.

In conclusion, this study provides an initial map of genes that may be modulated by CCL4 or IL-15 in prostate cancer. The determination of these differentially expressed genes can help elucidate the mechanisms underlying prostate cancer progression in tumors treated with CCL4 or IL-15. Furthermore, the characterization of the biological effects of these chemokines in prostate cancer is important to eventually introduce them into the clinic and complement current diagnostic methods. CCL4 and IL-15 may help differentiate between low grade and more aggressive cancers so unnecessary treatment is minimized and patients at risk of developing biochemical prostate cancer recurrence can be identified prior to the event.

The limitations of this study must also be acknowledged. It is important to note that these genes were only confirmed at mRNA and not protein level. Furthermore, it is important to remember that our model lets us study transcriptional patterns independently of the adaptive immune response. In order to draw a conclusion that can be extended to prostate cancer in humans, the expression of these genes must be confirmed in a model that has more direct relevance to humans. Future studies include confirming the expression of the

differentially expressed genes at a protein level. Furthermore, we will explore other pathways that are potentially regulated by CCL4 or IL-15 in prostate cancer, such as angiogenesis (for CCL4) and apoptosis (for IL-15).

References:

Aalinkeel, R., Nair, B.B., Reynolds, J.L., Sykes, D.E., Mahajan, S.D., Chadha, K.C., and Schwartz, S.A. (2011). Overexpression of MMP-9 contributes to invasiveness of prostate cancer cell line LNCaP. Immunol. Invest. *40*, 447–464.

Adunyah, S.E., Wheeler, B.J., and Cooper, R.S. (1997). Evidence for the involvement of LCK and MAP kinase (ERK-1) in the signal transduction mechanism of interleukin-15. Biochem. Biophys. Res. Commun. *232*, 754–758.

Affara, N.I., Ruffell, B., Medler, T.R., Gunderson, A.J., Johansson, M., Bornstein, S., Bergsland, E., Steinhoff, M., Li, Y., Gong, Q., et al. (2014). B cells regulate macrophage phenotype and response to chemotherapy in squamous carcinomas. Cancer Cell *25*, 809–821.

Alberts, B. (2015). Molecular biology of the cell: [MBOC] (New York, NY: GS, Garland Science).

American Cancer Society (2015). Cancer Facts & Figures 2015 (Atlanta: American Cancer Society).

Armitage, R.J., Macduff, B.M., Eisenman, J., Paxton, R., and Grabstein, K.H. (1995). IL-15 has stimulatory activity for the induction of B cell proliferation and differentiation. J. Immunol. Baltim. Md 1950 *154*, 483–490.

Axanova, L.S., Chen, Y.Q., McCoy, T., Sui, G., and Cramer, S.D. (2010). 1,25-dihydroxyvitamin D(3) and PI3K/AKT inhibitors synergistically inhibit growth and induce senescence in prostate cancer cells. The Prostate *70*, 1658–1671.

Bakin, A.V., and Curran, T. (1999). Role of DNA 5-methylcytosine transferase in cell transformation by fos. Science *283*, 387–390.

Baldin, V., Lukas, J., Marcote, M.J., Pagano, M., and Draetta, G. (1993). Cyclin D1 is a nuclear protein required for cell cycle progression in G1. Genes Dev. *7*, 812–821.

Blum, D.L., Koyama, T., M'Koma, A.E., Iturregui, J.M., Martinez-Ferrer, M., Uwamariya, C., Smith, J.A., Clark, P.E., and Bhowmick, N.A. (2008). Chemokine markers predict biochemical recurrence of prostate cancer following prostatectomy. Clin. Cancer Res. Off. J. Am. Assoc. Cancer Res. *14*, 7790–7797.

Brandt, B., Brinkmann, O., Griwatz, C., and Zanker, K.S. (1997). Circulating Prostate-Specific Antigen/CD14-Double-Positive Cells: a Biomarker Indicating Low Risk for Hematogeneous Metastasis of Prostate Cancer. JNCI J. Natl. Cancer Inst. *89*, 174–174.

Brusa, D., Simone, M., Gontero, P., Spadi, R., Racca, P., Micari, J., Degiuli, M., Carletto, S., Tizzani, A., and Matera, L. (2013). Circulating immunosuppressive cells of prostate cancer patients before and after radical prostatectomy: profile comparison. Int. J. Urol. Off. J. Jpn. Urol. Assoc. *20*, 971–978.

Burton, J.D., Bamford, R.N., Peters, C., Grant, A.J., Kurys, G., Goldman, C.K., Brennan, J., Roessler, E., and Waldmann, T.A. (1994). A lymphokine, provisionally designated interleukin T and produced by a human adult T-cell leukemia line, stimulates T-cell proliferation and the induction of lymphokine-activated killer cells. Proc. Natl. Acad. Sci. U. S. A. *91*, 4935–4939.

Chalhoub, N., and Baker, S.J. (2009). PTEN and the PI3-kinase pathway in cancer. Annu. Rev. Pathol. *4*, 127–150.

Davidsson, S., Ohlson, A.-L., Andersson, S.-O., Fall, K., Meisner, A., Fiorentino, M., Andrén, O., and Rider, J.R. (2013). CD4 helper T cells, CD8 cytotoxic T cells, and FOXP3(+) regulatory T cells with respect to lethal prostate cancer. Mod. Pathol. Off. J. U. S. Can. Acad. Pathol. Inc *26*, 448–455.

Edwards, J., Krishna, N.S., Mukherjee, R., and Bartlett, J.M.S. (2004). The role of c-Jun and c-Fos expression in androgen-independent prostate cancer. J. Pathol. *204*, 153–158.

Engelman, J.A., Luo, J., and Cantley, L.C. (2006). The evolution of phosphatidylinositol 3-kinases as regulators of growth and metabolism. Nat. Rev. Genet. *7*, 606–619.

Fang, L.-Y., Izumi, K., Lai, K.-P., Liang, L., Li, L., Miyamoto, H., Lin, W.-J., and Chang, C. (2013). Infiltrating macrophages promote prostate tumorigenesis via modulating androgen receptor-mediated CCL4-STAT3 signaling. Cancer Res. *73*, 5633–5646.

Frankel, T.L., Burns, W., Riley, J., Morgan, R.A., Davis, J.L., Hanada, K., Quezado, M., Rosenberg, S.A., and Royal, R.E. (2010). Identification and characterization of a tumor infiltrating CD56(+)/CD16 (-) NK cell subset with specificity for pancreatic and prostate cancer cell lines. Cancer Immunol. Immunother. CII *59*, 1757–1769.

Giri, J.G., Kumaki, S., Ahdieh, M., Friend, D.J., Loomis, A., Shanebeck, K., DuBose, R., Cosman, D., Park, L.S., and Anderson, D.M. (1995). Identification and cloning of a novel IL-15 binding protein that is structurally related to the alpha chain of the IL-2 receptor. EMBO J. *14*, 3654–3663.

Grabstein, K.H., Eisenman, J., Shanebeck, K., Rauch, C., Srinivasan, S., Fung, V., Beers, C., Richardson, J., Schoenborn, M.A., and Ahdieh, M. (1994). Cloning of a T cell growth factor that interacts with the beta chain of the interleukin-2 receptor. Science *264*, 965–968.

Hägglöf, C., and Bergh, A. (2012). The stroma-a key regulator in prostate function and malignancy. Cancers *4*, 531–548.

Hammarsten, P., Cipriano, M., Josefsson, A., Stattin, P., Egevad, L., Granfors, T., and Fowler, C.J. (2012). Phospho-Akt immunoreactivity in prostate cancer: relationship to disease severity and outcome, Ki67 and phosphorylated EGFR expression. PloS One *7*, e47994.

Hanahan, D., and Coussens, L.M. (2012). Accessories to the crime: functions of cells recruited to the tumor microenvironment. Cancer Cell *21*, 309–322.

Hanahan, D., and Weinberg, R.A. (2000). The hallmarks of cancer. Cell *100*, 57–70.

Hanahan, D., and Weinberg, R.A. (2011). Hallmarks of cancer: the next generation. Cell *144*, 646–674.

Hayflick, L. (1997). Mortality and immortality at the cellular level. A review. Biochem. Biokhimiia *62*, 1180–1190.

Hedlund, T.E., Duke, R.C., Schleicher, M.S., and Miller, G.J. (1998). Fas-mediated apoptosis in seven human prostate cancer cell lines: correlation with tumor stage. The Prostate *36*, 92–101.

Hedlund, T.E., Meech, S.J., Srikanth, S., Kraft, A.S., Miller, G.J., Schaack, J.B., and Duke, R.C. (1999). Adenovirus-mediated expression of Fas ligand induces apoptosis of human prostate cancer cells. Cell Death Differ. *6*, 175–182.

Hsieh, T.-C. (2009). Antiproliferative effects of resveratrol and the mediating role of resveratrol targeting protein NQO2 in androgen receptor-positive, hormone-non-responsive CWR22Rv1 cells. Anticancer Res. *29*, 3011–3017.

Hu, E., Mueller, E., Oliviero, S., Papaioannou, V.E., Johnson, R., and Spiegelman, B.M. (1994). Targeted disruption of the c-fos gene demonstrates c-fos-dependent and -independent pathways for gene expression stimulated by growth factors or oncogenes. EMBO J. *13*, 3094–3103.

Huntington, N.D., Puthalakath, H., Gunn, P., Naik, E., Michalak, E.M., Smyth, M.J., Tabarias, H., Degli-Esposti, M.A., Dewson, G., Willis, S.N., et al. (2007). Interleukin 15-mediated survival of natural killer cells is determined by interactions among Bim, Noxa and Mcl-1. Nat. Immunol. *8*, 856–863.

Hyer, M.L., Sudarshan, S., Schwartz, D.A., Hannun, Y., Dong, J., and Norris, J.S. (2003). Quantification and characterization of the bystander effect in prostate cancer cells following adenovirus-mediated FasL expression. Cancer Gene Ther. *10*, 330–339.

Inácio Pinto, N., Carnier, J., Oyama, L.M., Otoch, J.P., Alcântara, P.S., Tokeshi, F., and Nascimento, C.M. (2015). Cancer as a Proinflammatory Environment: Metastasis and Cachexia. Mediators Inflamm. *2015*, 791060.

Jeong, J.H., Bhatia, A., Toth, Z., Oh, S., Inn, K.-S., Liao, C.-P., Roy-Burman, P., Melamed, J., Coetzee, G.A., and Jung, J.U. (2011). TPL2/COT/MAP3K8 (TPL2) activation promotes androgen depletion-independent (ADI) prostate cancer growth. PloS One *6*, e16205.

Johnston, J.A., Bacon, C.M., Finbloom, D.S., Rees, R.C., Kaplan, D., Shibuya, K., Ortaldo, J.R., Gupta, S., Chen, Y.Q., and Giri, J.D. (1995). Tyrosine phosphorylation and activation of STAT5, STAT3, and Janus kinases by interleukins 2 and 15. Proc. Natl. Acad. Sci. U. S. A. *92*, 8705–8709.

Kanegane, H., and Tosato, G. (1996). Activation of naive and memory T cells by interleukin-15. Blood *88*, 230–235.

Karp, G. (2013). Cell and Molecular Biology Concepts and Experiments (New Jersey: John Wiley & Sons, Inc.).

Kennedy, M.A. (2010). A brief review of the basics of immunology: the innate and adaptive response. Vet. Clin. North Am. Small Anim. Pract. *40*, 369–379.

Kennedy, M.K., Glaccum, M., Brown, S.N., Butz, E.A., Viney, J.L., Embers, M., Matsuki, N., Charrier, K., Sedger, L., Willis, C.R., et al. (2000). Reversible defects in natural killer and memory CD8 T cell lineages in interleukin 15-deficient mice. J. Exp. Med. *191*, 771–780.

King, J.W., Thomas, S., Corsi, F., Gao, L., Dina, R., Gillmore, R., Pigott, K., Kaisary, A., Stauss, H.J., and Waxman, J. (2009). IL-15 can reverse the unresponsiveness of Wilms' tumor antigen-specific CTL in patients with prostate cancer. Clin. Cancer Res. Off. J. Am. Assoc. Cancer Res. 15, 1145–1154.

Klein, K.A., Reiter, R.E., Redula, J., Moradi, H., Zhu, X.L., Brothman, A.R., Lamb, D.J., Marcelli, M., Belldegrun, A., Witte, O.N., et al. (1997). Progression of metastatic human prostate cancer to androgen independence in immunodeficient SCID mice. Nat. Med. 3, 402–408.

Krzysiek, R., Lefèvre, E.A., Zou, W., Foussat, A., Bernard, J., Portier, A., Galanaud, P., and Richard, Y. (1999). Antigen receptor engagement selectively induces macrophage inflammatory protein-1 alpha (MIP-1 alpha) and MIP-1 beta chemokine production in human B cells. J. Immunol. Baltim. Md 1950 162, 4455–4463.

Lahn, M., Sundell, K., Gleave, M., Ladan, F., Su, C., Li, S., Ma, D., Paterson, B.M., and Bumol, T.F. (2004). Protein kinase C-alpha in prostate cancer. BJU Int. 93, 1076–1081.

Lapinet, J.A., Scapini, P., Calzetti, F., Pérez, O., and Cassatella, M.A. (2000). Gene expression and production of tumor necrosis factor alpha, interleukin-1beta (IL-1beta), IL-8, macrophage inflammatory protein 1alpha (MIP-1alpha), MIP-1beta, and gamma interferon-inducible protein 10 by human neutrophils stimulated with group B meningococcal outer membrane vesicles. Infect. Immun. 68, 6917–6923.

Lee, B., Sharron, M., Montaner, L.J., Weissman, D., and Doms, R.W. (1999). Quantification of CD4, CCR5, and CXCR4 levels on lymphocyte subsets, dendritic cells, and differentially conditioned monocyte-derived macrophages. Proc. Natl. Acad. Sci. U. S. A. 96, 5215–5220.

Li, L., Ittmann, M.M., Ayala, G., Tsai, M.-J., Amato, R.J., Wheeler, T.M., Miles, B.J., Kadmon, D., and Thompson, T.C. (2005). The emerging role of the PI3-K-Akt pathway in prostate cancer progression. Prostate Cancer Prostatic Dis. 8, 108–118.

Lin, H.-P., Lin, C.-Y., Huo, C., Jan, Y.-J., Tseng, J.-C., Jiang, S.S., Kuo, Y.-Y., Chen, S.-C., Wang, C.-T., Chan, T.-M., et al. (2015). AKT3 promotes prostate cancer proliferation cells through regulation of Akt, B-Raf, and TSC1/TSC2. Oncotarget 6, 27097–27112.

Liu, Y., Sæter, T., Vlatkovic, L., Servoll, E., Waaler, G., Axcrona, U., Giercksky, K.-E., Nesland, J.M., Suo, Z.-H., and Axcrona, K. (2013). Dendritic and lymphocytic cell infiltration in prostate carcinoma. Histol. Histopathol. 28, 1621–1628.

Lodolce, J.P., Boone, D.L., Chai, S., Swain, R.E., Dassopoulos, T., Trettin, S., and Ma, A. (1998). IL-15 receptor maintains lymphoid homeostasis by supporting lymphocyte homing and proliferation. Immunity 9, 669–676.

Mahner, S., Baasch, C., Schwarz, J., Hein, S., Wölber, L., Jänicke, F., and Milde-Langosch, K. (2008). C-Fos expression is a molecular predictor of progression and survival in epithelial ovarian carcinoma. Br. J. Cancer 99, 1269–1275.

Mandal, A. (2013). What are Cytokines?

Marks-Konczalik, J., Dubois, S., Losi, J.M., Sabzevari, H., Yamada, N., Feigenbaum, L., Waldmann, T.A., and Tagaya, Y. (2000). IL-2-induced activation-induced cell death is inhibited in IL-15 transgenic mice. Proc. Natl. Acad. Sci. U. S. A. 97, 11445–11450.

Marques, R.B., Aghai, A., de Ridder, C.M.A., Stuurman, D., Hoeben, S., Boer, A., Ellston, R.P., Barry, S.T., Davies, B.R., Trapman, J., et al. (2015). High Efficacy of Combination Therapy Using PI3K/AKT Inhibitors with Androgen Deprivation in Prostate Cancer Preclinical Models. Eur. Urol. 67, 1177–1185.

De Marzo, A.M., Platz, E.A., Sutcliffe, S., Xu, J., Grönberg, H., Drake, C.G., Nakai, Y., Isaacs, W.B., and Nelson, W.G. (2007). Inflammation in prostate carcinogenesis. Nat. Rev. Cancer 7, 256–269.

Maurer, M., and von Stebut, E. (2004). Macrophage inflammatory protein-1. Int. J. Biochem. Cell Biol. 36, 1882–1886.

McArdle, P.A., Canna, K., McMillan, D.C., McNicol, A.-M., Campbell, R., and Underwood, M.A. (2004). The relationship between T-lymphocyte subset infiltration and survival in patients with prostate cancer. Br. J. Cancer 91, 541–543.

McCarron, S.L., Edwards, S., Evans, P.R., Gibbs, R., Dearnaley, D.P., Dowe, A., Southgate, C., Easton, D.F., Eeles, R.A., and Howell, W.M. (2002). Influence of cytokine gene polymorphisms on the development of prostate cancer. Cancer Res. 62, 3369–3372.

Meehan, W.J., Samant, R.S., Hopper, J.E., Carrozza, M.J., Shevde, L.A., Workman, J.L., Eckert, K.A., Verderame, M.F., and Welch, D.R. (2004). Breast cancer metastasis suppressor 1 (BRMS1) forms complexes with retinoblastoma-binding protein 1 (RBP1) and the mSin3 histone deacetylase complex and represses transcription. J. Biol. Chem. 279, 1562–1569.

Mengus, C., Le Magnen, C., Trella, E., Yousef, K., Bubendorf, L., Provenzano, M., Bachmann, A., Heberer, M., Spagnoli, G.C., and Wyler, S. (2011). Elevated levels of circulating IL-7 and IL-15 in patients with early stage prostate cancer. J. Transl. Med. 9, 162.

Menten, P., Wuyts, A., and Van Damme, J. (2002). Macrophage inflammatory protein-1. Cytokine Growth Factor Rev. *13*, 455–481.

Miyazaki, T., Kawahara, A., Fujii, H., Nakagawa, Y., Minami, Y., Liu, Z.J., Oishi, I., Silvennoinen, O., Witthuhn, B.A., and Ihle, J.N. (1994). Functional activation of Jak1 and Jak3 by selective association with IL-2 receptor subunits. Science *266*, 1045–1047.

Miyazaki, T., Liu, Z.J., Kawahara, A., Minami, Y., Yamada, K., Tsujimoto, Y., Barsoumian, E.L., Permutter, R.M., and Taniguchi, T. (1995). Three distinct IL-2 signaling pathways mediated by bcl-2, c-myc, and lck cooperate in hematopoietic cell proliferation. Cell *81*, 223–231.

Munger, W., DeJoy, S.Q., Jeyaseelan, R., Torley, L.W., Grabstein, K.H., Eisenmann, J., Paxton, R., Cox, T., Wick, M.M., and Kerwar, S.S. (1995). Studies evaluating the antitumor activity and toxicity of interleukin-15, a new T cell growth factor: comparison with interleukin-2. Cell. Immunol. *165*, 289–293.

Murphy, K., Travers, P., Walport, M., and Janeway, C. (2012). Janeway's immunobiology (New York: Garland Science).

Nakanishi, H., Mazda, O., Satoh, E., Asada, H., Morioka, H., Kishida, T., Nakao, M., Mizutani, Y., Kawauchi, A., Kita, M., et al. (2003). Nonviral genetic transfer of Fas ligand induced significant growth suppression and apoptotic tumor cell death in prostate cancer in vivo. Gene Ther. *10*, 434–442.

National Cancer Institute NCI Dictionary of Cancer Terms.

Ness, N., Andersen, S., Valkov, A., Nordby, Y., Donnem, T., Al-Saad, S., Busund, L.-T., Bremnes, R.M., and Richardsen, E. (2014). Infiltration of CD8+ lymphocytes is an independent prognostic factor of biochemical failure-free survival in prostate cancer. The Prostate *74*, 1452–1461.

Neuhausen, S.L., Slattery, M.L., Garner, C.P., Ding, Y.C., Hoffman, M., and Brothman, A.R. (2005). Prostate cancer risk and IRS1, IRS2, IGF1, and INS polymorphisms: strong association of IRS1 G972R variant and cancer risk. The Prostate *64*, 168–174.

Oh, S., Berzofsky, J.A., Burke, D.S., Waldmann, T.A., and Perera, L.P. (2003). Coadministration of HIV vaccine vectors with vaccinia viruses expressing IL-15 but not IL-2 induces long-lasting cellular immunity. Proc. Natl. Acad. Sci. U. S. A. *100*, 3392–3397.

Oh, S., Perera, L.P., Terabe, M., Ni, L., Waldmann, T.A., and Berzofsky, J.A. (2008). IL-15 as a mediator of CD4+ help for CD8+ T cell longevity and avoidance of TRAIL-mediated apoptosis. Proc. Natl. Acad. Sci. U. S. A. *105*, 5201–5206.

Okada, K., Kojima, M., Naya, Y., Kamoi, K., Yokoyama, K., Takamatsu, T., and Miki, T. (2000). Correlation of histological inflammation in needle biopsy specimens with serum prostate- specific antigen levels in men with negative biopsy for prostate cancer. Urology 55, 892–898.

Oliva, A., Kinter, A.L., Vaccarezza, M., Rubbert, A., Catanzaro, A., Moir, S., Monaco, J., Ehler, L., Mizell, S., Jackson, R., et al. (1998). Natural killer cells from human immunodeficiency virus (HIV)-infected individuals are an important source of CC-chemokines and suppress HIV-1 entry and replication in vitro. J. Clin. Invest. 102, 223–231.

Vuk-Pavlović, S., Bulur, P.A., Lin, Y., Qin, R., Szumlanski, C.L., Zhao, X., and Dietz, A.B. (2010). Immunosuppressive CD14+HLA-DRlow/- monocytes in prostate cancer. The Prostate 70, 443–455.

Pilipow, K., Roberto, A., Roederer, M., Waldmann, T.A., Mavilio, D., and Lugli, E. (2015). IL-15 and T-cell Stemness in T-cell-Based Cancer Immunotherapy. Cancer Res. 75, 5187–5193.

Pirtskhalaishvili, G., Shurin, G.V., Esche, C., Cai, Q., Salup, R.R., Bykovskaia, S.N., Lotze, M.T., and Shurin, M.R. (2000). Cytokine-mediated protection of human dendritic cells from prostate cancer-induced apoptosis is regulated by the Bcl-2 family of proteins. Br. J. Cancer 83, 506–513.

Pittoni, P., and Colombo, M.P. (2012). The dark side of mast cell-targeted therapy in prostate cancer. Cancer Res. 72, 831–835.

Reiss, K., Wang, J.Y., Romano, G., Furnari, F.B., Cavenee, W.K., Morrione, A., Tu, X., and Baserga, R. (2000). IGF-I receptor signaling in a prostatic cancer cell line with a PTEN mutation. Oncogene 19, 2687–2694.

Reiss, K., Wang, J.Y., Romano, G., Tu, X., Peruzzi, F., and Baserga, R. (2001). Mechanisms of regulation of cell adhesion and motility by insulin receptor substrate-1 in prostate cancer cells. Oncogene 20, 490–500.

Ribot, J.C., Ribeiro, S.T., Correia, D.V., Sousa, A.E., and Silva-Santos, B. (2014). Human γδ thymocytes are functionally immature and differentiate into cytotoxic type 1 effector T cells upon IL-2/IL-15 signaling. J. Immunol. Baltim. Md 1950 192, 2237–2243.

Roberts, C.T. (2004). IGF-1 and prostate cancer. Novartis Found. Symp. 262, 193–199; discussion 199–204, 265–268.

Rohena-Rivera, K., Sanchez-Vazquez, M., Aponte-Colon, D., Forestier-Roman, I., Quintero-Aguilo, M., and Martinez-Ferrer, M. (2016). CCL-4 enhances prostate cancer migration and invasion by modulating integrin expression (Int J Clin Exp Med).

Rubin, M.A., Gerstein, A., Reid, K., Bostwick, D.G., Cheng, L., Parsons, R., and Papadopoulos, N. (2000). 10q23.3 loss of heterozygosity is higher in lymph node-positive (pT2-3,N+) versus lymph node-negative (pT2-3,N0) prostate cancer. Hum. Pathol. *31*, 504–508.

Rubinchik, S., Wang, D., Yu, H., Fan, F., Luo, M., Norris, J.S., and Dong, J.Y. (2001). A complex adenovirus vector that delivers FASL-GFP with combined prostate-specific and tetracycline-regulated expression. Mol. Ther. J. Am. Soc. Gene Ther. *4*, 416–426.

Saika, F., Kiguchi, N., Kobayashi, Y., Fukazawa, Y., and Kishioka, S. (2012). CC-chemokine ligand 4/macrophage inflammatory protein-1β participates in the induction of neuropathic pain after peripheral nerve injury. Eur. J. Pain Lond. Engl. *16*, 1271–1280.

Saito, S., Kitayama, J., Jin, Z.X., Tsuno, N., Kaisaki, S., Seto, Y., and Nagawa, H. (2003). Beta-chemokine, macrophage inflammatory protein-1beta (MIP-1beta), is highly expressed in diffuse type human gastric cancers. J. Exp. Clin. Cancer Res. CR *22*, 453–459.

Sallusto, F., Palermo, B., Lenig, D., Miettinen, M., Matikainen, S., Julkunen, I., Forster, R., Burgstahler, R., Lipp, M., and Lanzavecchia, A. (1999). Distinct patterns and kinetics of chemokine production regulate dendritic cell function. Eur. J. Immunol. *29*, 1617–1625.

Sansal, I., and Sellers, W.R. (2004). The biology and clinical relevance of the PTEN tumor suppressor pathway. J. Clin. Oncol. Off. J. Am. Soc. Clin. Oncol. *22*, 2954–2963.

Sato, N., Gleave, M.E., Bruchovsky, N., Rennie, P.S., Beraldi, E., and Sullivan, L.D. (1997). A metastatic and androgen-sensitive human prostate cancer model using intraprostatic inoculation of LNCaP cells in SCID mice. Cancer Res. *57*, 1584–1589.

Schimmer, A.D., Thomas, M.P., Hurren, R., Gronda, M., Pellecchia, M., Pond, G.R., Konopleva, M., Gurfinkel, D., Mawji, I.A., Brown, E., et al. (2006). Identification of small molecules that sensitize resistant tumor cells to tumor necrosis factor-family death receptors. Cancer Res. *66*, 2367–2375.

Schumacher, T.N., and Schreiber, R.D. (2015). Neoantigens in cancer immunotherapy. Science *348*, 69–74.

Sfanos, K.S., and De Marzo, A.M. (2012). Prostate cancer and inflammation: the evidence. Histopathology *60*, 199–215.

Sfanos, K.S., Isaacs, W.B., and De Marzo, A.M. (2013). Infections and inflammation in prostate cancer. Am. J. Clin. Exp. Urol. *1*, 3–11.

Shiao, S.L., Chu, G.C.-Y., and Chung, L.W.K. (2016). Regulation of prostate cancer progression by the tumor microenvironment. Cancer Lett.

Silverthorn, D.U., Johnson, B.R., Ober, W.C., Garrison, C.W., and Silverthorn, A.C. (2013). Human physiology: an integrated approach (Boston: Pearson Education).

Sramkoski, R.M., Pretlow, T.G., Giaconia, J.M., Pretlow, T.P., Schwartz, S., Sy, M.S., Marengo, S.R., Rhim, J.S., Zhang, D., and Jacobberger, J.W. (1999). A new human prostate carcinoma cell line, 22Rv1. In Vitro Cell. Dev. Biol. Anim. *35*, 403–409.

Steel, J.C., Waldmann, T.A., and Morris, J.C. (2012). Interleukin-15 biology and its therapeutic implications in cancer. Trends Pharmacol. Sci. *33*, 35–41.

Suzuki, K., Nakazato, H., Matsui, H., Hasumi, M., Shibata, Y., Ito, K., Fukabori, Y., Kurokawa, K., and Yamanaka, H. (2001). NK cell-mediated anti-tumor immune response to human prostate cancer cell, PC-3: immunogene therapy using a highly secretable form of interleukin-15 gene transfer. J. Leukoc. Biol. *69*, 531–537.

Tagaya, Y., Burton, J.D., Miyamoto, Y., and Waldmann, T.A. (1996). Identification of a novel receptor/signal transduction pathway for IL-15/T in mast cells. EMBO J. *15*, 4928–4939.

Tagaya, Y., Kurys, G., Thies, T.A., Losi, J.M., Azimi, N., Hanover, J.A., Bamford, R.N., and Waldmann, T.A. (1997). Generation of secretable and nonsecretable interleukin 15 isoforms through alternate usage of signal peptides. Proc. Natl. Acad. Sci. U. S. A. *94*, 14444–14449.

Taverna, G., Pedretti, E., Di Caro, G., Borroni, E.M., Marchesi, F., and Grizzi, F. (2015). Inflammation and prostate cancer: friends or foe? Inflamm. Res. Off. J. Eur. Histamine Res. Soc. Al *64*, 275–286.

Trudel, D., Fradet, Y., Meyer, F., Harel, F., and Têtu, B. (2003). Significance of MMP-2 expression in prostate cancer: an immunohistochemical study. Cancer Res. *63*, 8511–8515.

Waldmann, T.A. (2004). Targeting the interleukin-15/interleukin-15 receptor system in inflammatory autoimmune diseases. Arthritis Res. Ther. *6*, 174–177.

Waldmann, T.A., and Tagaya, Y. (1999). The multifaceted regulation of interleukin-15 expression and the role of this cytokine in NK cell differentiation and host response to intracellular pathogens. Annu. Rev. Immunol. *17*, 19–49.

Wolk, A., Mantzoros, C.S., Andersson, S.O., Bergström, R., Signorello, L.B., Lagiou, P., Adami, H.O., and Trichopoulos, D. (1998). Insulin-like growth factor 1 and prostate cancer risk: a population-based, case-control study. J. Natl. Cancer Inst. *90*, 911–915.

Wolpe, S.D., Davatelis, G., Sherry, B., Beutler, B., Hesse, D.G., Nguyen, H.T., Moldawer, L.L., Nathan, C.F., Lowry, S.F., and Cerami, A. (1988). Macrophages secrete a novel heparin-binding protein with inflammatory and neutrophil chemokinetic properties. J. Exp. Med. *167*, 570–581.

Woo, J.R., Liss, M.A., Muldong, M.T., Palazzi, K., Strasner, A., Ammirante, M., Varki, N., Shabaik, A., Howell, S., Kane, C.J., et al. (2014). Tumor infiltrating B-cells are increased in prostate cancer tissue. J. Transl. Med. *12*, 30.

Wright, W.E., Pereira-Smith, O.M., and Shay, J.W. (1989). Reversible cellular senescence: implications for immortalization of normal human diploid fibroblasts. Mol. Cell. Biol. *9*, 3088–3092.

Wu, J. (2013). IL-15 Agonists: The Cancer Cure Cytokine. J. Mol. Genet. Med. Int. J. Biomed. Res. *7*, 85.

Wu, Z., and Xu, Y. (2010). IL-15R alpha-IgG1-Fc enhances IL-2 and IL-15 anti-tumor action through NK and CD8+ T cells proliferation and activation. J. Mol. Cell Biol. *2*, 217–222.

Wu, J.D., Higgins, L.M., Steinle, A., Cosman, D., Haugk, K., and Plymate, S.R. (2004). Prevalent expression of the immunostimulatory MHC class I chain-related molecule is counteracted by shedding in prostate cancer. J. Clin. Invest. *114*, 560–568.

Wu, Y.-L., Ding, Y.-P., Tanaka, Y., Shen, L.-W., Wei, C.-H., Minato, N., and Zhang, W. (2014). γδ T Cells and Their Potential for Immunotherapy. Int. J. Biol. Sci. *10*, 119–135.

Xie, T., Dong, B., Yan, Y., Hu, G., and Xu, Y. (2015). Association between MMP-2 expression and prostate cancer: A meta-analysis. Biomed. Rep.

Yano, S., Nishioka, Y., Izumi, K., Tsuruo, T., Tanaka, T., Miyasaka, M., and Sone, S. (1996). Novel metastasis model of human lung cancer in SCID mice depleted of NK cells. Int. J. Cancer *67*, 211–217.

Yu, P., Steel, J.C., Zhang, M., Morris, J.C., and Waldmann, T.A. (2010). Simultaneous blockade of multiple immune system inhibitory checkpoints enhances antitumor activity mediated by interleukin-15 in a murine metastatic colon carcinoma model. Clin. Cancer Res. Off. J. Am. Assoc. Cancer Res. *16*, 6019–6028.

Zhang, M., Yao, Z., Dubois, S., Ju, W., Müller, J.R., and Waldmann, T.A. (2009). Interleukin-15 combined with an anti-CD40 antibody provides enhanced therapeutic efficacy for murine models of colon cancer. Proc. Natl. Acad. Sci. U. S. A. *106*, 7513–7518.

Appendices:

Appendix 1: *Supplementary Data-* IL-15 modulates genes related to lipid metabolism and lymphocyte development.

While performing the *in vivo* experiments with IL-15 (*see methods for experimental procedures*), an unexpected surprise was seeing an increased tumor volume in the tumor treated with IL-15 0.001 ng/mL as compared to the control. Because of that reason, we sought to identify genes that could help explain the observed phenotype. RNA from the previously extracted prostate cancer tumors was used for microarray analysis using the Affymetrix Human Gene 2.0 Gene Array. Afterwards, we used Ingenuity Pathway Analysis (IPA) to evaluate changes in gene expression and real time PCR to confirm those results. 952 genes were differentially expressed in tumors treated with IL-15 as compared to the control. We decided to further study genes related to fatty acids because previous data from our lab showed that tumors treated with IL-15 had increased number of adipocytes and Adiponectin expression as compared to the control. Additionally, we decided to study genes related to inflammation because prior data from our lab

had shown that these tumors had increased numbers of neutrophils and Neutrophil elastase expression. For such reasons, we studied the following genes related to lymphocyte development or transport of long chain fatty acids: RAC1, CPT2, CTR9, FABP4, TAPBP, STAT3, PLCG2, TCF4, ACSL3, GATA3, GOT2, DTX1, MSR1, and PLIN2. As can be appreciated in Figure 1 of this appendix, RAC1, CPT2, CTR9, and FABP4 mRNA expression is upregulated in tumors treated with IL-15 0.001 ng/mL as compared to the control. On the other hand, TAPBP, STAT3, PLCG2, TCF4, ACSL3, GATA3, GOT2, DTX1, MSR1, and PLIN2 mRNA expression is not differentially modulated by IL-15 as compared to the control (Figure 1E of Appendix 1).

Figure 1:
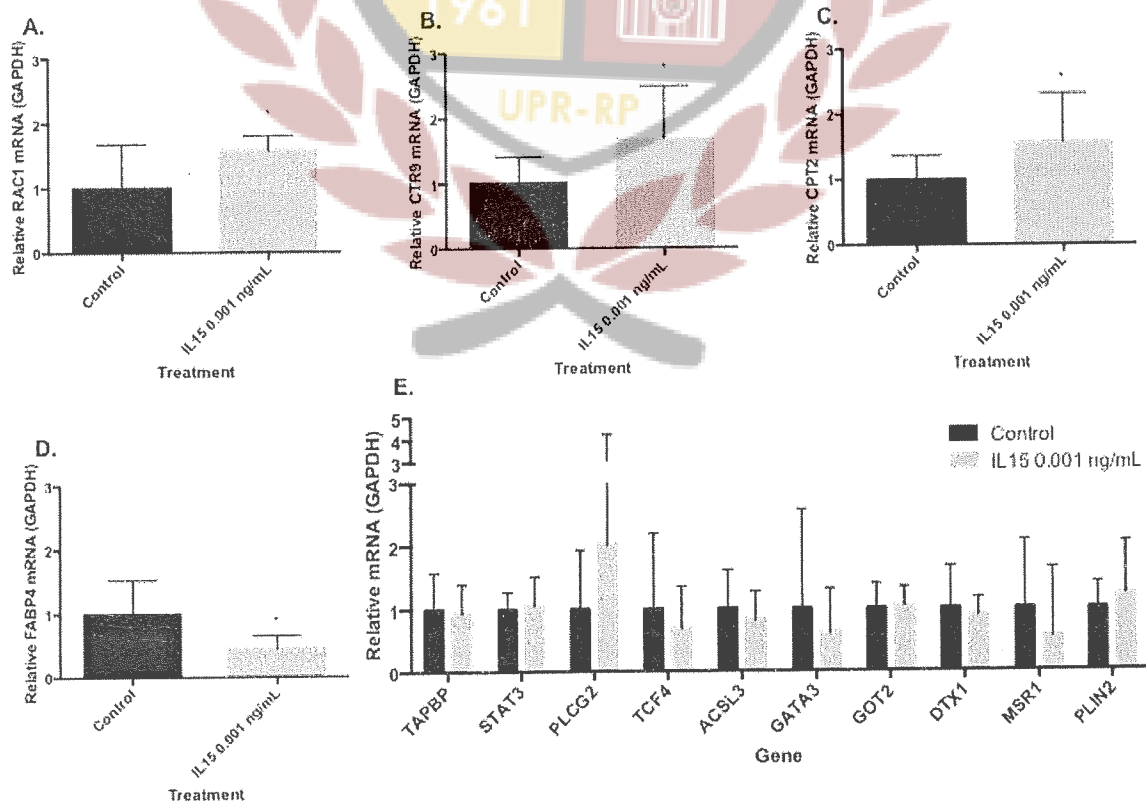
Figure 1. mRNA expression of genes related to lipid metabolism in prostate cancer tumors treated with IL-15. A. Quantitative real time PCR revealed RAC1 mRNA expression to be induced by IL-15 at a concentration of 0.001 ng/mL. B. Quantitative real time PCR revealed CTR9 mRNA expression to be induced by IL-15 at a concentration of 0.001 ng/mL. C. Quantitative real time PCR revealed CPT2 mRNA expression to be induced by IL-15 at a concentration of 0.001 ng/mL. D. Quantitative real time PCR revealed FABP4 mRNA expression to be induced by IL-15 at a concentration of 0.001 ng/mL. E. mRNA expression of genes that were differentially expressed when analyzed with Ingenuity Pathway Analysis (IPA) but not significantly modulated by IL-15 when confirmed through quantitative real time PCR. Real time PCR quantification was done using the $\Delta\Delta CT$ method. Values were normalized to GAPDH and relative to the control, Mean + SEM (*$P<0.05$). n = 5 tumors per group.
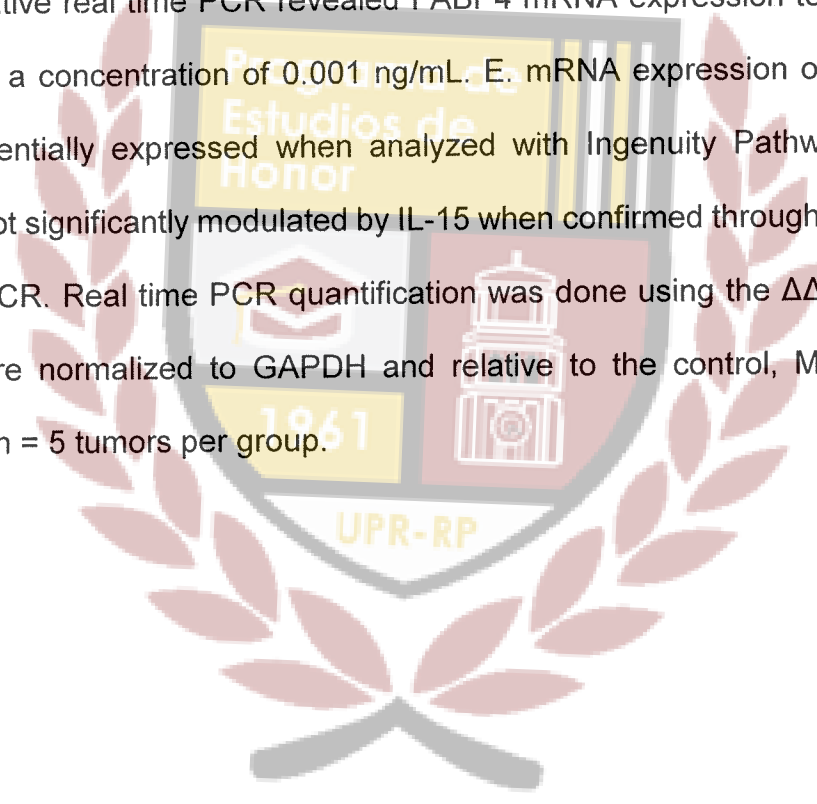
Appendix 2: Martínez-Ferrer Laboratory Protocols

Protocol: RNA Extraction

RNEasy Mini kit (Qiagen Cat No. 74106) (Please read their protocol)

1. Remove tissue from storage in -80 °C.

2. Extract a piece less than 30 mg, keep in dry ice.

3. Add 350 uL of buffer RLT with β-Mercapto Ethanol.

4. In Ice, homogenize tissue in 5 sec. intervals with a rotor stator homogenizer.

5. Clean homogenizer with nuclease free water 1x, 70% Ethanol 1x, and nuclease free water 3x between samples. Sterilization with a dry sterilizer is optional.

6. Add 590 uL nuclease free water, mix by pipetting.

7. Add 10 uL Proteinase K (Qiagen Cat No. 19131) Mix by pipetting.

8. Incubate for 10 min. at 55 °C.

9. Centrifuge for 1 min. at 10,000 rpm.

10. Transfer supernatant to a fresh microcentrifuge tube.

11. Add 475uL of molecular grade 200 °proof Ethanol. Mix by pipetting.

12. Transfer up to 700 µL of the sample, including any precipitate that may have formed, to an RNeasy Mini spin column placed in a 2 ml collection tube.

13. Centrifuge at 20–25°C for 15 s at 10,000 rpm. Discard the flowthrough. Reuse the collection tube.

14. Repeat step 12 and 13 until all sample is used. Discard the flowthrough. Reuse the collection tube.

15. Add 350 µL Buffer RW1 to the RNeasy spin column. Centrifuge at 20–25°C for 15 s at 10,000 rpm to wash the membrane. Discard the flow-through. Reuse the collection tube.

16. Add 10 µL DNase I (RNase Free DNase Set Qiagen Cat No. 79254) stock solution to 70 µL Buffer RDD. Mix by gently inverting the tube.

17. Add the DNase I incubation mix (80 µL) directly to the RNeasy spin column membrane, and incubate at room temperature for 15 min.

18. Add 350 µL Buffer RW1 to the RNeasy spin column. Centrifuge at 20–25°C for 15 s at 10,000 rpm to wash the membrane. Discard the flow-through. Reuse the collection tube.

19. Add 500 µL Buffer RPE to the RNeasy spin column. Centrifuge at 20–25°C for 15 s at 10,000 rpm to wash the membrane. Discard the flow-through. Reuse the collection tube.

20. Add 500 µL Buffer RPE to the RNeasy spin column. Close the lid gently, and centrifuge at 20–25°C for 2 min at 10,000 rpm to wash the membrane. Discard the flow-through and collection tube.

21. Place the spin column in a new 2 mL collection tube. Centrifuge at full speed for 1 min. Discard collection tube.

22. Place the RNeasy spin column in a new 1.5 mL collection tube.

23. Add 30 µL RNase-free water directly to the RNeasy spin column membrane. Incubate for 1 min at room temperature.

24. To elute the RNA, centrifuge for 1 min at 10,000 rpm at 20–25°C.

25. Reuse the eluate from the previous step and centrifuge for 1 min at 10,000 rpm to obtain a higher concentration.

26. Keep RNA at -80 °C.

References:

1. Qiagen RNeasy Mini Handbook. Available from: https://www.qiagen.com/resources/download.aspx?id=14e7cf6e-521a-4cf7-8cbc-bf9f6fa33e24&lang=en

Protocol: RT² Profiler PCR Array (Qiagen) for Step One Plus

cDNA Synthesis RT² First Strand Kit (Cat no. 330231) (Please read their protocol)

DNA Elimination

1. Prepare each sample in a PCR Tube

Reagent	Amount
RNA*	25ng-5ug (adjust to cell line and/or sample type)
GE Buffer (pink lid)	2 uL
RNase free H2O (light blue lid)	Depends on the sample amount
Adjust final volume to	10 uL

2. Put Samples on Thermal cycler at 42°C during 5 minutes to remove DNA

3. Put samples on ice 1 minute

cDNA Synthesis

1. Prepare reverse transcription mix

Reagent	Volume per sample (1)
BC3 Buffer (Red lid)	4 uL
Control P2 (Lilac lid)	1 uL
RE3 RT-Mix (Brown Lid)	2 uL
RNase Free H20	3 uL
VOLUME PER SAMPLE	10 uL

2. Add10uL of Reverse transcription mix to DNA elimination sample. (final volume 20uL)

3. Incubate @42C for 15 min, follow with 95C for 5 min. (thermocycler)

4. Place samples on ice.

5. Add 91uL to each reaction.
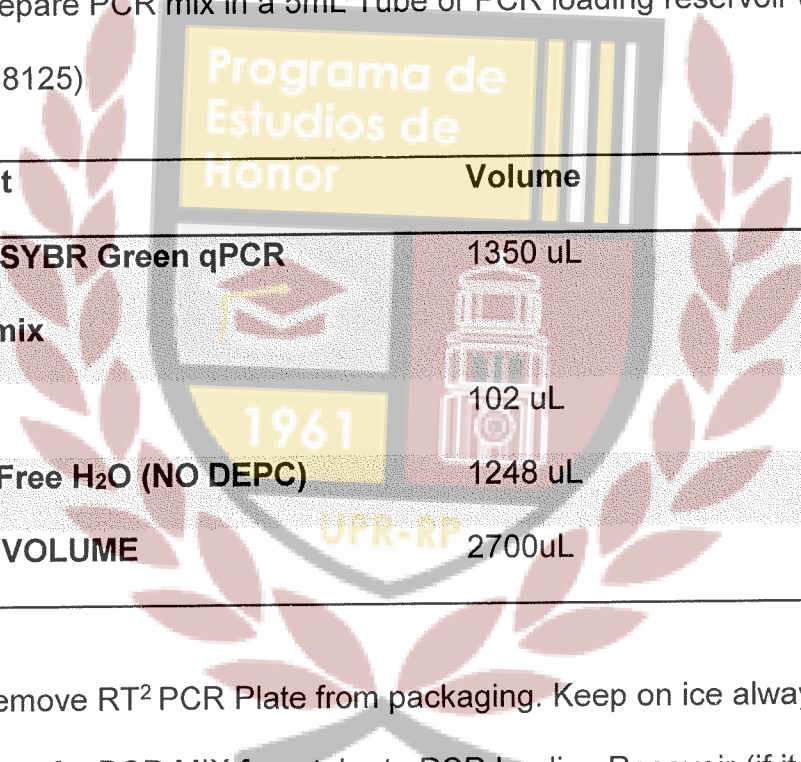
6. Keep at -20C if RT2-PCR is to be done other day

Real time PCR- RT^2 for Step one Plus (format C)

SYBR Green qPCR Mastermix (Cat no. 330500) (Please read their protocol)

Note: make sure you have at least two boxes of 200uL tips before starting.

SYBR Green is light sensitive (just direct light), keep covered or work with the lights off in the hood

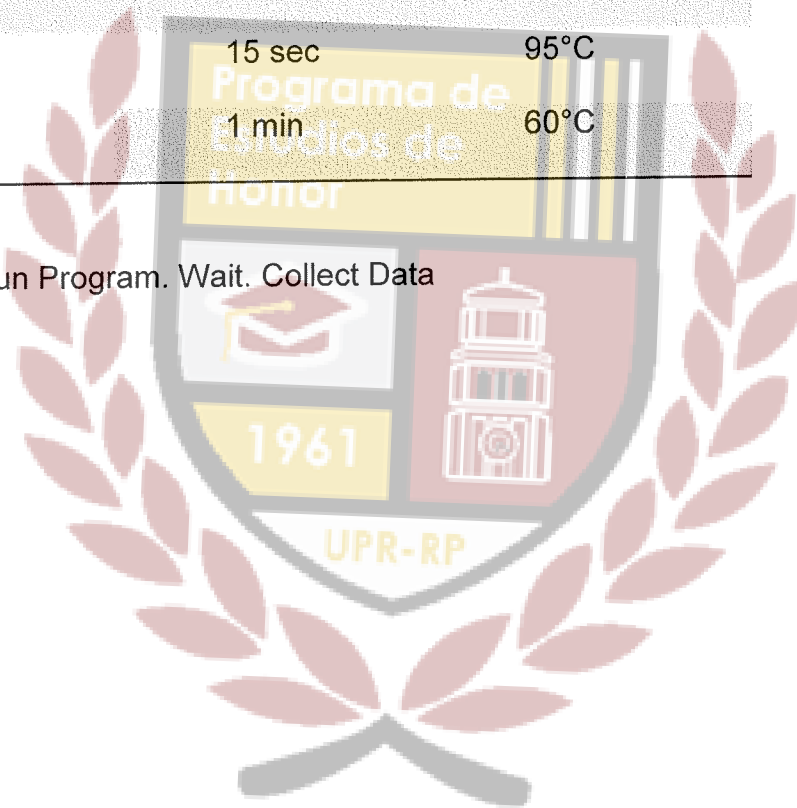1. Prepare PCR mix in a 5mL Tube or PCR loading reservoir (Cat no. 338125)

Reagent	Volume
2x RT2 SYBR Green qPCR Mastermix	1350 uL
cDNA	102 uL
RNase Free H$_2$O (NO DEPC)	1248 uL
TOTAL VOLUME	2700uL

2. Remove RT^2 PCR Plate from packaging. Keep on ice always!

3. Transfer PCR MIX from tube to PCR loading Resevoir (if it was not prepared there)

4. Add 25 uL of PCR Mix to each well using a multichannel. 8 wells at a time (left to right not up down)... (ALSO if covering with 8 cap strips.. make sure to cover each one at a time)

5. MAKE SURE TO CHANGE TIPS !!! PREVENT CONTAMINATION (remember primers are on each well) !!!

6. Cover your plate either with optical adhesive film (not provided) or with thin wall 8 cap strips (provided)

7. Centrifuge you plate. 1000g/1min RT.

8. Set up program in RT PCR machine.

Cycles	Time	Temperature
1	10 min	95°C
40	15 sec	95°C
	1 min	60°C

9. Run Program. Wait. Collect Data

Sample Plate Layout

Figure 1. RT2 Profiler PCR Array Formats A, C, D, F, H layout. RT2 Profiler PCR Array Formats A, C, D, F, H: Wells A1 to G12 each contain a real-time PCR assay for a pathway/disease/functionally related gene. Wells H1 to H5 contain a housekeeping gene panel to normalize array data (**HK1-5**). Well H6 contains a genomic DNA control (**GDC**). WellsH7 to H9 contain replicate reverse-transcription controls (**RTC**). Wells H10 to H12 contain replicate positive PCR controls (**PPC**).

References:

1. Qiagen RT^2 Profiler PCR array handbook. Available from: https://www.qiagen.com/us/resources/resourcedetail?id=6161ebc1-f60f-4487-8c9e-9ce0c5bc3070&lang=en

Protocol: cDNA Synthesis

BioRad iScript cDNA Synthesis **Kit (Cat No. 170-8891)** (Please read their

protocol)

1. Thaw all contents and resuspend 5x reaction buffer.

2. Prepare reaction mix:

Component	Volume Per Reaction
5x iScript Reaction Mix (Blue)	4 µL
iScript Reverse Transcriptase	1 µL
RNA Template (1 µg)*	Depends on sample concentration
Nuclease-Free Water	Depends on sample contents
Adjust Final Volume	10 µL

*If more RNA is needed, double the reaction accordingly

3. Prepare reactions in PCR tubes and run protocol in a thermal cycler.

   5 minutes at 25°C

   30 minutes at 42°C

   5 minutes at 85°C

   Hold at 4°C (optional)

4. Store at -20 °C if not using right away.

References:

1. BioRad iScript cDNA Synthesis kit. Available from: http://www.bio-rad.com/webroot/web/pdf/lsr/literature/4106228C.pdf

Protocol: Real-Time PCR

iQ SYBR Green Supermix BioRad (Cat No. 170-8884) (Please read their protocol)

1. In ice, thaw cDNA samples, SYBR Green Supermix and primers.

2. Prepare a 96-well template as a guide to load the samples.

3. Calculate how many reactions you have for each primer (Number of samples + 2 samples for pipetting errors and negative control)

4. Prepare master mix (all ingredients except cDNA) for each primer. Keep in ice. See example listed below.

Master Mix

Component	1x Reaction	50x Reactions
2x iQ SYBR Green	6.25 µL	312.5 µL
Primer (Forward)	0.25 µL	12.5 µL
Primer (Reverse)	0.25 µL	12.5 µL
Nuclease Free Water	4.75 µL	237.5 µL
Total Volume	11.5 µL	575 µL

5. Mix well, spin tubes for 10 sec, and aliquot 34.5 µL of the master mix in separate tubes corresponding to the number of samples.

6. Add 3 µL of the cDNA to the corresponding tube containing the master mix. (add 3 µL of nuclease-free water to the negative control) Mix well and spin for 10 sec.

7. Load, in triplicates, 10 µL of the sample to the 96-well plate following your model.

8. Place sealing film and spin plate for 30 sec at 1,000 rpm.

9. Place plate in real time PCR machine and run protocol.

Sample Protocol

Cycle Stage	Temperature	Time	Number of Cycles
Initial denaturation and enzyme activation	95°C	10 min	1
Denaturing	95°C	15 sec.	40
Annealing and extension	56-62°C (depending on primer)	1 min	
Melting Curve (Step and Hold)	95°C	15 sec.	1
	60°C	1min	
	95°C	15 sec.	

Protocol: Orthotopic Mouse Model

Cell preparation

1. Culture cells until confluent

2. Add Trypsin/EDTA to detach adherent cells and count.

3. Adjust cell concentration to 3.13×10^4 cells/mL

4. Aliquot 240 uL of cell suspension (per mouse lobes to be injected, keep cells on ice.

5. Aliquot 30 uL of collagen (per mouse lobes) in separate tubes, keep on ice.
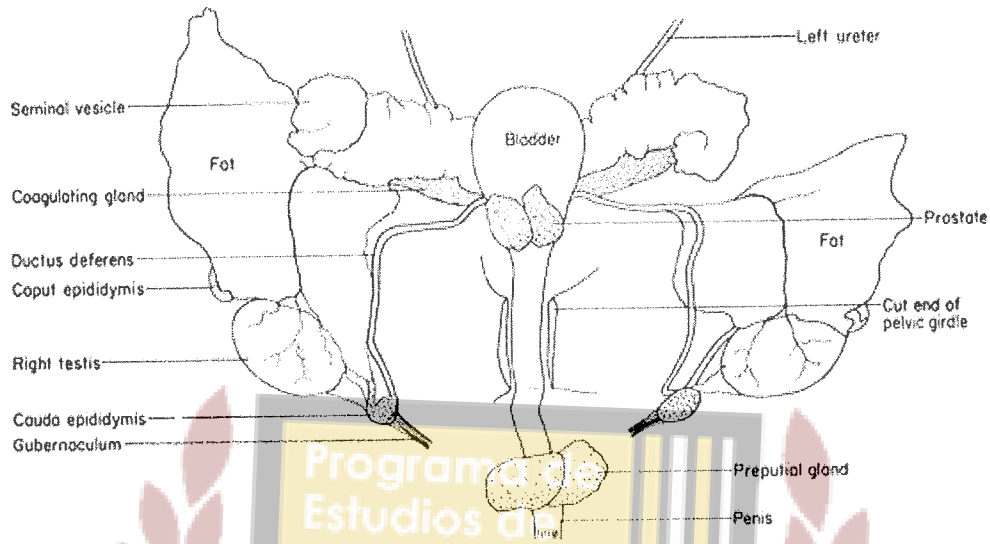
Mouse surgery

1. Anesthetize mouse with isofluorane. Keep mouse with anesthetic mask during the procedure.

2. Shave mouse if needed and disinfect with iodine solution

3. Keep mouse on heat pad at 37°C.

4. Make a small incision on the outer skin layer (low abdominal area)

5. Proceed with the inner skin layer.

6. Up front the urinary bladder will be seen, treat it carefully and empty it if necessary

7. Behind the urinary bladder, the seminal vesicles are found (appear white)

8. Load a syringe with cell suspension until 80 uL.

9. Mix the contents of the syringe in a tube containing 30 uL of collagen.

10. Load syringe with 100 uL of mixture.

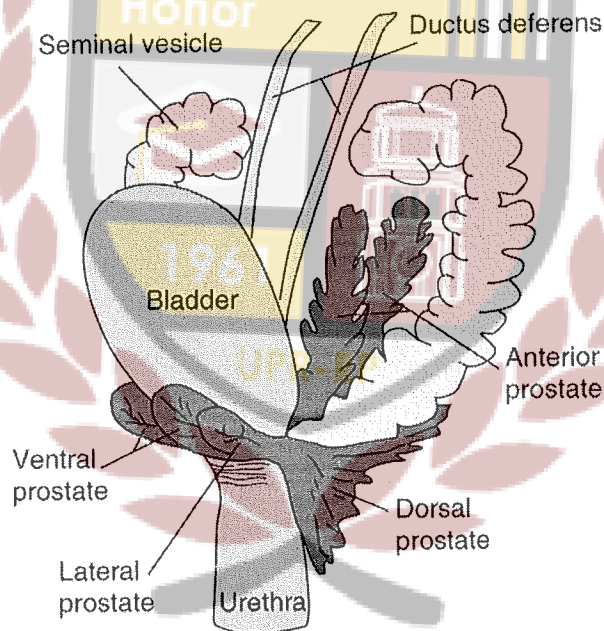11. Inject cell-collagen mixture to the anterior prostate lobes.

12. Make sure to keep all organs inside and close inner skin layer with absorbable sutures.

13. Close outer skin layer with clips.

14. Remove mouse from anesthetic mask and keep on 37°C heat pad for recovery.

15. Check mouse periodically after surgical procedure

Figures

Labels: Left ureter, Seminal vesicle, Bladder, Fat, Coagulating gland, Prostate, Ductus deferens, Caput epididymis, Fat, Right testis, Cut end of pelvic girdle, Cauda epididymis, Gubernaculum, Preputial gland, Penis

(1)

Labels: Seminal vesicle, Ductus deferens, Bladder, Anterior prostate, Ventral prostate, Dorsal prostate, Lateral prostate, Urethra

(2)

References

1. Cook MJ. The anatomy of the laboratory Mouse. Academic Press; 1965. p.143

2. Valkenburg KC, Williams BO. Mouse Models of Prostate Cancer. Prostate Cancer. 2011. p. 1–22.